PRESCRIBED FIRE & PINE STRAW: SOIL CARBON DYNAMICS IN LONGLEAF PINE STANDS UNDER TWO COMMON MANAGEMENT STRATEGIES

by

ALISON MOSS

(Under the Direction of Rebecca Abney)

ABSTRACT

Soil organic matter (SOM) composition was characterized in longleaf pine (*Pinus palustris*) stands managed with regular broadcast fire (Burned) or pine straw raking (Unburned) in the Coastal Plain of Georgia, USA. Proton nuclear magnetic resonance spectroscopy revealed that soil-water extractions isolate a dissolved organic matter pool (DOM) that is younger and faster-cycling than *in-situ* soil leachate DOM. One year of soil respiration monitoring captured higher carbon dioxide flux in Burned than Unburned stands. Burned stand soils contained a larger proportion of recently-fixed carbon (C) with SOM reflecting more fresh plant litter. Unburned stand SOM was dominated by more microbially-processed C due to historical tillage and modern pine straw removal. Our results show that soil C can persist for centuries to millennia, even in ecoregions facing rapid C loss to decomposition and leaching. Our study also highlights some methodological challenges of assessing SOM pools in this system and others.

INDEX WORDS: Pyrogenic carbon, leaching, water extractable organic matter, spectroscopy, stable isotopes, radiocarbon

PRESCRIBED FIRE & PINE STRAW: SOIL CARBON DYNAMICS IN LONGLEAF PINE STANDS UNDER TWO COMMON MANAGEMENT STRATEGIES

by

ALISON MOSS

B.S., Towson University, 2020

A Thesis Submitted to the Graduate Faculty of The University of Georgia in Partial

Fulfillment of the Requirements for the Degree

MASTER OF SCIENCE

ATHENS, GEORGIA

2023

© 2023

ALISON MOSS

All Rights Reserved

PRESCRIBED FIRE & PINE STRAW: SOIL CARBON DYNAMICS IN LONGLEAF PINE STANDS UNDER TWO COMMON MANAGEMENT STRATEGIES

by

ALISON MOSS

Major Professor: Rebecca Abney Committee: Mac A. Callaham, Jr.

David Clabo Nina Wurzburger

Electronic Version Approved:

Ron Walcott Vice Provost for Graduate Education and Dean of the Graduate School The University of Georgia August 2023

DEDICATION

This thesis is dedicated to my grandma, Janet Moss, whom I miss very much.

ACKNOWLEDGEMENTS

First, I would like to thank Mr. Mike Brumby for offering his beautiful property as a location for our study. Thank you to Rebecca for being such an inspiring, levelheaded, and fun mentor who guided me through a lot of self-doubt. I could not have completed this thesis without the support of my lab mates Courtney and Alexis. I look forward to many more years of laughter and adventure while we grow together as scientists. Thank you to my committee members David, Nina, and Mac for enriching my research with your considerable experience and insights – I have enjoyed being challenged to think more deeply by all of you. Many members of the UGA and the greater scientific community helped bring this project to fruition. This list includes, but is not limited to, John Glushka, Dave & Brandon Moorhead, Sherry Williford, Karan Rawlins, Joe O'Brien, Grant Snitker, Bayan Sheko, Dan Markewitz, Lori Sutter, Tom Maddox, Brad Smith, Ron Halstead, Jack Fitch, Morgan Kerpics, Kimber Moreland, Morgan Barnes, Fernanda Santos, Hayley Joyell Smith, The River Basin Center, and members of the Chung & Wurzburger Labs. Special thanks to Noelle Joy, Erica Head, and the rest of the folks at UGArden for maintaining a space that brought me joy during challenging moments. Finally, thank you to my parents, Rick and Catherine Moss, my sister Gengy, my partner Corey Allender, and our cat Bert. I am so lucky to have a supportive family to feed me and cheer me on. Bert, you are the most perfect being who ever lived. Corey, I love you too (more, if you can believe it).

TABLE OF CONTENTS

	Page
ACKNOWLEDGEMENTS	v
LIST OF TABLES	viii
LIST OF FIGURES	ix
CHAPTER	
1 INTRODUCTION AND LITERATURE REVIEW	1
Prescribed Fire in the Southeastern and in the Greater United States	s1
Pine Straw Harvesting in Southeastern Forest Management	2
Prescribed Fire Impacts on Soil Properties	3
Pyrogenic Carbon in Soils	6
2 LEACHING OF PYROGENIC CARBON AFTER A PRESCRIBED F	IRE.11
Abstract	12
Introduction	13
Materials & Methods	18
Results	33
Discussion	42
Conclusion	58
3 STABILITY OF CARBON IN STANDS MANAGED WITH AND	
WITHOUT PRESCRIBED FIRE	78
Abstract	79
Introduction	80

	Materials & Methods	84
	Results	90
	Discussion	94
	Conclusion	98
4	SUMMARY AND CONCLUSION	106
REFERE	NCES	108
APPEND	ICES	
A	CHAPTER 2 SUPPLEMENTARY MATERIALS	126
В	CHAPTER 3 SUPPLEMENTARY MATERIALS	173
С	FULL STUDY MAP	185

LIST OF TABLES

Page
Table 2.1: Description of soil characteristics
Table 2.2: Burned Stand species list
Table 2.3: Overstory structure in the Burned Stand as measured using approximately
1/40-hectare circular plots62
Table 2.4a: Density of shrubs in the Burned Stand by species, as measured using
approximately 1/400-hectare circular plots63
Table 2.4b: Density of shrubs in the Burned Stand by height, as measured using
approximately 1/400-hectare circular plots63
Table 2.5: Density and moisture content of herbaceous vegetation in the Burned Stand .64
Table 2.6: Weather conditions for 22 April 2021, during the prescribed fire in the Mature
and Burned Stands65
Table 2.7: Bulk soil chemical and physical properties
Table 2.8 Soil fraction chemical and physical properties
Table 3.1: Bulk soil chemical and physical properties

LIST OF FIGURES

Page
Figure 2.1: Map of the study location highlighting relevant stands and research plots68
Figure 2.2: Average monthly precipitation in Tifton, GA
Figure 2.3: Diagram of the lysimeter plot layout in the Burned Stand70
Figure 2.4: Duration and intensity of soil heating as a head fire passed over the
thermocouple array on the southeast side of the Burned Stand lysimeter plot
during the Rx fire on 22 April 202171
Figure 2.5: Average percent carbon, percent nitrogen, carbon to nitrogen (C:N) ratio, and
δ^{13} C72
Figure 2.6: Average percent C, percent N, C:N ratio, and δ ¹³ C in mineral associated
(MAOM) and particulate (POM) organic matter fractions73
Figure 2.7: Radiocarbon content (Δ^{14} C) of charcoal, mineral-associated organic matter
(MAOM), particulate organic matter (POM), and soil-water extract dissolved
organic matter (DOM) samples collected from 0-10 and 20-30 cm in the soil
profile
Figure 2.8: Mid-infrared spectra from Burned Stand soil sample 9 collected at 20-30 cm,
mineral associated organic matter (MAOM), and particulate organic matter
(POM) separated from that core

Figure 2.9: ¹ H-NMR data depicting the average proportion of dissolved organic matter
which is composed of aromatic, unsaturated, oxygenated, functionalized aliphatic,
and aliphatic functional groups
Figure 2.10: ¹ H-NMR data showing changes in DOM functional group composition over
the course of a 14-month sampling period
Figure 3.1: Map of the study location highlighting relevant stands and research plots100
Figure 3.2: Litterbag plot layout using Burned Plot 1 as an example101
Figure 3.3: Average percent carbon, percent nitrogen, (C:N) ratio, and δ ¹³ C102
Figure 3.4: Mid-infrared spectra from Burned and Unburned stand soil samples taken at
0-10 cm dried longleaf pine needle and longleaf pine needle PyC references103
Figure 3.5: Average CO ₂ flux (μmol CO ₂ m ⁻² s ⁻¹) from soils of forested stands (<i>n</i> =3)
managed with (Burned) and without (Unburned) Rx fire collected every two
months over one year
Figure 3.6: Fungal hyphae colonizing wood PyC in a litterbag collected from Unburned
Stand 2 on 29 March 2022, approximately 7 months after it was placed on the
forest floor105

CHAPTER 1

INTRODUCTION AND LITERATURE REVIEW

1.1 Prescribed Fire in the Southeastern and Greater United States

Prescribed fire is a land management tool in which fire is applied to the landscape to, among other aims, promote native plant diversity, decrease undesirable woody plant competition, improve wildlife habitat, increase stand accessibility, prepare a site for tree planting, and mitigate wildfire risk (Ryan et al., 2013). Prescribed (Rx) fire has a long history in the southeastern United States, where it used to maintain fire-adapted plant and animal communities – particularly the longleaf pine (Pinus paulstris) and wiregrass (Aristida stricta) savannah ecosystem (Fowler & Konopik, 2007; Mitchell et al., 2006; Noss, 1988). The objectives and operations of Rx fire differ from a related but distinct "good fire" practice: Indigenous cultural burning. Cultural burning is an umbrella term referring to Native tribes' specific fire-keeping practices, often woven within annual cycles of land-tending, which have been practiced extensively across lands which include what is now known as the U.S. Southeast (Johnson & Hale, 2002; Kimmerer & Lake, 2001; Munoz et al., 2014; Van Lear et al., 2005). Some definitions of Rx fire specify that it must occur within a legal framework (McLauchlan et al., 2020) that cultural burning traditions predate by millennia (Lake & Christianson, 2019), and many cultural burners intentionally deemphasize "fighting fire" as an objective (Levy, 2022). Thus, it is important to recognize these practices as distinct.

In the U.S., Rx fire has increased dramatically over the last decade, with approximately 70% of the country's Rx burned acres located in the Southeast (Kolden, 2019; Mitchell et al.,

2009). Private landowners in states such as Georgia and Florida are supported by increased legal protections against Rx fire liability (Brenner & Wade, 2003; Yoder, 2008) and 86% percent of Southeastern forested lands are privately owned (Hoover & Riddle, 2021), a scenario which reduces social, financial, and bureaucratic barriers to burning.

More than a century of fire suppression has dramatically altered the composition of U.S. forests and rangelands (Miller & Rose, 1999; Scholl & Taylor, 2010). One side effect of fire suppression is fuel accumulation which, coupled with climate change-associated heating and drying trends (Brown et al., 2004), has driven an increase in frequency and severity of wildfires, particularly in the West (Halofsky et al., 2020). The resulting mega fires represent a social (Xu et al., 2020) and ecological (Abella & Fornwalt, 2015) crisis that foresters, fire ecologists, and Indigenous practitioners argue must be remedied with the return of "good fire" to the land (Kelly et al., 2020; Kolden, 2019; North et al., 2021; Wood & Varner, 2023). In addition to restoring ecosystem resilience to climate change, Rx fire has been proposed as an emissions reduction strategy (Wiedinmyer & Hurteau, 2010). With recent legislation empowering land managers to further expand the use of Rx fire ("Civil Liability," 2021; "National Prescribed Fire Act of 2020," 2020; "Prescribed Fire Liability Pilot Program: Prescribed Fire Claims Fund," 2022), and Federal agencies beginning to incorporate the practice into "climate-smart" management plans (Forest Service Research & Development, 2021), research is needed to determine how these controlled, largely low-severity, burns impact the forest carbon (C) budget (Flanagan et al., 2019; Richter et al., 1982) and soil organic matter dynamics (Hobley et al., 2019).

1.2 Pine Straw Harvesting in Southeastern Forest Management

Pine straw is a forest product referring to the fresh layer of pine needles which are raked, baled, and sold for use as a landscaping mulch. In the U.S., almost all commercial pine straw is

produced in the Southeast, where it is shipped and sold throughout the country (Dickens et al., 2020). Longleaf pine is the most desirable species for aesthetics, durability and profitability, however slash (*Pinus elliottii*) pine straw composes a minor portion of the market (Dickens et al., 2020). Pine straw represents an attractive opportunity for landowners to collect income from stands before they have generated merchantable timber (Susaeta et al., 2012). As a result, the market has grown quickly over the past several decades (Dickens et al., 2020).

The act of raking pine straw is generally a low impact practice which does not substantially alter the understory community (Kelly et al., 2000), however when considered holistically, pine straw management may impact forest health in several ways. Herbicide is commonly used to suppress understory growth, which may influence soil biological functions through changes to microbial community (Ratcliff et al., 2006; Wardle & Parkinson, 1990) and macrofauna (Zaller et al., 2014), particularly applied at higher than recommended rates. Tractors and other vehicles driven through stands to apply chemicals, create bales, and transport bales offsite may generate soil compaction, with potential to negatively affect stand productivity. Finally, harvesting needles represents a reduction in organic matter inputs to soil, potential creating changes to soil moisture and nutrient dynamics which may necessitate management adjustments (Dickens et al., 2020).

1.3 Prescribed Fire Impacts on Soil Properties

The effects of Rx fire management on soils have been understudied, leading to many knowledge gaps (Hiers et al., 2020). While we can look to wildfire studies, which are more numerous, wildfire and Rx fire represent two entirely different disturbance regimes. A major challenge in aggregating data from Rx fire studies comes from inconsistent reporting of pre- and during-fire conditions (Bonner et al., 2021). Ideally, landscapes are managed regularly with Rx

fire, however most Rx fire studies sample soils after a single burn event, which increases the potential to miss long term trends (Alcañiz et al., 2018). The geographic distribution of Rx fire studies is dominated by Australia and the U.S., particularly the Southeastern states – as a result, many ecosystem and soil types are underrepresented (Fontúrbel et al., 2021). Depending on weather, topography, burn unit size, and fuel complexity, Rx fires can burn with a spatial heterogeneity which can be difficult to capture (Hiers et al., 2020). Due to these challenges, and the fact that many prescribed fires burn at low to moderate intensities which compare poorly to wildfire, our knowledge of how Rx fire impacts soil properties is incomplete.

In general, changes to soil properties from Rx fire are minor and temporary, often reverting to pre-fire state after less than one year (Alcañiz et al., 2018; Callaham et al., 2012). Most Rx fires do not burn intensely enough to change soil mineralogy, so effect on texture is negligible, however Guinto et al. (2001) reported a decrease in clay content under a 2-year fire regime. Prescribed fires may temporarily increase soil hydrophobicity (Alcañiz et al., 2018), though this is rarely reported in southeastern forest ecosystems (Callaham et al., 2012). Increases in bulk density have been recorded after Rx fire, likely due to the destruction of aggregates during soil heating. However the opposite trend has also been observed – bulk density may decrease post-fire, possibly due to an increase in OM inputs to soils (Alcañiz et al., 2018). It is typical for soils to experience a pulse of nitrogen (N) after Rx fire due to ash deposition. In some long-term studies, repeated burning resulted in reduced concentrations of plant available N (NH⁴⁺, NO³⁻) (Bell & Binkley, 1989; Hunt & Simpson, 1985). However, these nutrients can also increase after Rx fire (Augustine et al., 2014; Choromanska & DeLuca, 2001; White, 1986). In a regularly burned mixed pine-hardwood Coastal Plain forest, Gilliam (1991) reported that N volatilized during Rx fire would be re-accumulated from precipitation during the inter-burn

period. Most often no change is observed (Fontúrbel et al., 2021). Another commonly documented result of ash deposition is a temporary increase in pH from base cations (Ca²⁺, Mg²⁺, K⁺) (Alcañiz et al., 2018). Across Coastal Plain sites, pH increases after Rx fire were found to persist longer in greater percent clay soils than in sandier soils (McKee, 1982) which may lose these cations more quickly due to rapid infiltration and leaching.

The impact of Rx fire on soil organisms is severely understudied (Callaham et al., 2012; Fontúrbel et al., 2021). In general, fire can result in mortality of microorganisms, often with fast recovery (Hart et al., 2005). Because this initial die off is attributed to soil heating, low intensity Rx burns may have little direct effect on microbial communities (Kranz & Whitman, 2019). Instead, Rx fire likely shapes the soil microbiome through altered C and N cycling, which has a greater impact with increasing fire frequency (Bastias et al., 2009; Bastias et al., 2006). Choromanska and DeLuca (2001) suggested that Rx fire may help to build soil microbial resilience to wildfire. Some studies report shifts to fungal community composition with repeated burning (Brown et al., 2013; Oliver et al., 2015). Efforts are underway to determine whether a "fire-adapted microbiome" can be defined. Some "pyrophilic" microbial taxa, which increase in abundance after wildfires, have been identified (Glassman et al., 2016; Whitman et al., 2019), including those which can metabolize PyC (Fischer et al., 2021),

In general, soil fauna display resilience to Rx burns (Jacobs et al., 2015), but recover to pre-burn population levels more slowly than microorganisms (Fontúrbel et al., 2021) with postfire effects varying by taxon (Wikars & Schimmel, 2001). After a fire in a clearcut, Malmström et al. (2008) showed that depth and intensity of soil heating influenced postburn recovery of microarthropod populations. Rx fire can shape mesofauna populations indirectly by altering litter composition, which can result in population increases (Lussenhop, 1976) or

decreases (Metz & Farrier, 1973) depending on the season of burn and litter layer characteristics (Coyle et al., 2017).

1.4 Pyrogenic Carbon in Soils

The benefits of prescribed burning to Georgia's fire-adapted plant and animal communities—such as longleaf pine ecosystems—are well documented (Brockway, 1997; Diemer, 1986; Van Lear et al., 2005). Less is known about how regular, low intensity burns impact soil health parameters such organic matter (OM) composition (Alcañiz et al., 2018; Richter et al., 1982). During a fire, incomplete combustion of organic matter creates pyrogenic carbon (PyC), a range of materials from soot to charcoal (Masiello, 2004). Because PyC is typically more resistant to microbial degradation than unburned OM (Bird et al., 2015), leading to longer soil residence times, it has received considerable research focus on its capacity to act as a C-sink. But not all PyC remains in soil for as long as was once thought (Masiello, 2004). While early research suggested PyC might persist in soil for millennia (Glaser et al., 2001), growing evidence shows that most PyC cycles on centennial or even decadal time scales (Abney et al., 2019a; Bird et al., 2015).

PyC is a critical component of global soil C stocks estimated to compose an average of 14% of soil organic carbon (Reisser et al., 2016). Certain components of the global PyC cycle, such PyC concentrations in soils (Bird et al., 2015), the flux of dissolved pyrogenic carbon (dPyC) from rivers to oceans (Jaffé et al., 2013) and emissions of PyC from fires to the atmosphere as soot (van der Werf et al., 2010), have been well described, however, many pools and fluxes, particularly those connecting terrestrial and aquatic systems, have yet to be quantified (Santín et al., 2016). To understand the long-term fate of PyC in soils we must investigate its mechanisms of loss from, and stabilization within, the soil profile. In this thesis, I examine *in*-

situ leaching, decomposition, and mineral association of PyC in the soil of longleaf pine stands managed with and without prescribed fire. This will help to fill gaps in our knowledge of the PyC cycle, contributing to the knowledge base required to increase the accuracy and resolution of global C models and understand Rx fire's role in "climate smart" land management.

1.4.1 Leaching of Pyrogenic Carbon

After a fire, PyC deposited on the soil surface is subject to various mechanisms of loss. PyC is mostly lost to erosion (Abney & Berhe, 2018; Abney et al., 2019b), while a smaller portion is respired by microorganisms (Wang et al., 2015; Whitman et al., 2014a). As PyC moves vertically through the soil profile via infiltration and bioturbation, exposure to transformational processes such as chemical oxidation result in the addition of surface O- and Hcontaining functional groups, such as carboxylic structures, which increase PyC solubility and thus susceptibility to leaching (Abiven et al., 2011; Cheng et al., 2006; Schiedung et al., 2020). This environmental processing of PyC may increase its availability for chemical stabilization through mineral associations, which can promote long-term retention in soil (Brodowski et al., 2005a; Hobley, 2019). PyC leached into groundwater is eventually carried to long-term storage in marine sediments (Coppola et al., 2014). Globally, an estimated 26 Tg of PyC flows from rivers to oceans each year (Jaffé et al., 2013), which accounts for approximately 10% of riverine dissolved organic carbon (DOC). PyC in rivers is likely derived from a mixture of sources: atmospheric deposition from burning of fossil fuels, soil runoff carried via overland flow, and subsurface hydrologic transport of DOC. The relative contribution of each of these fluxes to riverine PyC has yet to be quantified (Santín et al., 2015).

PyC leaching has rarely been studied *in-situ* (Bellè et al., 2021; Major et al., 2010; Santos et al., 2017), with most studies relying on in-lab extractions or leaching simulations (Hilscher &

Knicker, 2011; Santos et al., 2022; Schiedung et al., 2020; Wozniak et al., 2020). Recent laboratory soil heating experiments showed that temperatures as low as 175 °C can destabilize soil aggregates, leading to increased DOC in water extracts (Jian et al., 2018). This may lead to increased leaching; however, it is unclear how well these in-lab extractions simulate conditions in an intact soil profile. Most PyC, including compounds isolated from marine and freshwater samples, has a chemical structure that would suggest it is insoluble (Wagner et al., 2017), and the mechanisms responsible for increasing the apparent solubility are still unknown. One hypothesis from Wagner et al. (2017) proposes that PyC may form supramolecular structures with DOM which enable molecules composed of highly condensed aromatic ring structures to enter the aqueous phase. An effort by Butnor et al. (2017) to elucidate long-term C storage in soils of longleaf pine forests across the Southeast highlighted incongruities between estimates of PyC production and PyC stocks. These authors noted that high regional precipitation suggests leaching may be an important contributor to this loss, however studies of aqueous transport in longleaf stands have yet to incorporate *in-situ* soil water sampling (Wagner et al., 2019).

1.4.2 Stabilization of Pyrogenic Carbon

Typically, PyC stability is attributed to its structure of condensed aromatic rings which require from microbes a considerable energetic investment to disassemble (Lehmann & Joseph, 2009). However, a recent paradigm shift de-emphasizes static "recalcitrant" and "labile" classifications of SOM components, including PyC (Czimczik & Masiello, 2007; Lehmann et al., 2020; Lehmann & Kleber, 2015). Currently, SOM is understood to be a heterogenous range of materials whose stability is largely conferred by mechanisms of physical and chemical protection within the soil matrix (Kleber, 2010). In a simplified system proposed by (Lavallee et al., 2020), SOM can be conceptualized into two main pools: particulate (POM) and mineral associated

(MAOM) organic matter. POM is defined as particles 53-2,000 μm in size which are less microbially processed (higher C:N), exist freely or in large aggregates, and tend to cycle on annual to decadal timescales. MAOM comprises smaller particles (< 53 μm) which have experienced substantial microbial processing (lower C:N), are more protected from microbial degradation than POM through complexation with minerals, and tend to cycle on decadal to centennial scales.

It's not entirely clear where PyC falls into the POM/MAOM concept. While inherent resistance to decomposition is likely more important in PyC than unburned SOM (Lavallee et al., 2019), variability in estimated mean residence times for PyC suggests that environmental context also plays a role (Schmidt et al., 2011). Several ¹³C labelling experiments have found that PyC may enter the MAOM within months or even days (Hilscher & Knicker, 2011; Schiedung et al., 2020; Singh et al., 2014), however the few studies which investigate PyC-mineral associations as they occur naturally in soils assign PyC to soil fractions in very different proportions (Brodowski et al., 2006; Glaser et al., 2000; Laird et al., 2008; Vasilyeva et al., 2011). The soil or ecosystem characteristics controlling this variability in PyC fractionation have yet to be identified.

1.4.3 Decomposition of Pyrogenic Carbon

The chemical nature of PyC is influenced by the starting materials from which it is formed, as well as the temperature and duration of heating (Masiello, 2004). This range of materials formed under low to progressively higher temperatures is conceptualized as the combustion continuum (Hedges et al., 2000). The heterogeneity of these materials has implications for the fate of PyC in soil. For example, a low intensity prescribed fire which pyrolyzes mostly herbaceous understory material will produce PyC with less highly ordered structures than a crown fire which burns entire trees (Czimczik & Masiello, 2007; Hedges et al.,

2000). PyC produced in the low intensity scenario may be more chemically reactive and thus susceptible to transformative processes in soils such as decomposition, chemical oxidation, physical fragmentation, and leaching (Hobley, 2019). Conversely, the crown fire PyC created at higher temperatures may be composed of more condensed aromatic structures, and thus be more chemically inert, with larger pore spaces which could increase its potential for adsorption.

Adsorbed compounds may provide PyC protection from degradation by intercepting microbial enzymes, but can also result in supramolecular structures that are more hydrophilic and thus susceptible to leaching (Keiluweit et al., 2010; Masiello, 2004). The frequency with which fire is applied to the landscape can influence the soil microbial community, potentially shaping its ability to break down PyC (Brown et al., 2013). Recent PyC incubation experiments have challenged the previous characterization of PyC as resistant to microbial decomposition (Whitman et al., 2014b); however incubation experiments may overestimate degradability (Bird et al., 2015), highlighting the need to study PyC decomposition in-situ.

CHAPTER 2

LEACHING OF PYROGENIC CARBON AFTER A PRESCRIBED FIRE

¹ Moss, A., Clabo, D., Moreland, K.C., and Abney, R.B. 2023. To be submitted to *Journal of Geophysical Research: Biogeosciences*

2.1 Abstract

Pyrogenic carbon (PyC) may be an important persistent (C) pool in forests managed with prescribed (Rx) fire, however the mechanisms of its post-fire distribution through soil remain poorly understood. We established a study in two longleaf pine stands, one managed with (Burned Stand) and one without (Unburned Stand) regular Rx fire. Lysimeters were installed immediately post-Rx fire and used to collect leachate for 14 months. Soils were separated into particulate (POM) and mineral associated (MAOM) organic matter fractions. Soil-water extractions were used to obtain dissolved organic matter (DOM). Soils, soil fractions, leachate DOM, and extract DOM were analyzed for total C, total N, δ^{13} C, and radiocarbon. Organic matter (OM) composition was characterized using mid-infrared and proton nuclear magnetic resonance spectroscopies. DOM composition differed significantly between extracts and leachate. Extract DOM was substantially younger and dominated by oxygenated functional groups characteristic of fresh OM, while leachate DOM was composed of mostly aliphatic functional groups indicating microbial byproducts and degradation-resistant plant materials. Results show that the MAOM was vertically mobile and much younger than POM, suggesting that it cycles rapidly while POM contains more persistent C. In the DOM, PyC signal was not stronger in extracts from postburn soils. An apparent spike of PyC in the Burned Stand leachate was observed ~8 months postburn, highlighting the importance of PyC "aging" for it to enter the aqueous phase. Our results suggest that in-lab extractions may not accurately recreate in-situ soil water and that OM dynamics in sandy soils may not be captured by our current MAOM/POM model. These results provide key methodological insights which can inform future studies of PyC stabilization and leaching, advancing the research necessary to close PyC cycle knowledge gaps and incorporate Rx fire management into global C models.

2.2 Introduction

2.2.1 Soil Carbon Cycling and Pyrogenic Carbon Persistence

Pyrogenic carbon (PyC) is a subset of soil organic matter (SOM), which is defined broadly as those compounds existing within or on top of soil which are of biological origin (Baldock & Broos, 2011). SOM may include plant residues, decomposing soil fauna, microbial derived compounds, root exudates, microbial biomass, and more (Kögel-Knabner & Amelung, 2014). The great variety of inputs that form SOM create a diversity of carbonaceous compounds in soil, each with its own degree of chemical reactivity and susceptibility to microbial attack (Kleber & Johnson, 2010). It was once thought that the inherent recalcitrance of certain chemical forms, referred to as humic substances, controlled SOM stability in soil however there has been a recent paradigm shift away from the humus concept (Kleber, 2010; Lehmann & Kleber, 2015). Currently, SOM is understood as a heterogenous range materials whose stability is largely conferred by mechanisms of physical and chemical protection within the soil matrix (Baldock & Skjemstad, 2000).

During a fire, incomplete combustion of organic matter (OM) creates a chemically diverse range of materials from lightly charred wood to charcoal to soot, referred to collectively as pyrogenic organic matter (PyOM) (Masiello, 2004). The terms pyrogenic carbon (PyC) or black carbon (BC) are used to refer specifically to the carbon component of PyOM. PyC is of scientific interest for several reasons, including its influence on global climate, use in radiocarbon dating, and relative resistance to decomposition (Bird et al., 2015). Once considered a chemically "recalcitrant" material that remained in soil for millennia, research over the last two decades has revealed that PyC is, in fact, susceptible to microbial decomposition (Santos et al., 2012) and that much of this material may cycle on a decadal to centennial scale (Abney & Berhe,

2018; Bird et al., 2015). PyC is a critical subset of global carbon (C) stocks, estimated to compose an average of 14% of soil organic carbon (Reisser et al., 2016). Thus, the details of its persistence in soil are of great interest for resolving carbon cycle models and informing land management strategies (Glaser, 2007).

SOM may be stabilized in soil via three major mechanisms: 1) resistance of the chemical structure to decomposition 2) physical protection within soil aggregates 3) association with soil minerals. While the role of recalcitrant humic structures in controlling SOM stability has been radically deemphasized over the last two decades, the degree to which PyC chemical structure controls its fate in soil remains unclear. For microorganisms to breakdown aromatic structures, they must produce costly oxidative enzymes in a process that is less energetically rewarding than, for example, hydrolytic cellulose degradation (Lehmann & Joseph, 2009). Organisms such as *Pyronema* fungi, which may specialize in liberating nutrients from PyC, are rare and appear to occupy a brief post-fire temporal niche (Fischer et al., 2021). Inherent resistance to decomposition is likely more important in PyC than unburned SOM, but variability estimated mean residence times for PyC suggests environmental context also plays a role (Schmidt et al., 2011).

2.2.2 The Combustion Continuum of Pyrogenic Carbon

The chemical nature of PyC is influenced by the starting materials from which it is formed, as well as the temperature and duration of heating (Masiello, 2004). This range of materials formed under low to progressively higher temperatures is conceptualized as the combustion continuum (Hedges et al., 2000). The heterogeneity of these materials has implications for the fate of PyC in soil. For example, a low intensity prescribed fire which pyrolyzes mostly herbaceous understory material will produce PyC with less highly ordered

structure than a crown fire which burns entire trees (Czimczik & Masiello, 2007; Hedges et al., 2000). PyC produced in the low intensity scenario may be more chemically reactive and thus susceptible to transformative processes in soils such as decomposition, chemical oxidations, physical fragmentation, and leaching (Hobley, 2019). Conversely, the crown fire PyC created at higher temperatures may be composed of more condensed aromatic structures, and thus be more chemically inert, with larger pore spaces which could increase its potential for adsorption.

2.2.3 Dissolution, Leaching and Stabilization of Pyrogenic Carbon in Soils

After a fire, PyC deposited on the soil surface is subject to various mechanisms of loss. PyC is mostly lost to erosion (Abney & Berhe, 2018; Abney et al., 2019b), while a smaller portion is respired by microorganisms (Wang et al., 2015; Whitman et al., 2014a). As PyC moves vertically through the soil profile via infiltration and bioturbation, exposure to transformational processes such as chemical oxidation result in the addition of surface O- and Hcontaining functional groups, such as carboxylic structures, which increase PyC solubility and thus susceptibility to leaching (Abiven et al., 2011; Cheng et al., 2006; Schiedung et al., 2020). This processing of PyC may increase its availability for chemical stabilization through mineral associations, which can promote long-term retention in soil (Brodowski et al., 2005a; Hobley, 2019). PyC leached into groundwater is eventually carried to long-term storage in marine sediments (Bird et al., 2015). Globally, an estimated 26 Tg of PyC flows from rivers to oceans each year (Jaffé et al., 2013), which accounts for approximately 10% of riverine dissolved organic carbon (DOC). PyC in rivers is likely derived from a mixture of sources: atmospheric deposition from burning of fossil fuels, soil runoff carried via overland flow, and subsurface hydrologic transport of DOC. The relative contribution of each of these fluxes to riverine PyC has yet to be quantified (Santín et al., 2015).

PyC leaching has rarely been studied *in-situ* (Bellè et al., 2021; Major et al., 2010; Santos et al., 2017), with most studies relying on in-lab extractions or leaching simulations (Hilscher & Knicker, 2011; Santos et al., 2022; Schiedung et al., 2020; Wozniak et al., 2020). Recent laboratory soil heating experiments showed that temperatures as low as 175 °C can destabilize soil aggregates, leading to increased DOC in water extracts (Jian et al., 2018). This may lead to increased leaching; however, it is unclear how well these in-lab extractions simulate conditions in an intact soil column. Most PyC, including compounds isolated from marine and freshwater samples, has a chemical structure that would suggest it is insoluble (Wagner et al., 2017), and the mechanisms responsible for increasing the apparent solubility are still unknown. One hypothesis from Wagner et al. (2017) proposes that PyC may form supramolecular structures with DOM which enable molecules composed of highly condensed aromatic ring structures to enter the aqueous phase. An effort by Butnor et al. (2017) to elucidate long-term C storage in soils of longleaf pine forests across the Southeast highlighted incongruities between estimates of PyC production and PyC stocks. These authors noted that high regional precipitation suggests leaching may be an important contributor to this loss.

Typically, PyC stability is attributed to its structure of condensed aromatic rings which require from microbes a considerable energetic investment to disassemble (Lehmann & Joseph, 2009). However, a recent paradigm shift de-emphasizes static "recalcitrant" and "labile" classifications of SOM components, including PyC (Czimczik & Masiello, 2007; Lehmann et al., 2020; Lehmann & Kleber, 2015). Currently, SOM is understood to be a heterogenous range of materials whose stability is largely conferred by mechanisms of physical and chemical protection within the soil matrix (Kleber, 2010). In a simplified system proposed by (Lavallee et al., 2020), SOM can be conceptualized into two main pools. The first pool is particulate organic matter

(POM), defined as particles 53-2,000 μm in size which are less microbially processed (higher C:N), exist freely or in large aggregates, and tend to cycle on the annual to decadal timescale. The second pool is MAOM, defined as smaller particles (< 53 μm) which have been more processed by microbes (lower C:N), are more protected from microbial degradation than POM through complexation with minerals, and tend to cycle on the decadal to centennial scale.

It's not entirely clear where PyC falls into the POM/MAOM concept. While inherent resistance to decomposition is likely more important in PyC than unburned SOM (Lavallee et al., 2019), variability in estimated mean residence times for PyC suggests that environmental context also plays a role (Schmidt et al., 2011). Several ¹³C labelling experiments have found that PyC may enter the MAOM within months or even days (Hilscher & Knicker, 2011; Schiedung et al., 2020; Singh et al., 2014), however the few studies which investigate these associations as they occur *in-situ* assign PyC to soil fractions in very different proportions (Brodowski et al., 2006; Glaser et al., 2000; Laird et al., 2008; Vasilyeva et al., 2011). The soil or ecosystem characteristics controlling this variability in PyC fractionation have yet to be identified.

To improve our understanding of the mechanisms controlling PyC persistence in soils, it is necessary to investigate those processes occurring within the soil profile which contribute to PyC loss and stabilization. Entrance into the aqueous phase is a key process which controls the ability of OM to encounter and enter stabilizing relationships with minerals (Kleber et al., 2015). Considerable uncertainty remains concerning the conditions under which PyC may enter the aqueous phase (Wagner & Jaffé, 2015). In-lab extractions have failed to recreate these conditions (Wagner et al., 2017), highlighting the need to study PyC leaching *in-situ*.

2.2.4 Study Objectives and Hypotheses

The overall objective of our study was to investigate the leaching and stabilization of OM in the soils of longleaf stands managed with Rx fire and pine straw raking, the two most common management strategies for longleaf pine in the southeastern U.S. In particular, we set out to track the vertical movement of PyC down the soil profile. We hypothesized that 1) there would be an initial spike of dPyC in the soil water immediately after Rx fire, 2) there would be a larger proportion of dPyC in the soils of a stand managed with regular broadcast fire (Burned) compared to a stand from which fire was excluded (Unburned), 3) POM would be older in the Burned than the Unburned stand, and 4) proportion of C stored as MAOM versus POM would increase with depth.

2.3 Materials & Methods

2.3.1 Southeastern Plains

Our study was conducted within the region of Georgia below the Piedmont plateau which is often generalized as the Southern Coastal Plain. This area experiences a humid subtropical climate with hot summers and mild winters. Precipitation follows a bimodal pattern, with a primary peak during the summer thunderstorm and tropical storm season and a smaller peak in early spring (Bauer et al., 2020). More specifically, the study site is located on the border between the Atlantic Southern Loam Plains (also known as the Vidalia Upland) and Tifton Upland ecoregions of the Southeastern Plains, as defined by the U.S. Environmental Protection Agency (Griffith et al., 2001). The topography at this interface is flat with gently rolling hills. Soils are poorly-consolidated sand, silt, and clay derived from Cretaceous or Tertiary-age sedimentary materials, mainly marine deposits (Lawton et al., 1976). Argillaceous sands weather to gritty, mottled soils with deposits of plinthite – a quartz and iron-oxide material found in

highly-weathered soils as a product of pedogenesis (Aide et al., 2004; Stephenson et al., 1915). Landscapes include well-drained uplands suited to cropping, poorly-drained bottomlands dominated by forest, and excessively-drained sand dunes (Griffith et al., 2001).

Before European colonization, the Southern Coastal Plain experienced frequent low-intensity fires due to the prevalence of lightning strikes (Mitchener & Parker, 2005), with anthropogenic fire expanding the spatial and temporal extent of burning (Van Lear et al., 2005). This fire regime maintained plant communities such as longleaf pine-wiregrass savannas in the uplands and longleaf pine-turkey oak (*Quercus cerris*)-sandhill rosemary (*Ceratiola ericoides*) on sand ridges. Wetter bottomlands would have been populated with mixed pine-hardwood forests with key species including loblolly pine (*Pinus taeda*), slash pine (*Pinus elliottii*) and sweetgum (*Liquidambar styraciflua*).

2.3.2 Study Site

The study site is a privately-owned 584- hectare property (Fig 2.1) near Tifton, within Tift County, GA (31.543181, -83.467122). Uplands on the property are primarily planted in longleaf-, slash-, and loblolly pine, and naturally regenerated pine-hardwood forest types are located along stream drainages. Dominant understory species include wiregrass (*Aristida stricta*), *Dicanthelium spp.*, gallberry (*Ilex glabra*), and wax myrtle (*Morella cerifera*). Much of the property was reforested after having been in row crop agriculture (e.g., peanuts, cotton, corn, sweet potato), though there are some areas of the property that were never in agricultural production including approximately 22 hectares of naturally regenerated longleaf pine. In 2011, a dam was constructed at the confluence of Middle Creek and Pine Log Creek to create Lake Henry, an approximately 150-hectare water body at the center of the property.

Tifton's mean annual precipitation is 1,212.3 mm with mean annual minimum and maximum temperatures of 12.7 °C and 25.2 °C, respectively. This rainfall follows the bimodal pattern typical of the region, with a major precipitation peak in June through August and a smaller peak in January through February. The driest months are October, November, and May, respectively. Our study was initiated in spring 2021 and concluded during summer 2022. During this time, the bimodal precipitation trend was notably more dramatic than the historic regime.

Tifton received 1,546.9 mm of precipitation in 2021, 27.6% more than the historical average, with dry months experiencing less precipitation than usual and wetter months experiencing more (Fig 2.2). Historically, the wettest month has been July, with an average of 137.9 mm of rain. In 2021, Tifton's bimodal precipitation peaks were much more intense than normal – the area received 50.1% more rain in July and 108.8% more in February than the historical average. While 2022 was slightly drier than usual, overall, Tifton still received 66.8% more rain in August and 54% more in January than in an average year. Less rain fell in May of 2021 than the historical average (–69.2%), with a similar deficit (–62.8%) in 2022. The spring of 2022 was quite dry, with much of Tift County in Moderate (D1) Drought through June (Georgia Automated Environmental Monitoring Network, 2023).

The mean maximum temperatures for 2021 and 2022 matched the historical average, while mean minimum temperatures were higher at 14.0 °C and 13.7 °C, respectively. Climatic data were obtained from the Georgia Automated Environmental Monitoring Network's Coastal Plain Experimental Station, which is located approximately 8 km west/southwest from the Brumby property (Georgia Automated Environmental Monitoring Network, 2023). Historical averages were calculated using precipitation records from 1923 to 2016.

2.3.3 Stand Descriptions

Two longleaf pine stands, referred to as the Burned and Unburned Stand, were used to compare management impacts on soil properties. Soils in each stand were described on 28 February 2022, from a 1.5 m soil core removed using a hand auger (Table 2.1). A species list for the Burned Stand (Table 2.2) was compiled by identifying understory species along a 30 m transect. Shrub and tree species were identified while characterizing fuels.

Burned Stand: This previously clearcut stand was planted with longleaf pine in 2014 and is bisected by a road, with an approximately 1.27 ha section to the east of the road and 0.85 ha section west of the road, adjacent to the lake. Our study took place in the latter section. The stand was burned during April 2018, then on 22 April 2021 (see *Prescribed Fire at the Burned Stand*) and has been managed with a 3- to 5-year fire return interval since the mid-1980's. The stand has an open canopy with diverse understory vegetation (Table 2.2), including characteristic longleaf bog ecosystem species (e.g. *Sarracenia flava*) occupying wetter areas and more upland locations populated by longleaf savanna species such as wiregrass (*Aristida stricta*), savanna meadow beauty (*Rhexia alifanus*), and toothache grass (*Ctenium aromaticum*). Soils are Cowarts series (fine-loamy, kaolinitic, thermic Typic Kanhapludults) with textures: loamy sand (0-10 cm), loamy clay sand (10-23 cm), sandy clay loam (23-30 cm), sandy clay (30-122 cm), and sandy clay/loamy sand (122-152+ cm) (Williford, 2022). Soil chromatic evidence of a water table begins at approximately 74 cm.

<u>Unburned Stand:</u> This approximately 1.16 ha stand was in agricultural production for at least 30 years prior to establishment, with cotton and peanuts in the crop rotation. Longleaf pine was planted at 1,495 trees ha⁻¹ during 2004 through the United States Department of Agriculture, Farm Service Agency's Conservation Reserve CP36 Program (CRP). The most recent broadcast

burn was conducted for site preparation in fall 2003. The canopy is closed with minimal understory vegetation. Herbaceous vegetation within canopy gaps is treated periodically with herbicide to maintain weed-free conditions for pine straw harvest, which occurs annually in the winter or early spring. Small, randomly-spaced slash piles are burned as part of the raking process. This stand is located along the northern shore of Lake Henry. Trees within 10 m of the lake sustained damage during October 2018 during hurricane Michael. Soils are Dothan series (fine-loamy, kaolinitic, thermic Plinthic Kandiudults) with textures: loamy sand (0-33 cm), sandy loam (33-51 cm), sandy loam/sandy clay loam (51-71 cm), sandy clay loam (71-152+ cm) (Williford, 2022). Soil chromatic evidence of a water table begins at 122 cm; however, water is consistently observed filling holes at 30 cm or higher, suggesting that establishment of Lake Henry has altered groundwater hydrology in this stand.

2.3.4 Prescribed Fire in the Burned Stand

An approximately 27-hectare prescribed fire was conducted in the Burned Stand along with an adjacent stand of mature, open canopy longleaf pine (Mature Stand), on 22 April 2021. A pre-fire vegetation survey was completed on 30 March 2021, to create an estimate of woody stem densities and an herbaceous vegetation species list. To determine overstory structure, two 1/40-hectacre plots were established in the Burned Stand. Within these plots, species, height, and diameter at breast height (DBH) were recorded for all trees with DBH greater than 1.2 cm. These values were used to calculate average stem count, height, and DBH per hectare for each species (Table 2.3). To characterize shrub density in the Burned Stand, two 1/400-hectare plots were established. Shrubs were identified to either species or genus and individuals of each taxon were tallied within four height classes (Tables 2.4a and 2.4b).

Before the prescribed fire, one 12 m x 12 m plot was established in each stand to contain a 4 x 4 grid of lysimeters. Hereafter, these plots will be referred to as lysimeter plots within the Burned Stand (Fig. 2.3) and the Unburned Stand. Herbaceous vegetation was sampled to determine fuel loads in the Burned Stand at 0800h on the morning of the fire, approximately one hour before ignition. Aboveground biomass was harvested within four 0.25 m² quadrats, each located approximately 3 m from one side of the lysimeter plot (Fig 2.3). Biomass was stored in sealed plastic bags, then dried in an oven at 60 °C for 26 h until a constant weight was reached. The moisture content of herbaceous vegetation on the morning of the burn averaged 35.60%, with fuel loading of 5.54 MT/ha (Table 2.5).

To monitor soil heating temperature and duration, a CR1000 datalogger (Campbell Scientific, Logan, UT, USA) fitted with five type K thermocouples was installed on the east-southeast side of the lysimeter array (planned direction of approach for the flanking fire) (Fig 2.3). Thermocouple wires were secured in the ground with a staple made of medium gauge steel wire, then buried under approximately 1 mm of soil. Thermocouple probes were left exposed at the soil surface. To protect temperature-sensitive equipment while minimizing disruption to both fuel continuity and soils within the leaching study area, a hole was dug in a relatively bare spot between wiregrass clumps outside the lysimeter array (Fig. 2.3). The datalogger placed in a plastic tub and buried inside the hole for the duration of the Rx fire.

Pre-fire weather conditions were obtained from the Georgia Automated Environmental Monitoring Network's Coastal Plain Experimental Station. Weather conditions during the prescribed fire were monitored using a Kestrel weather meter (Kestrel Instruments, Boothwyn, PA, USA). Temperature, in-stand wind speed, wind direction, dew point, humidity, and barometric pressure were recorded at beginning (0910h), middle one (1110h), middle two

(1220h) and end (1311h) time points. Open wind speed was recorded at the beginning and end time points.

Atmospheric conditions were relatively dry in the weeks leading up to the prescribed fire. Tifton received 11.2 mm of rain during the first three weeks of April 2021, with the last precipitation events before the fire being 1.8 and 0.5 mm of rain on 17 April and 18 April, respectively. On the day of the fire, in-stand wind speeds were between 1.3 and 9.7 kilometers per hour (Table 2.6).

A backing fire was ignited at approximately 0900h by walking a drip torch along the southwestern perimeter of the Mature Stand. Once the back line was secured, flanking fire was ignited in strips while walking north along the southeast perimeter. A second flanking fire was ignited in the same direction along the edge of the lake (Fig. 2.1). During the burn, wind direction shifted between N and NE – one such change from N to N-NE at around 1300h caused the southeast flanking fire to turn into a head fire and move more quickly over the lysimeter plot than anticipated. The atmospheric temperature at ignition was 11.9 °C and humidity was 36.0%. By the fire's end at 1311h, the temperature had risen to 22.0 °C and humidity had dropped to 22.4%.

Soil heating results are presented in Figure 2.4. The duration of soil heating was brief—all thermocouples experienced a temperature spike then returned to their baseline within three minutes. Temperature spikes recorded by the datalogger as the head fire passed over the thermocouples were quite variable. Thermocouple 1 recorded the highest maximum temperature of 809 °C, followed by Thermocouple 3, which reached 412.4 °C. The other three thermocouples recorded less intense heating, from 218.2 °C to 278.5 °C).

2.3.5 Soil Sampling & Preparation

Four soil cores were collected adjacent to each lysimeter plot (Fig 2.3) by brushing aside the organic layer and using a hand auger to remove soils at three depths: 0-10 cm, 10-20 cm, and 20-30 cm. Soils were collected at two time points in the Unburned Stand: 22 April 2021 and March 29, 2022 (referred to as Unburned and 11-month Unburned, respectively) and three time points in the Burned Stand: 21 April 2021; 22 April 2021; and 29 March 2022 (referred to as Preburn, Postburn, and 11-month Postburn, respectively). Sampled soils were stored in Ziploc bags in a cooler with ice before they were transferred to a 4 °C refrigerator, then air dried on the lab bench. Once dry, soils were passed through a 2-mm sieve. A subsample of each soil was ground in a mixer mill for 12 minutes. Pieces of charcoal greater than 2 mm were removed during sieving and stored in tight-lidded plastic petri dishes. Bulk density cores were collected from the soil surface adjacent to the soil cores using a 5.5 cm diameter brass cylinder before the Rx fire (Preburn samples) and after (Postburn samples) (Fig. 2.3). Weights were recorded after drying in an oven at 105 °C and until a stable weight was reached.

2.3.6 Soil Separation into Mineral associated- and Particulate Organic Matter

A small subset of bulk soils (*n*=4; Burned Core A 0-10 cm and 20-30 cm and Unburned Core at 0-10 and 20-30 cm) were size separated into mineral associated- (MAOM) and particulate organic matter (POM) fractions using the definitions proposed by Lavallee et al. (2020). For each sample, soil aggregates were dispersed by filling two Falcon tubes with 18 g of bulk soil and 36 mL of 0.5% sodium hexametaphosphate solution, then agitated on an oscillating shaker at 325 RPM for 20 hours (Cotrufo et al., 2019). Samples were then wet-sieved through a 0.53 μm sieve using Milli-Q type II pure water (MilliporeSigma, Burlington, MA, USA) and collected in acid-washed glass beakers. The fraction which passed through the sieve (<0.53 μm)

is considered MAOM, while the fraction collected on the sieve (>0.53 μ m) is POM. Beakers were placed in a drying oven at 60 °C until all liquid evaporated, and samples reached a consistent weight. Both fractions were ground in a mixer mill for 12 minutes and stored in glass scintillation vials.

2.3.7 Lysimeter Installation & Sampling

In both lysimeter plots, tension lysimeters (Soil Moisture Equipment Corp., Goleta, CA, USA) were installed at a depth of 30 cm in four positions down a hillslope adjacent to the lake. Slope in the Burned Stand was 3% and the Unburned Stand was <1%. This was replicated four times perpendicular to the slope, creating a grid of sixteen lysimeters (Fig. 2.3). Lysimeters were installed in both plots on the afternoon of 22 April 2021, immediately after the prescribed burn in the Burned Stand.

Lysimeters were sampled at 1-week, 2-month, 3-month, 4-month, 8-month, and 14-month post-burn time points, with the first collection occurring on 30 April 2021 and the final collection occurring on 16 June 2022. In between samplings, lysimeters were not under tension. Sampling occurred within 24-48 hours of a precipitation even (except for the 30 April sampling, which was 6 days after a major storm) and tension was applied immediately prior to collection. Soil-water was drawn through polyethylene tubing into a plastic syringe, then emptied into acid-washed 250 mL Nalgene bottles and stored on ice in a cooler until it could be transferred to a 4 °C walk-in cooler (approximately 8 hours).

2.3.8 Pyrogenic Carbon Production

Pyrogenic carbon was produced in-lab for use as a reference in spectroscopic analyses.

Longleaf pine needles and birch wood popsicle sticks were trimmed to ~2 cm pieces. Wide-form porcelain crucibles (Fisher Scientific, Waltham, MA, USA) were filled to approximately two-

thirds of 250 mL capacity with either 60 g wood or 15 g pine needle pieces. Crucibles were tightly enclosed with aluminum foil to minimize airflow and pyrolyzed in a muffle furnace at 350 °C for 1 hour, simulating a low-intensity fire (Abney et al., 2019a; Majidzadeh et al., 2015). Samples will be referred to as "pine needle PyC" and "wood PyC", respectively. A portion of each PyC type, along with unburned longleaf pine needles were ground in a mixer mill for 12 minutes. The unburned pine needles were dried in an oven for 24 hours at 60 °C to facilitate grinding.

2.3.9 Dissolved Organic Matter Preparation

Leachate samples were filtered within seven days of collection using $0.7~\mu m$ Whatman GF/F filters, stored in acid-washed 50~mL Falcon tubes at $-20^{\circ}C$, and lyophilized to isolate DOM. The DOM originating from these lysimeter samples will be referred to as "leachate DOM."

To obtain soil water extractable organic matter (WEOM) for spectroscopic characterization, 18 g of soil from each bulk soil sample was added to an acid-washed 50-mL Falcon tube with 36 mL Milli-Q water and agitated on an oscillating shaker at 425 RPM for 1 hr. The soil-water suspensions were then centrifuged at 10,000 x g for 15 min. The supernatant was poured off centrifuged samples, filtered, and lyophilized. To generate a mass of WEOM sufficient for radiocarbon analysis, 45 g of soil from each Core (A, C, F, H; Fig. 2.3) at two depths (0-10 and 20-30 cm) for Burned and Unburned samples was homogenized for a total of 180 g soil and 360 mL water per extraction.

Water extractable organic matter was isolated from ~2 cm pieces of unburned pine needles, pine needle PyC, and wood PyC. For each reference OM type, 1.5 g of material was added to an acid-washed 50-mL Falcon tube with 30 mL Milli-Q water and agitated on an

oscillating shaker at 425 RPM for 1 hr. Samples were centrifuged, filtered, and lyophilized as described above. Lyophilized WEOM from soil and reference OM extractions will be referred to as "extract DOM."

2.3.10 Bulk Soil Analysis

Bulk density was determined by weighing oven-dried soil cores and dividing the dry mass of soil by the volume of the 5.5 cm diameter, 3 cm tall soil core. Bulk cores were prepared by removing coarse roots and rocks. For all soil core samples, pH was quantified at a 1:1 ratio in both water Milli-q ultrapure (H₂O) and 0.01M calcium chloride (CaCl₂) solution using a Fisherbrand accumet AB200 pH/Conductivity meter (Fisher Scientific, Pittsburgh, PA, USA). Particle size distribution was assessed using the hydrometer method (Bouyoucos, 1962).

2.3.11 Soil Organic Matter Characterization

All ground soil samples (n=52) and the soil fractions (n=8) were sent to University of New Mexico Center for Stable Isotopes for total C, total N, and δ ¹³C analysis. Two analytical replicates were prepared for all ground soil and soil fraction samples by rolling 8-12 mg of material in each tin capsule (Costech Technologies, Montréal, Quebec, CA). Two analytical replicates were prepared for leachate DOM when possible. Total C/N and isotope ratios were measured by Elemental Analyzer Continuous Flow Isotope Ratio Mass Spectrometry using a Costech ECS 4010 Elemental Analyzer (Costech, Technologies, Montréal, Quebec, CA) coupled to a ThermoFisher Scientific Delta V Advantage mass spectrometer via a CONFLO IV interface (ThermoFisher Scientific, Waltham, MA, USA). A representative subset of soils was screened for carbonates using 1M hydrogen peroxide. No effervescence was detected, indicating that soils would not need to be treated to remove carbonates. These results were corroborated with the

Natural Resources Conservation Service (NRCS) Web Soil Survey, which reports no carbonates in soils within the study area (Soil Survey Staff).

The soil fractions (*n*=8) as well as subsets of leachate DOM (*n*=4), charcoal (*n*=4), and extract DOM (*n*=4) were analyzed for radiocarbon at Lawrence Livermore National Laboratory Center for Accelerator Mass Spectrometry. The charcoal samples were isolated from the same soil cores from which the soil fractions were derived (Burned Core A 0-10 cm and 20-30 cm and Unburned Core at 0-10 and 20-30 cm). Due to low organic matter content, more soil was required to extract sufficient DOM for radiocarbon analysis than was feasible to use from Core A. Thus, soils were pooled as described in *Section 2.3.8: Dissolved Organic Matter Preparation*, then extracted. Charcoal samples were pre-treated using the acid-base-acid extraction to remove adsorbed organic material (Rebollo et al., 2016). All other samples were untreated since there was no detection of inorganic carbon using pH, and 1M hydrochloric acid tests.

Radiocarbon (Δ^{14} C) analyses were conducted on samples after sealed-tube combustion of organic carbon (Broek et al., 2021) to carbon dioxide (with CuO and Ag) that was then reduced onto Fe powder in the presence of H₂ (Vogel et al., 1984). Radiocarbon values were measured in 2022 on the National Electrostatic Corporation (NEC) 1 MV Pelletron tandem accelerator at the Center for Accelerator Mass Spectrometry at the Lawrence Livermore National Laboratory (Broek et al., 2021). Radiocarbon isotopic values were corrected for mass-dependent fractionation with measured δ^{13} C values and were reported in Δ -notation corrected for 14 C decay since 1950 (Stuiver & Polach, 1977).

Organic matter composition of soil samples (n=52), soil fractions (n=8), PyC (n=2), and unburned longleaf pine needle (n=1) were spectroscopically characterized using a Thermo Scientific Nicolet iS10 FT-IR Spectrometer (ThermoFisher Scientific, Waltham, MA, USA)

operated with OMNIC Series Software (ThermoFisher Scientific, Waltham, MA, USA). Ground samples were placed in a drying oven at 60 °C for 48 hours to ensure dehydration before analysis. Samples were run using a diffuse reflectance infrared Fourier transform (DRIFTS) experiment at a resolution of 4. Absorbance was measured between 4000 and 400 cm⁻¹ with an aperture of 4 mm; 64 scans were performed and averaged. A background was run every 120 min using spectroscopy-grade potassium bromide (KBr) and used for atmospheric baseline correction. Spectra from a subset of samples were visualized in R. Peaks were assigned by consulting previous mid-IR analyses of soil, biochar, and plant root samples (Calderón et al., 2011; Hall et al., 2018; Keiluweit et al., 2010; Parikh et al., 2014; Strakova et al., 2020).

2.3.12 Dissolved Organic Matter Characterization

Dissolved organic matter composition of all leachate and extract samples was characterized using solution-state proton magnetic resonance spectroscopy (¹H NMR) at the University of Georgia Complex Carbohydrate Research Center. To reduce water content in samples, leachate and extract DOM was suspended in deuterium oxide (D₂O), re-lyophilized, and stored in a glass scintillation vial. Prior to analysis, DOM was re-suspended in D₂O and spun in a microcentrifuge at 5000 RPM for 1 minute. Approximately 600 µL of supernatant was removed and pipetted into a 5 mm tube NMR fitted with a Bruker SampleJet compatible cap (SP Wilmad-LabGlass, Vineland, NJ, USA).

Samples were run on the Bruker 600 MHZ Avance III spectrometer running Topspin 3.6.4 (Bruker Corporation, Billerica, MA, USA) and fitted with a 5 mm cryoprobe and SampleJet autosampler. Spectra were recorded using the 1D NOESY pulse sequence with presaturation (noesygppr1d) at 472 scans with 4 s acquisition time and 4 s relaxation delay. Spectra were manually phase corrected and subjected to the Whittaker Smoother baseline

correction in Mnova (Mestrelab Research, Santiago, Spain), then integrated into five regions, adapted from Santos et al. (2016): aliphatic (0.0-1.9 ppm), functionalized aliphatic (1.9-3.1 ppm), oxygenated (3.1-4.6 ppm), unsaturated (4.9-7.0), and aromatic (7.0-10.0 ppm). The proportion of the whole spectrum for which the integral for each region of interest composed was calculated and interpreted as percent of carbon structures in the total sample. Due to extremely low signal in the unsaturated region, integral values for some leachate samples were made slightly negative (the most negative unsaturated proportion was -0.23%), by the base correction. For these samples, the absolute value for the unsaturated region was corrected to zero, and proportions were recalculated post-correction. Lack of peaks in the unsaturated region of the leachate but not extract samples may indicate that unsaturated structures do not exist in leachate in concentrations within our detection threshold. It is also possible that signal interference due to the presence of minerals (e.g. iron) within the soil solution has suppressed peaks in this region.

2.3.13 Statistical Analysis

Total carbon, total nitrogen, C:N ratio, δ^{13} C, and pH were analyzed for differences across treatment groups using mixed linear effects models run with the lmer() function in the lme4 package (Bates et al., 2015). We included burn status, depth, and collection date as fixed effects with and without the interaction between burn status and depth. Aikake information criterion (AIC) was calculated for models with and without interaction using the aictab() function in the AICcmodavg package (Mazerolle, 2023), and the model with lowest AIC was selected. Each soil core's ID was included in the model as a random effect.

Because the Postburn treatment existed only in 0-10 cm samples from April 2021 collection, this treatment was excluded from the primary models. For each response variable (percent C, percent N, C:N ratio, δ^{13} C, pH in H₂O, and pH in CaCl₂), a one-way ANOVA was

run for April 2021 topsoil samples only using the lm() function in the cars package (Fox & Weisberg, 2019). To test for significant differences between the Burned and Postburn treatments, pairwise comparisons were conducted using the Sidak method via the emmeans() function in the emmeans package (Lenth, 2022). The effect of burn status on bulk density was analyzed using a one-way ANOVA with pairwise comparisons as previously described.

Aromatic, oxygenated, functionalized aliphatic, and aliphatic proportions were analyzed for differences across treatment groups using separate mixed linear effects models for leachate and extract samples. No models were run for the unsaturated proportion of leachate DOM due to extremely small and many corrected to zero values, however the unsaturated proportion of extract DOM was analyzed.

Leachate only models were run using burn status and collection date as fixed effects both with and without interaction and models were selected using AIC as described above. Leachate models for all functional groups had a better fit (lower AIC) without the interaction term. Each lysimeter's ID was included as a random effect to account for repeated measurements.

Extract samples were analyzed using burn status, depth, and collection date as fixed effects, with and without interaction of burn status and depth and models were selected using AIC as described above. Extract models for all functional groups had a better fit (lower AIC) when the interaction between burn status and depth was included. Each soil core's ID was included in this model as a random effect. Because the Postburn treatment was only collected in topsoil (0-10 cm) samples from April 2021, these samples were excluded from the primary extract models. As described above, one-way ANOVAs were run and pairwise comparisons were conducted to test for significant differences between Burned and Postburn treatments.

To analyze the influence of sample type on DOM composition, two-way ANOVAs were run to analyze the influence of burn status, sample type, and their interaction for each functional group (aromatic, oxygenated, functionalized aliphatic, and aliphatic proportions) in leachate and 20-30 cm extract samples, both collected in April 2021. Pairwise comparisons were assessed using the emmeans() function as described above.

Data were collected in either a lab notebook (lab experiments) or data sheet (field experiments) then organized and archived in Microsoft Excel. Statistical analysis and data visualizations were completed in R version 4.2.0 (R Core Team, 2020) using the ggplot2 package (Wickham, 2016). For all models, significance was quantified using a likelihood ratio test: for each variable of interest, a null model was constructed which excluded that variable, then testing the significance of the null model when compared to the full model using the anova() function. No statistical analysis was run on radiocarbon data or soil fractions due to the lack of sample replication.

2.4 Results

2.4.1 Bulk Soil Analysis

Soil physical and chemical characteristics are summarized in Table 2.7. Topsoil bulk density was lower in the Burned Stand than in the Unburned Stand, though this difference was not statistically significant ($F_{2,9} = 3.747$, p = 0.065). Bulk density in the Burned Stand was unchanged by Rx fire (p = 0.93). For full model results see Appendix A, Figure A.13.

Soils were acidic, with pH values ranging from 4.05 to 5.19 in H_2O and 3.63 to 4.83 in $CaCl_2$. Contrary to frequently reported trends after both wildfire and Rx fires (Alcañiz et al., 2018; Gonzalez-Perez et al., 2004), topsoil pH in the Burned Stand decreased after the Rx fire. This effect was significant for pH measured in H_2O (p = 0.0004), but not for pH measured in

CaCl₂ (p=0.08). Though topsoil pH did not differ significantly between the Burned and Unburned Stand, a trend of lower pH in the Burned Stand became significant for both pH in H₂O (χ^2 (1) = 8.117, p=0.004) and CaCl₂ (χ^2 (1) = 40.789, p<0.0001), as pH declined with depth in Burned Stand soils but increased in those from the Unburned Stand. *For full model results see Appendix A, Figures A.5, A.6, A.11, and A.12*.

Soil texture in the Burned Stand was determined by particle size distribution as sandy loam at 0-10 and 10-20 cm and sandy clay loam at 20-30 cm. Soils at all depths in the Unburned Stand were sandy loam. There was no difference in soil texture between the April 2021 and March 2022 sampling dates or in samples collected before and after the Rx fire.

2.4.2 Soil Organic Matter Characterization

Organic matter concentrations were low in both the Burned and Unburned Stand (Fig. 2.5). Carbon concentrations in Burned Stand 0-10 cm soils were higher (χ^2 (1) = 5.027, p = 0.02), ranging from 1.3% in April 2021 to 1.4% March 2022, while Unburned Stand 0-10 cm soils experienced an increase of 0.8% to 1.3%. A similar trend was displayed in N concentrations, which increased significantly (χ^2 (1) = 6.810, p = 0.009) in Unburned Stand 0-10 cm soils, from 0.04% in April 2021 to 0.07% in March 2022 and were significantly (χ^2 (1) = 7.112, p = 0.007) higher in the Burned Stand (0.07% to 0.08%). There was no significant change to C and N concentrations in the Burned stand 0-10 cm soils after the Rx fire (p < 0.93 and 0.89, respectively). Both C and N declined significantly with depth (χ^2 (1) = 89.366, p < 0.0001; χ^2 (1) = 68.029, p < 0.0001).

There was a significant influence of both depth (χ^2 (1) = 102.6, p < 0.0001) and burn status (χ^2 (1) = 43.751, p < 0.0001) on δ^{13} C isotope values (Fig. 2.5). In April 2021, 0-10 cm soils from the Burned Stand collected in April 2021 were depleted in 13 C (-24.4 %) compared to

soils collected at 20-30 cm (-24.1 ‰). Carbon-13 values in Unburned Stand soils were depleted when compared to the Burned Stand, but showed the same trend with depth: δ^{13} C was -25.9 ‰ in 0-10 cm soils and -24.5 ‰ at 20-30 cm. Though our model did not find the effect of collection date statistically significant, it is notable that during March 2022, δ^{13} C decreased to -26.6‰ in Unburned Stand 0-10 cm soils. There was no significant difference in 13 C values for 0-10 cm soils collected before and after the Rx fire (p = 0.58). *For full model results see Appendix A, Figures A.1 through A.4 and A7 through A.10*.

Properties of soil fractions are summarized in Table 2.8. Across all samples, about 70% of soil mass separated into the POM fraction and about 30% separated into the MAOM. Due to the low OM content of these soils, N was below the detection limit for all POM except that isolated from the Burned Stand at 0-10 cm. For soils collected at 0-10 cm, the MAOM fraction was 2.75 times more C-rich than the POM in both Burned and Unburned Stand soils. This trend was more pronounced, with 20-30 cm the MAOM fractions 9 times more C-rich in the Burned and 6 times more C-rich in the Unburned Stand (Fig. 2.6). Carbon to nitrogen ratios were much lower in the MAOM fractions (12.7-13.9) than in the Burned topsoil POM (28.1). The δ^{13} C isotopic values did not differ between fractions at 0-10 cm, but Burned and Unburned plot 20-30 cm POM fractions were ~2\% lighter than their MAOM counterparts, suggesting POM that was less microbially processed. Following the trend observed in bulk soil, δ^{13} C values were ~1% higher in Burned versus Unburned Stand fractions at both depths – this may indicate elevated decomposition in Burned Stand soils, but could also be the influence of C₄ grasses, primarily wiregrass, which have a higher δ^{13} C isotopic signature than C₃ grasses and forbs (Cerling et al., 1997).

In general, samples from the Unburned Stand had a lower Δ ¹⁴C values than those from the Burned Stand indicating the Burned Stand had more newly fixed C compared to the Unburned Stand (Fig. 2.7). The Δ ¹⁴C values were lower with depth indicating older, deep carbon (Fig 2.7). Charcoal samples were an exception to this trend, with Δ ¹⁴C values only 5.7 per mil lower in Burned and 1.8 per mil lower in Unburned Stands from 0-10 cm to 20-30 cm, suggesting the pieces of charcoal we sampled from both depths may have been created at the same time, possibly from roots smoldering down through the soil profile. In both stands, POM samples had lower Δ ¹⁴C values than MAOM samples, indicating that in these soils, more persistent SOM exists in the POM fraction. At 20-30 cm, Unburned Stand POM Δ ¹⁴C was - 128.3 per mil, indicating it is substantially older than Burned Stands POM at the same depth, which had a Δ ¹⁴C value of -66.0 per mil. The same relationship could be seen at 0-10 cm where the Δ ¹⁴C value of POM in the Unburned Stand was -45.7 per mil compared to 16.4 in the Burned Stand. All MAOM samples, as well as POM from Burned Stand topsoil, had Δ ¹⁴C values which reflect a modern origin.

Extract Δ^{14} C values indicated modern C both in the topsoil and at depth, suggesting this is a fast-cycling and highly mobile OM pool. Leachate samples had much lower Δ^{14} C values than Extracts, indicating they are older and cycling on a centennial timescale. Following the trend we see in the POM, leachate DOM Δ^{14} C was much lower in the Unburned (-100 per mil), compared to the Burned Stand (-50 per mil).

To facilitate qualitative comparison between soil and soil fractions, absorption spectra from a small subset of soils and soil fractions were plotted (Fig. 2.8) along with spectra from dried longleaf pine needle (PN), longleaf pine needle PyC (PN PyC), and birch popsicle stick PyC (W PyC). The spectrum from a Burned Stand soil collected at 20-30 cm (Soil-9) is depicted

alongside its mineral associated (MAOM-9) and particulate (POM-9) organic matter fractions. The spectrum for a second soil from the Burned Stand (Soil-12) was included because it contains a higher clay content (28.2%, compared to 16.2% in Soil-9) which allows us to see the influence of soil texture on specific mid-infrared regions.

Peaks at 3700 and 3625 cm⁻¹ are associated with stretching of free alcoholic and phenolic hydroxyl O-H (Fig. 2.8), including O-H stretching of hydroxyl groups in clay (Nguyen et al., 1991), in particular kaolinite (Guillou et al., 2015). These peaks are absent in the pine needle sample but present as a small shoulder on the larger intermolecular O-H peak in the PyC and POM samples. The free O-H peaks are largest in the higher-clay soil and sharpest in the MAOM. From 3200-3600 cm⁻¹ there is a broad peak created by intermolecularly bonded O-H and N-H stretching (Parikh et al., 2014) which has greatest absorption in the fresh pine needle sample – this peak can be observed to decrease substantially with charring as O-containing plant materials like cellulose are transformed by dehydration. In the soil and soil fractions, this broad peak is largest in the MAOM, then smaller in the higher-clay soil (12), lower-clay soil (9), and POM, respectively. Peaks at 2931 and 2854 cm⁻¹, which are associated with asymmetric and symmetric aliphatic C-H stretching, respectively, are barely visible in soil samples but large in the pine needle (Hall et al., 2018). There is a reduction in aliphatic peak absorbance from uncharred to charred pine needles (PN PyC), another indication that cellulose-associated functional groups are destroyed with charring (Keiluweit et al., 2010).

A series of three peaks between 1790 and 2000 cm⁻¹, commonly associated with quartz overtones from sand, is most prominent in the POM and lower-clay soil, followed by the higher-clay soil and MAOM, respectively (Calderón et al., 2011; Nguyen et al., 1991). Logically, these quartz peaks are absent in the OM references. The peak presenting at 1684 cm⁻¹ in soil and soil

fractions, 1733 cm⁻¹ in pine needles, and 1710 cm⁻¹ in PyC samples was interpreted as carboxylic acid C=O (Calderón et al., 2011; Strakova et al., 2020) with possible contribution from C=O stretching in aldehydes and ketones. The peak at 1610 cm⁻¹ interpreted variously as aromatic C=C, carboxylate C=O, and some combination of the two (Calderón et al., 2011; Kaiser et al., 2012). Some studies also assign conjugated carbonyl C-O, ketone C=O, and aromatic C-H deformations to this region (Parikh et al., 2014). Among our samples, this peak is sharper and more prominent in samples composed of more lignified or charred OM (e.g., POM, pine needle and wood PyC), suggesting aromatic functional groups are the largest contributors. A second peak associated with aromatic C=C was identified at 1513 cm⁻¹. This peak was sharpest in the pine needle and shrunk with charring, consistent with studies where it has been assigned in particular to lignin (Parikh et al., 2014). In a study by Calderón et al. (2013) charring of corn stover reduced absorbance in this region from a sharp peak in fresh material to no peak in biochar pyrolyzed at 500 °C. Modelling approaches consider a decrease in this area relative to other aromatic regions to indicate increasing PyC content (Chatterjee et al., 2012).

Two peaks associated with amides suggest microbial biomass such chitin, a major component of fungal cell walls, (Andrade et al., 2004) and microbial proteins. A small peak at 1550 cm⁻¹, most prominent in the MAOM sample, is commonly attributed to amide II N-H bending and C-N stretching (Parikh et al., 2014). A corresponding peak at 1641 cm⁻¹, which is associated with amide I C=O stretching, appears to be present in the MAOM but is affected by a deformation from clay which occurs in the same region. This peak can be seen in the soil samples as a small, rounded shoulder on the larger peak at 1610 cm⁻¹. The contribution of clay can be seen by comparing this region in the lower-clay to the higher-clay sample. The large peak at 1360 cm⁻¹ in POM and bulk soil and 1320 cm⁻¹ in MAOM is attributed mainly to C-O from

carboxylate and phenolic groups, with contributions from ester C-O and aliphatic C-H. This peak is sharper in POM and lower % clay soil. The shift of the MAOM peak, 1320 cm⁻¹, may indicate a larger relative contribution from ester and aliphatic groups (Parikh et al., 2014). Another explanation is that the 1320 cm⁻¹ peak represents an amide III band, with the C=O peak appearing as a gradually sloping shoulder at 1360 cm⁻¹ (Calderón et al., 2013). This is the most prominent peak in soil and soil fraction samples but is not present in PyC and appears as a small peak at ~1370 cm⁻¹ in the pine needle.

The region from about 1190 to 1000 cm⁻¹, frequently associated with C-O-C esters and aliphatic O-H groups indicative of cellulose, hemicellulose, and other polysaccharides (Keiluweit et al., 2010; Parikh et al., 2014), is prominent in the pine needle sample as a broad and complex series of peaks that do not exist in the soils or soil fractions. This region becomes more flattened in the pine needle PyC as fresh plant components are transformed during pyrolysis. A series of peaks at from 885 to 752 cm⁻¹ are associated with aromatic C-H out of plane aromatic deformations, where degree of substitution decreases with decreasing wavenumber (Keiluweit et al., 2010; Parikh et al., 2014). However the sharp, tall peak at 813 cm⁻¹ followed by two smaller peaks at, 792, and 722 cm⁻¹ seen in soil and soil fractions closely resembles an absorbance pattern indicating O-Si-O bonds in quartz (Calderón et al., 2013; Guillou et al., 2015). If the smaller aryl C-H peak we see in pine needle and biochar samples are present in soils, they are obscured by, or incorporated into, the stronger signal from quartz. Keiluweit et al. (2010) speculated that peaks near 815 and 750 cm⁻¹ in biochar spectra indicate O-containing aromatic structures such as quinones. A small, sharp peak at 672 cm⁻¹, which is most prominent in the POM and whole soil, can be attributed to alcohol O-H out of plane bending (Parikh et al., 2014)

and is also attributed to O-Si-O bands (Guillou et al., 2015). This peak has also been identified in biochar but is not present in our lab produced PyC samples (Parikh et al., 2014).

2.4.3 Dissolved Organic Matter Characterization

Aromatic proportion ranged from 1.25 to 7.44% of leachate DOM and was larger in the Burned Stand than the Unburned Stand for all collections except for the final (June 2022) sampling, when this trend reversed (Fig. 2.10). The effect of burn treatment was not significant (χ^2 (1) = 1.441, p = 0.23), however the effect of collection date was (χ^2 (1) = 8.1445, p = 0.004). The oxygenated proportion ranged from 4.89 to 20.30% of leachate DOM and also differed significantly by collection date (χ^2 (1) = 0.7745, p = 0.38), but not between Burned and Unburned Stands (χ^2 (1) = 4.968, p = 0.02). Functionalized aliphatic proportion ranged from 4.64 to 9.92% throughout most of the sampling period and did not change significantly over time (χ^2 (1) = 2.317, p = 0.12), but was significantly higher in the Burned than the Unburned Stand (χ^2 (1) = 5.661, p = 0.02) likely due to a sharp increase to 17.65% of DOM during the June 2022 sampling. Aliphatic functional groups were the largest contributor to leachate, composing a range from 62.77 to 83.26% of DOM, a proportion which was significantly higher in the Unburned than in the Burned Stand (χ^2 (1) = 4.413, p = 0.04). For full model results see Appendix A, Figures A.14 through A.17.

Dissolved organic matter composition in Burned and Unburned Stand extracts showed opposite trends down the soil profile for all functional groups besides functionalized aliphatic (Fig. 2.9). The proportion of aromatic functional groups in extract DOM was significantly influenced by depth (χ^2 (2) = 18.623, p < 0.0001) and burn status (χ^2 (2) = 19.609, p < 0.0001). For example, for extracts from April 2021 soils, Unburned Stand aromatic proportion increased from 0.66% at 0-10 cm to 3.34% at 20-30 cm while Burned stand aromatic proportion decreased

from 1.11 at 0-10 cm to 0.69% in 20-30 cm. There was no increase in aromatic proportion of extract DOM from Burned Stand 0-10 cm soils collected after the Rx fire, in fact this value decreased, nonsignificantly, to 0.75% (p=0.82). The aliphatic proportion of extract DOM followed a similar trend. The Unburned Stand aliphatic proportion increased from 25.66% in April 2021 0-10 cm soils to 36.60% with depth and was significantly (χ^2 (2) = 49.279, p < 0.0001) larger than the Burned Stand aliphatic proportion which was about 18% at all depths. Oxygenated functional groups were the largest component of extract DOM, making up significantly (χ^2 (2) = 36.163, p < 0.0001) more, 61.72-65.58%, of the DOM from the Burned than from the Unburned Stand (57.44-46.17%). The unsaturated proportion was also significantly (χ^2 (2) = 48.167, p < 0.0001) larger in the Burned stand, a trend which became more pronounced with depth. For all functional groups, no model reported significant differences between extracts from the April 2021 and March 2022 soils. *For full model results see Appendix A, Figures A.18 through A.27*.

Comparison of DOM composition from leachate collected on 30 April 2021 and extracts from 20-30 cm soils collected on 21 and 22 April 2021 showed a significant influence of sample type on aromatic ($F_{1,12} = 9.731$, p = 0.009), oxygenated ($F_{1,12} = 91.887$, p < 0.0001), and aliphatic ($F_{1,12} = 117.529$, p < 0.0001) proportions but not on functionalized aliphatic proportion ($F_{1,12} = 0.000$, p = 0.999). Aromatic proportion of spectra was a significantly (p = 0.02) larger component of Burned Stand leachate than extract DOM. This difference was not seen in the Unburned Stand, where extract and leachate DOM had similar aromatic proportions (p = 0.9845). The largest differences between sample types were observed in oxygenated and aliphatic proportions. For example, in the Burned stand, oxygenated DOM proportion comprised 20.30% of leachate and 65.58% of extracts (p < 0.0001), while aliphatic DOM comprised

62.77% of leachate, but only 18.14% of extracts (p < 0.0001). These differences, though less extreme, followed the same statistically significant trends in the Unburned Stand (p < 0.0001). For full model results see Appendix A, Figures A.28 through A.31.

2.5 Discussion

We conducted an in-depth characterization of organic matter composition across several SOM pools, comparing the soils of a longleaf pine stand managed with regular Rx fire to one raked for pine straw. We expected to see an immediate spike in the aromatic proportion of Burned Stand DOM postfire, representing the infiltration of PyC compounds with higher inherent solubility (Wagner et al., 2018) into soil. We also expected a stronger overall dPyC signal in the Burned Stand DOM, reflecting the influence of current fire management. Our ¹H NMR results from both leachate and extract DOM showed no immediate postburn increase in aromatic proportion, but a relative increase in Burned Stand aromatic proportion ~8 months postfire. In the soil fractions, we predicted that POM in the Burned Stand would be older due to higher inputs of PyC compared to the Unburned Stand, however we found the opposite – Unburned Stand POM was substantially older at both 0-10 and 20-30 cm depths. Finally, we hypothesized that in both stands, a higher proportion of C would be stored as MAOM versus POM at 20-30 cm when compared to 0-10 cm fractions, reflecting an increased amount of time in the soil profile and thus greater chance of encountering, and entering into association with, a mineral. This hypothesis was supported by our results, which show C is about evenly split across MAOM and POM in 0-10 cm samples from both stands, but MAOM contains about 4 times and 2 times as much C at 20-30 cm in the Burned and Unburned Stand, respectively.

2.5.1 Characterizing Soil Organic Matter Quality in a Coastal Plain Sandy Loam

MAOM and POM fractions were consistent with the framework outlined by Lavallee et al. (2020) in several ways. The C:N ratio of MAOM was 12-14, reflective of microbial residues and lower molecular weight (LMW) plant compounds including leached materials (e.g. pectins and sugar alcohols) and decomposition products such as depolymerized components of cellulose. The C:N ratio of 28-29 in POM is more typical of charcoal or structural plant materials like cellulose and lignin. At 20-30 cm in the Burned and Unburned Stand, MAOM had δ^{13} C values of -22.10 to -23.35 %, respectively, about 2% higher than the POM, suggesting it is more microbially processed. Overall, δ^{13} C values were about 1-2% higher in the Burned Stand than corresponding fractions in the Unburned Stand, possibly reflecting substantial contribution of from C₄ grasses, especially wiregrass, to SOM in this stand.

Our SOM separations appear to have isolated the expected components of MAOM and POM, however our fractions deviate from the dominant paradigm in one key way: MAOM is generally thought to cycle on a decadal to centennial timescale, while POM is estimated to turn over within years to decades (Cotrufo et al., 2019; Lavallee et al., 2020). In the Burned Stand, radiocarbon values indicate that POM is modern in the topsoil, but POM at 20-30 cm originated an average of 480 years ago. In the Unburned Stand, topsoil POM is much older, with an average origin of 305 ya while the material at 20-30 cm originated an average of 1035 ya. MAOM is modern down to 20-30 cm in both the Burned and Unburned Stand soils, suggesting it is highly vertically mobile, and is likely composed leachable C compounds which were mobilized relatively quickly after being fixed by a plant.

Because the MAOM fraction appears to be recently fixed C that has also been highly processed by microbes, we may assume it does not experience much protection by minerals.

Amide peaks visible in mid-infrared spectra from MAOM, but not POM suggest a higher concentration of microbial proteins (Parikh et al., 2014). Strong peaks in O-H and N-H regions of the MAOM spectra may also indicate microbially-derived compounds, like polysaccharides or amino sugars, though these signals are likely also influenced by the separation of clay particles into this fraction. In our soils, clay ranged from 13.2-18.2%. Redoximorphic features and plinthite suggest Fe oxides are present in the soil, indicating that opportunities for mineral association exist, however soils are poorly aggregated, limiting opportunities for physical protection. The MAOM is composed of recently fixed C, even at depth, with a high proportion of -OH functional groups that could indicate an origin as hydrophilic fresh plant substances such as simple sugars leached from recently senesced leaves or exuded into the rhizosphere to stimulate microbial interaction.

Our results suggest that the most persistent C in our soils may exist in the POM as inherently decomposition resistant compounds, such as PyC. Butnor et al. (2017) investigated PyC stability in longleaf pine forests across a range of mostly low clay content soils by chemically fractionating soils into oxidation resistant (SOC_R) and oxidizable (SOC_{OX}) pools. These researchers found that ~92% of PyC was found in the SOC_{OX}, which had a mean residence time (MRT) of 63-274 years at 0-10 cm and 520-743 at 20-50 cm and concluded that PyC in soils was not an important long-term C sink in the longleaf pine system. This assessment of MRT is generally consistent with our results, especially considering that removal of fresh needle cast during pine straw harvest and previous agricultural tillage has likely increased the mean age of SOM in the Unburned Stand (discussed in more detail in subsequent sections). While the majority of SOC in the Butnor et al. (2017) study was found to be SOC_{OX}, a smaller SOC_R pool cycled on millennial timescales (1,223-22,626 year MRT), potentially displaying longevity due

to mineral stabilization. It is possible that a longer-term mineral-associated C pool does exist in our soils, but was collapsed into the POM during size fractionation, for example, because it was adsorbed within the pore spaces of larger PyC particles (Brodowski et al., 2005a). Density fractionation may be required to investigate this phenomenon (Brodowski et al., 2006).

Mid-infrared spectroscopy provides information about mineral and organic components of soils, at once a strength and a drawback of this technique. Mineral signatures can interfere with organic regions, making interpretation complicated (Parikh et al., 2014). Our results provide insight into how peaks commonly attributed to carboxylic acid C=O and aromatic C=C bonds can present very differently in predominantly sand versus more clayey soils (Calderón et al., 2011; Hall et al., 2018). The prominence of C=O and C-O associated peaks compared to that of C-H and C-O-C peaks indicating fresh cellulosic materials reflects a soil environment with highly decomposed OM (Kaiser et al., 2012). Due to the complexity of the main OM informational region (1750-1210 cm⁻¹) in mid-IR spectra (Guillou et al., 2015), estimation of PyC proportions will require modelling techniques that are beyond the scope of this thesis (Chatterjee et al., 2012; Cotrufo et al., 2016; Uhelski et al., 2022). Thus, we are not able to present a comparison of PyC stocks across the Burned and Unburned Stands at this time.

2.5.2 Extract DOM is Substantially Younger than DOM from *In-situ* Leachate

In our study, leachate DOM collected at 30 cm was primarily composed of aliphatic compounds, with proportions ranging from 63-81% of C compounds in the Burned and 71-83% in the Unburned Stand. The prominence of aliphatic groups in the DOM, as analyzed by ¹H NMR, is interpreted to indicate decomposed plant material and microbial biomass. This is in contrast to the mid-IR spectra of bulk soils, soil fractions, and OM references, for which aliphatic groups were interpreted to indicate fresh organic matter. Aliphatic plant materials are resistant to

decomposition and inherently hydrophobic (e.g. waxes, resins, fatty acids), often characterized by long hydrocarbon chains with little affinity for water (Kögel-Knabner & Amelung, 2014). Alkane degradation is energy-intensive (Wershaw, 2004); most microbes utilizing the C in these materials are generalists that will preferentially pursue other C sources (Rojo, 2009), so degradation of aliphatic compounds likely occurs more often in nutrient-limited conditions. For an aliphatic material like a plant cuticle wax to become dissolved, it must be oxidized into shorter alkane chains adequately substituted with polar functional groups. This pool of decomposition-associated aliphatics may also include microbial biomass such as bacterial, fungal, and algal cell wall components (Nzila, 2018; Weete, 1972).

Hydrophobic secondary plant metabolites, such as oleoresins, may be another important pool of aliphatic materials in coniferous forests. One example is turpentine, which is produced in high concentrations by the roots of longleaf pine (Anderson et al., 2018). Turpentine is a fragrant material owing its scent to terpenes, which pine trees also produce in their needles (Ormeño et al., 2009). Terpenes are very flammable – during Rx fire, they may be lost from the litter layer in a higher proportion than other forest floor components (White, 1991). These LMW compounds are insoluble in water and possess antimicrobial properties that make them generally resistant to microbial transformation (Masyita et al., 2022). Pine-derived terpenes occur in cyclic (unsaturated) forms, such as pinene, a dominant monoterpene in longleaf pine wood (Adamczyk et al., 2015; Eberhardt et al., 2009) which exhibits lower resistance to oxidation by microbes (Wershaw, 2004), and acyclic (aliphatic) forms including linalool (da Silva Rodrigues-Corrêa et al., 2013) with linear structures that are more environmentally persistent. Despite their insolubility, terpenes have been identified in the DOM, possibly brought into the aqueous phase through association with carbohydrates such as plant hemicelluloses and bacterial cell wall

components (Wershaw et al., 2005). In addition to terpenes, oleoresins are composed of higher molecular weight hydrophobic compounds, such as gums, resins, and waxes (da Silva Rodrigues-Corrêa et al., 2013).

Extract DOM samples were dominated by oxygenated functional groups, particularly in the Burned (62-66%) but also in the Unburned Stand (46-57%). This suggests a high concentration of polysaccharides from fresh plant litter (Kögel-Knabner & Amelung, 2014), such hemicelluloses and pectins, as liberated OH-containing ring structures from decomposing lignin. Many of these O-containing compounds have a high inherent solubility and do not require microbial processing to enter the soil solution (Santos et al., 2022). Low molecular weight root exudates (e.g., sugars, amino acids, and organic acids), which are secreted into the rhizosphere to regulate plant-microbe interaction (Sasse et al., 2018), are another potential source of oxygenated compounds.

Compositional differences in the quality of *in-situ* leachate versus extract DOM are reinforced by radiocarbon results which suggest these SOM pools cycle on different timescales. Based on the radiocarbon values from pooled lysimeter samples collected in April 2021, Burned and Unburned Stand leachate DOM originated an average of 340 and 775 years ago, respectively. On the other hand, extract DOM has radiocarbon values reflecting C fixed during the modern era, both in the topsoil and at 20-30 cm in both stands. Leachate DOM is predominantly composed of chemically insoluble aliphatic molecular structures, suggesting it is highly influenced by in-soil processes such as the formation of colloids and mineral-association that were not recreated during our 1-hour shaking event.

These same processes likely play an important part in PyC entering the soil water, as results from the aromatic proportion of DOM follow a similar trend. Leachate DOM ranged from

2.56 to 7.44% in the Burned and 1.25 to 6.27% in the Unburned Stand, significantly larger proportions than in extract DOM at 20-30 cm, where it ranged from 0.45 to 0.93% and 0.33 to 6.28% in those stands, respectively. Notably, the aromatic proportion of extract DOM was not higher in postburn extract samples. This is consistent with results from (Hobley et al., 2019), who reported that water extractable organic carbon (WEOC) decreased in 0-2 cm soils from unburned to low frequency Rx fire treatments, and again from low to high frequency Rx fire treatments. These decreases in WEOC were correlated with a shift in UV-Vis spectral peaks, suggesting WEOC components in frequently burned soils had a greater proportion of aromatic components and that those aromatic structures were less-substituted. This decrease in WEOC was attributed to a relative increase in aromatic functional groups with increasing Rx fire frequency. Speculatively, the small proportion of aromatic compounds seen in Burned Stand and Unburned Stand extracts may be the type of LMW, less condensed, and more highly Osubstituted aromatic compounds which are inherently able to enter the aqueous phase. These types of aromatic structures may have developed from more highly condensed PyC undergoing oxidative processes, or their relative solubility may be conferred by low intensity burning of more herbaceous starting material. Either scenario is possible in our system, with the former possibly predominating in the Unburned and the latter more likely in the Burned Stand (discussion continued in the next section).

The greater representation of aromatic compounds in leachate than extract DOM suggests that PyC unavailable for dissolution during extraction can enter the soil solution under the correct conditions. For example, Wagner et al. (2017) hypothesize that highly condensed and inherently insoluble PyC compounds form supramolecular associations with more polar DOM components that bring them into the aqueous phase, however they were unable to support this

hypothesis when comparing char-only to soil-water-char extractions obtained during a 72-hour shaking extraction. One notable anomaly in our data is the large proportion of aromatic compounds found in some Unburned Stand extracts at 20-30 cm. This may be the result of solubility conferred to PyC through association with iron (Fe) oxide compounds in plinthite. While plinthite was not recorded in our soil descriptions until the Bt layer at 51 cm (Table 2.1), it was observed in 20-30 cm cores from the Unburned Stand during sieving. The spatial discontinuity of plinthite deposits could explain the wide range in aromatic proportion values found in Unburned Stand extract DOM at 20-30 cm (Fig. 2.9) when compared to other to all other treatments.

2.5.3 Impact of Stand Management on Dissolved and Bulk Soil Organic Matter Composition

A global meta-analysis showed that frequent low intensity fires tend to reduce C and N stocks at 0-20 cm in savannah and grassland ecosystems while increasing C and N in warm climate conifer forests (Pellegrini et al., 2021) and building concentrations of persistent C in both. This is consistent with other studies showing Rx fire reduces total soil C and N storage (Pellegrini et al., 2020), including in longleaf pine (Lavoie et al., 2010). Our ability to assess this trend within our Coastal Plain longleaf stands is complicated by site history as well as by the removal of fresh OM from the Unburned Stand during pine straw harvesting. Total C and N in both stands was generally low, but within expected values for Cowarts and Dothan series (Soil Survey Staff). Both stands displayed evidence of persistent C. Despite a moist, warm climate which facilitates rapid OM decomposition, POM and leachate DOM in the Unburned Stand were found to contain C fixed over 700 and 1,000 ya, respectively, which is younger than, but still comparable to, charcoal found in Terra Preta soils (Glaser et al., 2001).

Carbon in the Unburned Stand POM fraction was fixed an average of 305 ya in the topsoil and 1,035 ya at 20-30 cm, while in the Burned Stand those values were modern and 480 ya, respectively. Likewise, radiocarbon values in the Unburned Stand leachate DOM indicate it is derived from plant materials originating an average of 775 years ago, versus Burned Stand plant materials that were substantially younger (480 ya). This disparity can be explained by current management which, along with stand age and structure, influences SOM inputs between both above and below the soil surface. Differences in site history between the two stands over the ~150-year period between European settlement and initiation of the current management regime likely contributed to shaping these trends as well.

The Burned Stand was established 7 years before study initiation, on a site that had been clearcut. This site was never tilled, as evidenced by the presence of wiregrass. Permanently wet areas in this stand would have made it unsuitable to cultivation, and the persistence of bog species like *Sarracenia spp.*, *Utricularia sp.*, and *Drosera sp.* suggest that soil disturbance has been minimal. The Unburned Stand was planted 17 years before study initiation in a field that was in agricultural production for an undetermined length of time, but likely not less than three decades. Several lines of evidence indicate that agricultural practices have altered soil properties in this. Though an Ap layer was not identified during soil delineation, higher bulk density relative to the Burned Stand suggests degraded soil structure due to tillage. Agricultural legacy effects may also explain pH dynamics. Contrary to what is generally observed in longleaf and most other landscapes managed with Rx fire (Alcañiz et al., 2018; McKee, 1982), pH was lower in the Burned than Unburned Stand. This may be an effect of previous land managers adding lime to neutralize naturally acidic Coastal Plain soils for crops like cotton, corn, and peanuts, which all require a soil pH of ~6-6.5 (Gascho & Parker, 2001). This difference was not

significant at 0-10 cm but became significant at 10-20 and 20-30 cm, with pH decreasing with depth in the Burned but increasing with depth in the Unburned Stand. This may indicate soils beginning to recover their characteristic pH after reforestation.

Teasing apart the relative influence of current versus historical management on SOM dynamics in these stands is challenging. The Unburned Stand is more densely planted, with more mature trees that form a closed canopy. Understory vegetation is scattered herbaceous growth that is treated with herbicide. Conversely, the Burned Stand is less densely planted and younger, with an open canopy and thickly-vegetated understory dominated by wiregrass. Thus, modern inputs to SOM are quite different, however quantifying these differences is a significant challenge. Existing research on C allocation in longleaf stands can provide insight, but not to the extent that we can extrapolate a full C budget for each stand. Hendricks et al. (2016) estimated both pine needle and ectomycorrhizal fungi (EMF) production in a 35-year-old longleaf plantation at the Jones Ecological Research Center in southwestern GA. Annual pine needle production was 543 g m⁻² yr⁻¹, about twice as much biomass as EFM production, which was 279 g m⁻² yr⁻¹. EMF constituted standing biomass of 30 g m⁻² which turned over approximately 10 times per year. Guo et al. (2004) measured standing biomass of fine roots in a 24-year-old longleaf plantation, also at the Jones Center, isolating 13 g m⁻² of first order roots, which turn over approximately once per year (Guo et al., 2008), 24 g m⁻² of second- and third order roots, which turn over about every 2-2.5 years, and 40 g m⁻² of fourth- and fifth order roots, which likely turn over at an average rate of every 4-6 years (Matamala et al., 2003). Due to differences in stand age and planting densities, it is not possible to compare EFM versus fine root standing biomass directly across these two studies, and these values are likely higher than in our less mature stands, but they do highlight the complexity in estimating inputs to SOM, especially

belowground. Across all categories of SOM pools, materials enter the soil at annual rates which differ by biomass type, specific even to the level of fine root order, with site and stand characteristics likely influencing turnover as well.

Beyond fine roots, longleaf pines grow extensive woody lateral roots, vertical sinker roots, and taproots which pose a considerable challenge to measure using current methodologies. Samuelson et al. (2014) utilized planted (5-, 12-, and 21-year-old) and naturally regenerated (64and 87-year-old) longleaf stands at Fort Moore military installation, which spans the Georgia-Alabama border, to investigate C allocation across a gradient of stand ages. Groundcover and residual taproot were significant C contributors in the 5-year stand, but not in the older stands, where aboveground live woody plant C was dominant (and residual taproot was not measured). This study found fine root C to be a relatively small proportion of longleaf pine biomass and which increased non-linearly with total stand C suggesting longleaf pine find roots reach their maximum density at relatively low basal area (7-8 m² ha⁻¹). While a small pool, fine roots are key to SOM dynamics due their fast turnover and colonization by EFM. Taproots represent a medium-term C pool in longleaf pine stands, which can persist for several decades after harvest (Samuelson et al., 2014). A coarse root decay model by Anderson et al. (2018) predicted that 25% of taproot necromass would remain in soil 100 years after a tree was cut. An ecosystem C allocation model created by Samuelson et al. (2017) estimated that lateral roots contribute substantially more to C storage in longleaf pine than other forest types, with a predicted average root:shoot ratio of 0.54 (standard deviation 0.19). While coarse roots represent a substantial C pool in longleaf pine forests, contributing to C stocks while influencing soil properties such as bulk density and hydraulic connectivity, their lignified composition and relative resistance to rot suggests they have a longer temporal path to DOM than other OM types.

While the effects of reforestation in the Unburned Stand have begun to reduce 0-10 cm pH, C stocks have likely not begun to recover from loss via agricultural practices. In an analysis of soils in longleaf stands established on marginal agricultural lands, Markewitz et al. (2002) reported no evidence of soil C sequestration over the first 14 years. Hastened decomposition or removal of stumps, taproots, and lateral roots during tillage and row cropping represents was likely a strong contributor to reducing the average age of SOM in the Unburned compared to the Burned Stand. Tillage represents a loss of a medium-term C pool which would be slow to recover. We also see a modern loss of a shorter term C pool – pine needles – which are removed annually. Thus, fact cycling belowground SOM inputs such as fine roots and EFM along with very slow cycling, persistent, components such as PyC and mineral-protected OM probably play a disproportionately large role in shaping SOM quality in the Unburned Stand.

The Burned Stand may be characterized by dynamics similar to the 5-year-old stand characterized by (Samuelson et al., 2014), with the wiregrass understory and residual taproots from the previous clearcut contributing strongly to SOM. In general, promotion of perennial grasses in savannah systems leads to SOM stabilization through the production of deep roots and associations with arbuscular mycorrhizal fungi (AMF) that can increase aggregation (Pellegrini et al., 2021). While wiregrass does allocate the majority of its biomass to a thick perennial root system (Saterson & Vitousek, 1984), it is fairly shallow, mostly occurring within 20 cm of the soil surface and generally not extending past 46 cm (Uchytil, 1992). Colonization of wiregrass roots by AMF is not well studied, but it is thought to be minimal (Anderson & Menges, 1997), thus contribution of fungal biomass may be lower in the Burned versus the Unburned Stand. Finally, the ability of perennial grasses to promote persistent C is stronger in clayey than in sandy soils (Pellegrini et al., 2021), possibly due to its positive effects on aggregation. While the

wiregrass understory is likely an important SOM contributor in the Burned Stand, it may not necessarily promote C longevity at our study site.

PyC deposited every 3-5 years during controlled burns is another important addition of newly-fixed C to the Burned Stand. Thermocouple readings indicate that soil heating during our Rx fire was highly variable, potentially creating a of range of PyC compounds across the combustion continuum. Those formed at temperatures between 200-300 °C might be quite soluble and thus mobile while those formed at >800 °C would be highly condensed and more resistant to decomposition. Herbaceous materials like grasses and forbs burned <300 °C would create PyC with relatively high O-substitution. These materials would tend to be more vertically mobile and decomposable when compared to woodier materials like shrubs and bark, which might be more likely to endure heating temperatures >800 °C, resulting in more highly-condensed, persistent PyC. Despite soil heating and vegetation conditions suggesting the formation of relatively soluble, O-substituted PyC, the lack of any significant increase in aromatic proportion from Burned to Postburn extract DOM indicates that these materials still require "aging" to enter the soil solution (Abiven et al., 2011).

In extracts, differences between Burned and Unburned Stand DOM become more pronounced with depth. Radiocarbon values indicate that at 20-30 cm, Burned Stand extract DOM is composed on average of more recently-fixed C compounds than those in the Unburned Stand extract DOM, however this effect is not so dramatic that it can be confidently interpreted without sample replication. Where we do see significant differences is in DOM quality. Burned Stand extract DOM is significantly more oxygenated than Unburned Stand DOM. Conversely, Unburned Stand extract DOM is more aliphatic. Each of these disparities increases down the soil profile. These trends echo what is seen in the radiocarbon: SOM in the Burned Stand tends to be

newer, leading to a DOM pool with compounds more reflective of fresh plant material, while the Unburned Stand DOM contains materials that are more decomposed. We see the same differences in the leachate DOM – despite its overall compositional difference from the extracts, leachate DOM is still significantly more oxygenated in the Burned and aliphatic in the Unburned Stand.

Another between-stand difference potentially controlling Burned versus Unburned Stand DOM composition may be qualitative difference in belowground inputs from roots and associated fungi. Forbs and wiregrass in the Unburned Stand may contribute more labile, oxygenated material from fine roots, approximately 50% of which are sloughed off perennial grasses annually (Gill & Jackson, 2000). The Unburned Stand is more densely stocked with longleaf pine, contributing coarse roots, fine roots, and associated EMF fungi. Pine needles are removed from the Unburned Stand, representing a considerable reduction in oxygenated fresh plant materials. Because of previously discussed losses of coarse root necromass due to agricultural tillage and the slower turnover of coarse roots (Anderson et al., 2018; Zhang & Wang, 2015) coarse root necromass available for incorporation into DOM may be minimal. Live longleaf pine roots may deposit substantial aliphatic exudates via turpentine secretion (Eberhardt et al., 2009), while fungal biomass contributes aliphatic cell wall materials like chitin. As mentioned previously, wiregrass does not appear to associate strongly with AMF, and due to the lower stand age and density of the Burned Stand, EMF is probably substantially less dense. These differences may be responsible for the higher representation of oxygenated proportion in the Burned and of aliphatic proportion in the Unburned Stand DOM.

Overall, aromatic proportion is larger in leachate DOM from the Burned Stand than Unburned Stand, though not significantly. There was no noticeable increase in aromatic

proportion in Burned Stand DOM during the initial postfire sampling. This may be because freshly deposited PyC was not soluble enough to infiltrate down to lysimeters at 30 cm. However, it may also be because this first flush of PyC occurred during the initial precipitation event – a major storm resulting in 162 mm of rain that fell over a 24-hour period three days after the Rx burn in the Burned Stand. Due to logistical challenges, soil water was not sampled until 7 days after this rain event and an initial pulse of the most mobile compounds was probably missed (Schiedung et al., 2020).

There is an overall decrease in aromatic proportion of Burned Stand DOM throughout the postfire sampling period. For the most part, general compositional trends seem to follow a seasonal pattern across both stands, with two notable exceptions. In general, patterns in leachate DOM composition are mirrored in the Burned and Unburned Stand until the final sampling date. However, we see an increase in Burned Stand aromatic proportion from August to December 2021, while this proportion decreases sharply in the Unburned Stand. This may be the effect of PyC from the Rx fire becoming decomposed enough to enter the soil water and travel to 30 cm at about 8 months postburn.

A second compositional departure between the stands occurs during the final sampling on June 2022. Unburned Stand leachate DOM appears to have generally returned to the same composition that can be observed in samples from June 2021. Leachate DOM in the Burned Stand, however, shows a drop in the least soluble (aromatic and aliphatic) functional groups and a strong increase in functionalized aliphatic compounds. We propose that these differences indicate a compositional shift in DOM caused by an extended period of abnormally dry weather, including three months of moderate drought. Drought effects would be buffered in the Unburned Stand due to the raised water table created by the dam on Middle Creek. Functionalized aliphatic

compounds include plant materials that confer drought resiliency, such as cutan and suberin (Boom et al., 2005; Harman-Ware et al., 2021). It is possible that the assembly of supramolecular structures required to bring insoluble compounds into the aqueous phase require some period of soil saturation that was not met by rapid infiltration of a 46 mm rain event that occurred under drought conditions on 14 June two days before the 16 June 2022, sampling, and thus aromatic and aliphatic compounds were not mobilized.

2.5.4 Future Directions and Limitations

Two major limitations of this study are the lack of replication across management treatments and the fact that SOM pools are described, but not quantified. According to dominant statistical conventions, our study was pseudoreplicated and we are not statistically supported in drawing conclusions about the impact of regular Rx fire versus pine straw raking in outside the boundaries of our study stands (Hurlbert, 1984). This also applies to our findings comparing leachate and extract DOM composition – we would encourage researchers using soil-water extracts to simulate leaching to investigate this disparity within their systems. That said, there is considerable logistical difficulty in replicating management-scale Rx burn treatments, not to mention that unburned "control" stands are essentially nonexistent in fire-obligate communities like longleaf-wiregrass, so the need to balance ecologically meaningful interpretations with statistical rigor and practical constraints must be accounted for (Hargrove & Pickering, 1992).

Our results highlight the importance of using *in-situ* soil water to study soil DOM pools. Tension lysimeters are a relatively low-cost and easily installed system for sampling *in-situ* soil water. To study terrestrial to aquatic movement of PyC, these lysimeters could be placed along a subsurface flow path and sampled along with adjacent water bodies such as creeks, ponds, and rivers in a post-Rx fire time series experiment. Combining advanced spectroscopy, radiocarbon,

and stable isotopes with DOC and direct PyC quantification methods like benzene polycarboxylic acid (BPCA) (Brodowski et al., 2005b) or hydrogen pyrolysis (hypy) (Wurster et al., 2013), would provide insight into in-soil transformation processes and their role in PyC export from soil to sea.

BPCA and hypy are two of our most quantitative PyC methods but they can be prohibitively cost- and time intensive. One promising development is recent modelling approaches which use BPCA and hypy values to train models that can predict PyC concentrations in MIR datasets using partial least squares regression (MIR-PLSR) (Cotrufo et al., 2016; Uhelski et al., 2022). This cutting-edge approach is being developed in soils with little or no utilization in DOM. Future directions for research include exploring the potential of MIR-PLSR to expand the interpretive value of our MIR dataset.

2.6 Conclusion

Burned Stand SOM pools were younger on average and characterized by OM more representative of fresh plant material, while Unburned Stand SOM was older and showed more evidence of decomposition. There was no significant increase in aromatic proportion for either extract or leachate DOM immediately post-Rx fire, but an increase was observed in the leachate after about 8 months, highlighting the need for most PyC to be oxidized or become associated with supramolecular structures in order to enter the soil solution. Extract DOM was younger and predominantly composed of inherently soluble oxygenated structures, while leachate DOM was older and composed mostly of aliphatic structures reflecting the chemical and microbial processes that allow hydrophobic compounds to enter the soil solution. Counter to our expectations, C isolated in the MAOM fraction was fast cycling, vertically mobile, and fixed in the modern era while C in POM originated >1000 ya to the modern era and increased in age with

depth. This suggests that size fractionation may not have isolated mineral-stabilized C in our soils. Despite low OM stocks and well drained sandy loam soils in which SOM faces high leaching potential and minimal protection in aggregates, we found evidence of C persisting from centuries to millennia.

2.7 Tables

Table 2.1. Description of soil characteristics.

Depth	Horizon	Matrix Color	Texture	Structure ¹		Redoximorphic	Concentrations	Ped/V. Surface
(cm)		(Wet)		Grade	Type	Features	Concentrations	Features
Burned Star	nd							
0-6	A1	10YR 3/3	Loamy sand	Wk	G	-	-	-
6-10	A2	10YR 4/1	Loamy sand	Wk	G	-	-	-
10-23	E	10YR 5/2	Loamy clay sand	Wk	G to Sg	-	-	-
23-30	BE	10YR 5/3	Sandy clay loam	Wk	Sbk	10YR 6/2 (few)	10YR 5/6 (few)	-
30-51	Bt1	10YR 5/3	Sandy clay	Mod	Sbk	10YR 6/2 (common)	10YR 5/8 (common)	-
51-99	Bt2	Multi	Sandy clay	Str	Sbk	10YR 6/2 (many)	10YR 5/8 (many)	-
99-122	Bc1	Multi	Sandy clay	Ma	assive	10YR 6/2 (many)	7.5YR 5/4 / 2.5YR 5/8 (common)	-
122-152+	Bc2	Multi	Sandy clay/loamy sand	Ma	assive	2.5Y 7/1 (many)	10YR 5/8 / 2.5YR 5/8 (common)	-
Unburned S	tand							
0-33	A	10YR 4/2	Loamy sand	Wk	G	-	-	-
33-51	BE	10YR 6/3	Sandy loam	Wk	G/Sbk	-	5YR 5/8 (few)	-
51-71	Bt	10YR 6/6	Sandy loam/sandy clay loam	Wk	Sbk	-	5YR 5/8 (common)	Plinthite 2%
71-114	Btv1	10YR 6/6	Sandy clay loam	Wk	Sbk	-	5YR 5/8 (common)	Plinthite 30%
114-127	Btv2	10YR 6/4	Sandy clay loam	Mod	Sbk	10YR 7/2 (common)	5YR 5/8 (many)	Plinthite 30%
127-152+	Btv3	10YR 5/8	Sandy clay loam	Mod	Sbk	10YR 7/2 (many)	10YR 6/6 (many)	Plinthite 15%

¹Wk = weak, Mod = moderate, Str = strong; G = granular, Sg = single grain, Sbk = subangular blocky

Table 2.2. Burned Stand species list.

Botanical Name	Common Name	Type	
Acer rubrum	Red maple	Tree	
Agalinus sp.	False foxglove	Forb	
Anaphalis margaritaceae	Pearly everlasting	Forb	
Andorpogon virginicus	Broom sedge	Graminoid	
Aristida stricta	Wiregrass	Graminoid	
Baccharis halimifolia	Groundseltree or Salt bush	Shrub	
Balduina sp.	Honeycomb head	Forb	
Carex sp.	Sedge	Graminoid	
Chaptalia tometosa	Wooly sunbonnet	Forb	
Ctenium aromaticum	Common toothache grass	Graminoid	
Dicanthelium sp.	Panicgrass	Graminoid	
Drosera sp.	Sundew	Forb	
Dryopteris sp.	Wood fern	Fern	
Eriocaulon sp.	Pipewort	Forb	
Eupatorium roundifolium	Roundleaf thoroughwort	Forb	
Helenium sp.	Sneezeweed	Forb	
Hypericum sp.	St. John's Wort	Forb	
Ilex glabra	Gallberry	Shrub	
Licania michauxii	Gopher apple	Shrub	
Lycoris sp.	Spider lily	Forb	
Magnolia virginiana	Sweetbay magnolia	Tree	
Morella cerifera	Southern wax myrtle	Shrub	
Pinus elliottii	Slash pine	Tree	
Pinus palustris	Longleaf pine	Tree	
Pinus taeda	Loblolly pine	Tree	
Pityopsis graminifolia	Narrowleaf silkgrass	Forb	
Polygula nana	Candy root	Forb	
Prunus serotina	Black cherry	Tree	
Quercus nigra	Water oak	Tree	
Quercus phellos	Willow oak	Tree	
Quercus pumila	Runner oak	Shrub	
Rhexia alifanus	Savanna meadow beauty	Forb	
Rhus copallinum	Winged sumac	Shrub	
Rubus sp.	Blackberry	Forb	
Rudbeckia sp.	Coneflower	Forb	
Sabatia sp.	Rose gentian	Forb	
Sarracenia flava	Yellow pitcher plant	Forb	
Sarracenia minor	Hooded pitcher plant	Forb	
Sisyrinchium sp.	Blue-eyed grass	Forb	
Smilax, sp.	Greenbrier	Forb	
Sphagnum sp.	Sphagnum moss	Bryophyte	
Urticularia sp.	Bladderwort	Forb	
Vaccinium sp.	Blueberry	Shrub	
Viola lanceolata	Lance-leaved violet	Forb	
Vitis rotundifolia	Muscadine	Forb	
Xyrix sp.	Yellow-eyed grass	Forb	

Table 2.3. Overstory structure in the Burned Stand as measured using approximately 1/40-hectare circular plots.

Species	Density (trees ha ⁻¹)	Basal Area (m² ha-1)	Average Height ¹ (m)
Longleaf pine	445	1.71	5.8
Loblolly pine	12	0.04	5.8
Water oak	272	0.55	4.0
Willow oak ²	12	-	0.8
Red maple ²	49	-	0.5
Sweetbay magnolia ²	12	-	2.1
Black cherry ²	25	-	0.6
Miscellaneous hardwoods ²	49	-	0.6
Total	876	2.3	-

¹Mean across two randomly located plots

²Height and DBH not recorded for trees with DBH <1.2 cm

Table 2.4a. Density of shrubs in the Burned Stand by species, as measured using approximately 1/400-hectare circular plots.

Species	Stems ¹ ha ⁻¹				
Vaccinium	741				
Gallberry	44,089.5 123.5				
Sumac					
Wax myrtle	1482 370.5				
Baccharis					
Runner oak	741				

¹Mean across two randomly located plots

Table 2.4b. Density of shrubs in the Burned Stand by height, as measured using approximately 1/400-hectare circular plots.

Height Class (cm)	Stems ¹ ha ⁻¹		
0-30	101		
30.1-60	224		
60.1-90	59		
90.1-120	1		

¹Mean across two randomly located plots

Table 2.5. Density and moisture content of herbaceous vegetation in the Burned Stand.

Quadrat	Fuel Loading (MT/ha)	Moisture (%)		
1	5.13	36.52		
2	6.87	31.38		
3	7.50	33.06		
4	2.77	41.44		
Average	5.54	35.60		

Table 2.6. Weather conditions for 22 April 2021, during the prescribed fire in the Mature and Burned Stands.

Time	Temperature (°C)	In-stand Wind Speed (km/h)	Open Wind Speed (km/h)	Wind Direction	Humidity (%)	Dew Point (°C)	Barometric Pressure (hPa)
9:10	11.9	3.2-8.0	8.0-16.0	NE	36.0	-1.7	29.92
11:10	18.7	3.2-9.7	-	N-NE	30.1	-2.4	29.95
12:20	18.7	2.7-5.3	-	N	27.0	2.8	29.97
13:11	22.0	1.3-2.3	1.3-2.3	N-NE	22.4	-1.1	29.95

Table 2.7. Bulk soil chemical and physical properties.

Depth (cm)	Bulk Density (g/cm ³)	pH in H ₂ O	pH in CaCl ₂	Sand %	Silt %	Clay %	%N	%C	C:N	δ ¹³ C (‰)
Burned S	Burned Stand									
Preburn										
0-10	1.26 (0.10)	4.45 (0.07)	4.11 (0.11)	69.6 (2.2)	12.7 (0.8)	17.2 (1.6)	0.07 (0.01)	1.3 (0.2)	19.9 (0.6)	-24.4 (0.4)
10-20	-	4.19 (0.06)	3.69 (0.04)	70.5 (2.9)	10.6 (0.4)	18.6 (2.8)	0.04 (0.00)	0.9 (0.1)	21.2 (1.0)	-24.3 (0.4)
20-30	-	4.29 (0.14)	3.63 (0.03)	65.9 (3.4)	11.4 (0.9)	22.7 (2.5)	0.04 (0.00)	0.8 (0.1)	19.8 (0.8)	-24.1 (0.3)
Postburn										
0-10	1.20 (0.07)	4.05 (0.08)	3.81 (0.10)	69.6 (1.1)	13.9 (0.9)	16.5 (1.1)	0.07 (0.01)	1.4 (0.1)	20.4 (1.0)	-23.8 (0.5)
11-month	Postburn									
0-10	-	4.79 (0.11)	4.08 (0.11)	65.0 (4.6)	14.2 (0.5)	20.8 (4.7)	0.08 (0.00)	1.4 (0.0)	16.9 (0.6)	-23.6 (0.3)
10-20	-	4.64 (0.06)	4.03 (0.05)	73.5 (1.4)	10.8 (0.2)	15.8 (1.3)	0.05 (0.01)	0.9 (0.1)	19.4 (0.3)	-23.6 (0.3)
20-30	-	4.77 (0.02)	3.96 (0.03)	63.0 (3.8)	8.2 (2.7)	28.9 (1.8)	0.04 (0.00)	0.6 (0.1)	16.2 (0.3)	-23.0 (0.3)
Unburne	d Stand									
Unburned	d									
0-10	1.48 (0.50)	4.52 (0.09)	4.23 (0.05)	74.7 (0.8)	12.3 (0.4)	13.0 (0.5)	0.04 (0.00)	0.8 (0.0)	19.1 (0.4)	-25.9 (0.1)
10-20	-	4.89 (0.08)	4.54 (0.06)	76.9 (0.8)	9.8 (0.8)	13.3 (0.3)	0.03 (0.00)	0.5 (0.0)	20.6 (0.4)	-24.9 (0.1)
20-30	-	4.83 (0.05	4.47 (0.05)	74.4 (1.0)	11.1 (0.8)	14.6 (0.6)	0.02 (0.00)	0.4 (0.1)	20.0 (1.2)	-24.5 (0.1)
11-month	11-month Unburned									
0-10	-	4.75 (0.04)	4.22 (0.05)	75.2 (1.1)	11.7 (0.8)	13.2 (0.4)	0.07 (0.00)	1.3 (0.1)	19.9 (1.0)	-26.6 (0.2)
10-20	-	5.20 (0.06)	4.78 (0.09)	77.2 (0.4)	10.1 (0.4)	12.7 (0.2)	0.03 (0.00)	0.8 (0.1)	23.0 (0.8)	-25.6 (0.1)
20-30	-	5.19 (0.03)	4.83 (0.03)	76.7 (1.5)	10.4 (1.3)	13.0 (0.3)	0.03 (0.00)	0.6 (0.0)	21.3 (0.1)	-25.0 (0.1)

Values are reported as mean (standard error) with n=4 replicates

Table 2.8. Soil fraction chemical and physical properties.

Donth (am)	Fraction	%N	%C	C:N	δ ¹³ C (‰)	Recovered	Fraction N	Fraction C
Depth (cm)	Fraction			C.N		Weight (g)	(g/sample)	(g/sample)
Burned Stand	!							
0-10	MAOM	0.17	2.2	13.3	-22.85	7.21	1.23 x 10 ⁻²	1.6 x 10 ⁻¹
0-10	POM	0.03	0.8	28.1	-22.95	17.94	5.38 x 10 ⁻³	1.5 x 10 ⁻¹
20-30	MAOM	0.07	0.9	12.8	-22.10	7.46	5.22 x 10 ⁻³	6.3 x 10 ⁻²
20-30	POM	-	0.1	-	-24.40	16.84	-	1.7 x 10 ⁻²
Unburned Sta	Unburned Stand							
0-10	MAOM	0.09	1.1	12.7	-25.00	7.31	6.58 x 10 ⁻³	8.0 x 10 ⁻²
0-10	POM	-	0.4	-	-24.40	17.07	-	6.8 x 10 ⁻²
20-30	MAOM	0.04	0.6	13.9	-23.35	6.55	2.62 x 10 ⁻³	3.9 x 10 ⁻²
20-30	POM	-	0.1	-	-25.40	17.50	-	1.8 x 10 ⁻²

2.8 Figures

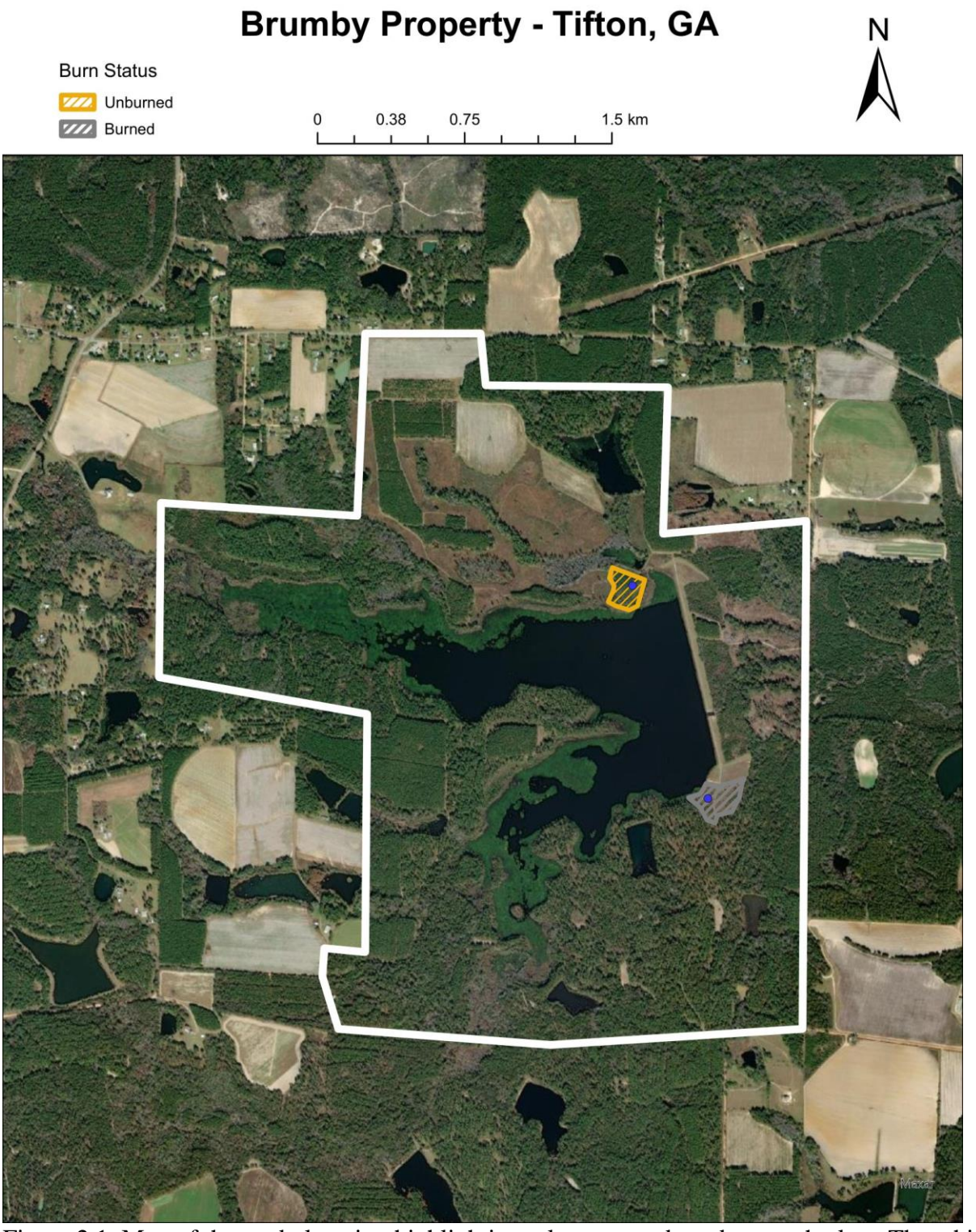


Figure 2.1. Map of the study location highlighting relevant stands and research plots. The white line indicates property boundaries.

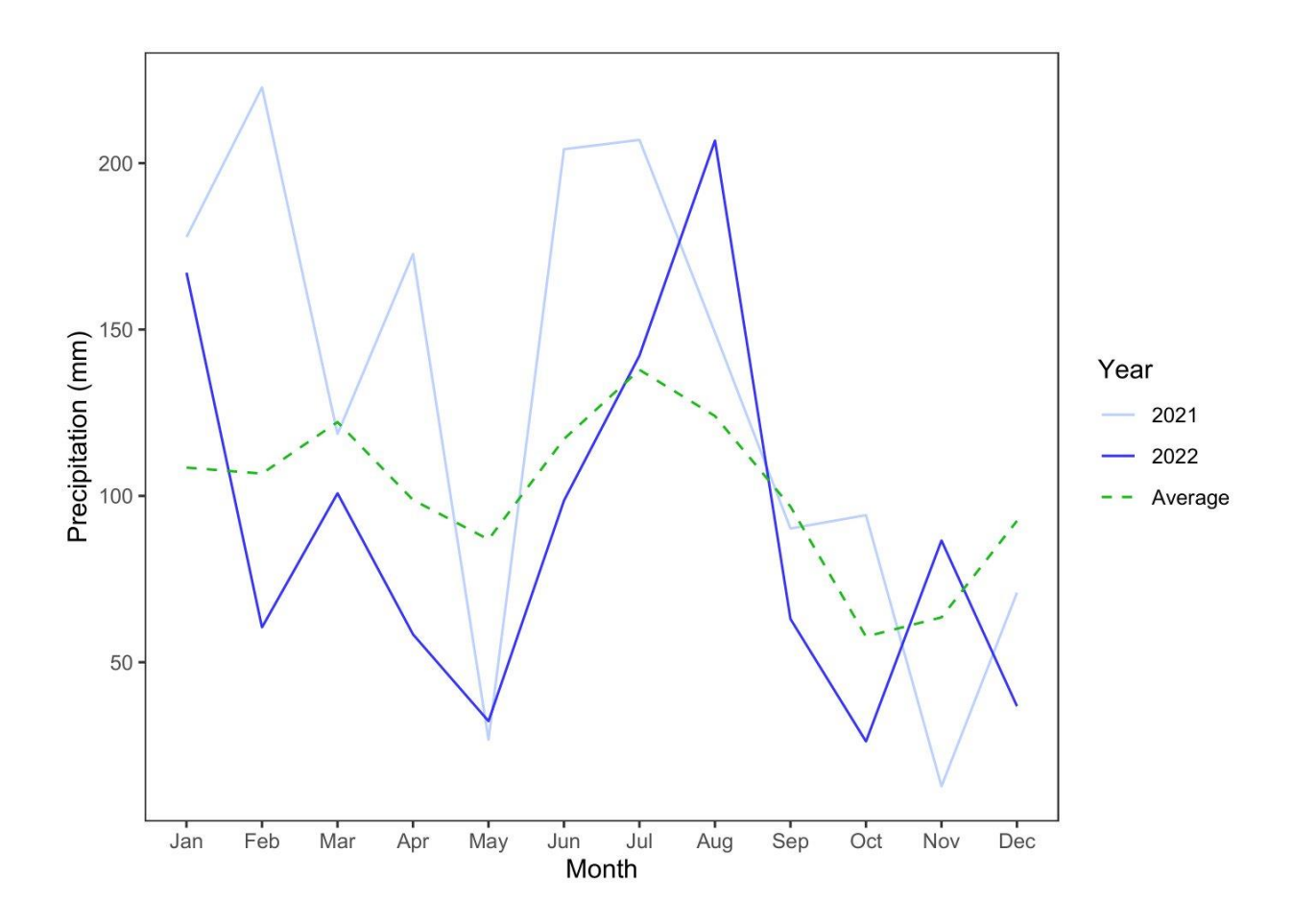


Figure 2.2. Average monthly precipitation in Tifton, GA. Data are from the Coastal Plain Experimental Station, part of the Georgia Automated Environmental Monitoring Network, about 8 km west/southwest from the Brumby property. Historical average was calculated from precipitation records from 1923 to 2016 (Georgia Automated Environmental Monitoring Network, 2023).

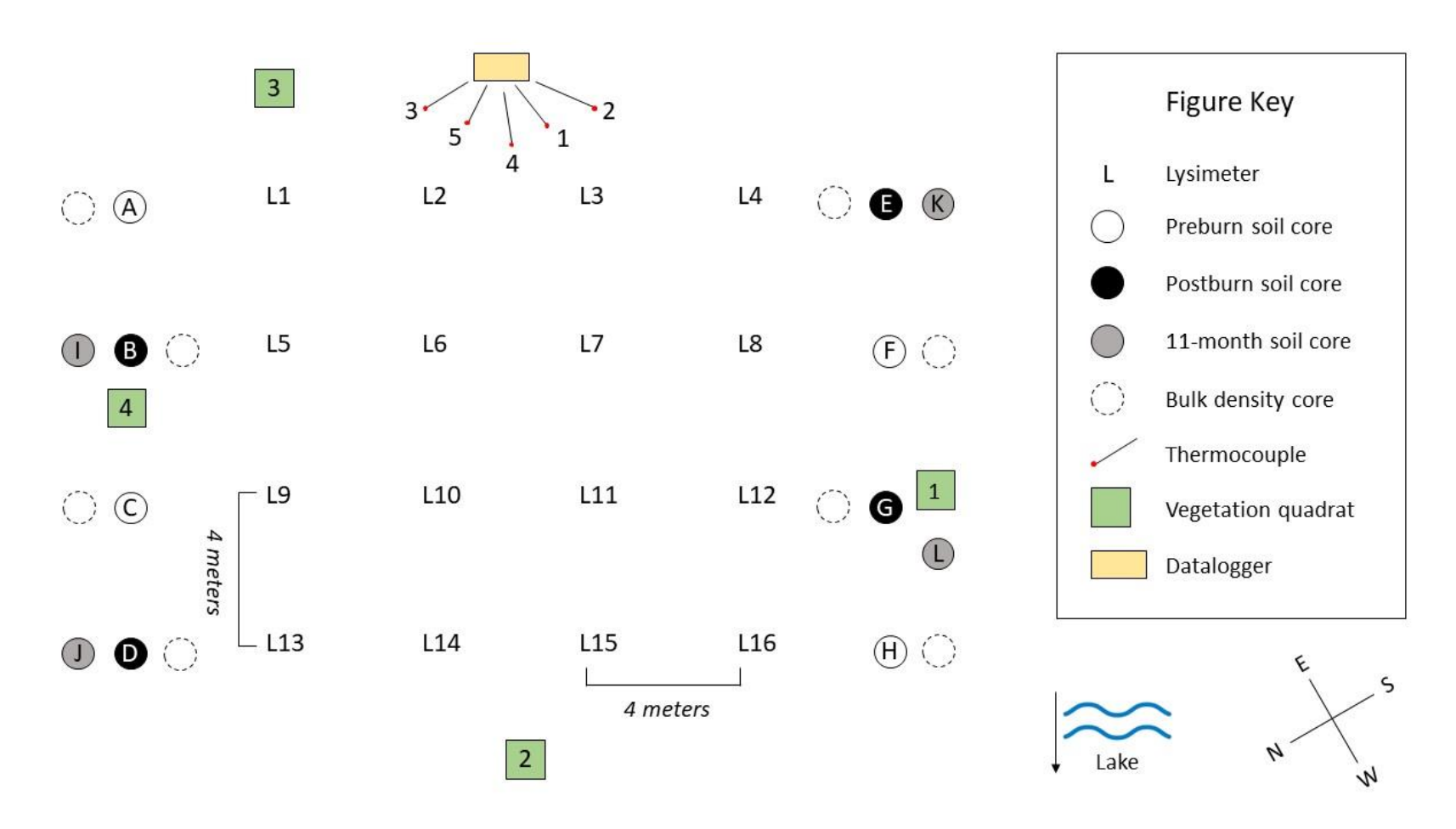


Figure 2.3. Diagram depicting the layout of the lysimeter plot in the Burned Stand. Image is not to scale.

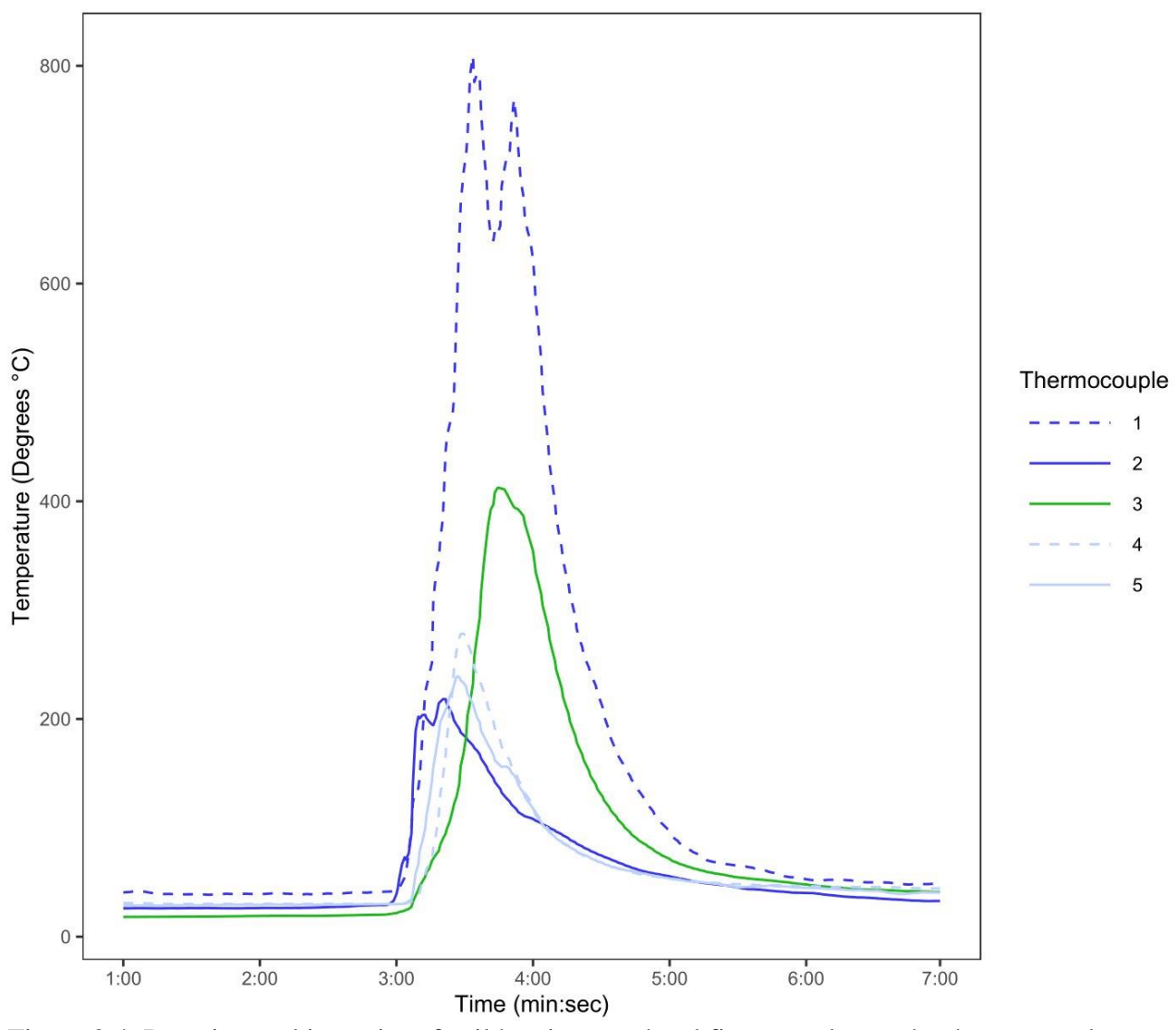


Figure 2.4. Duration and intensity of soil heating as a head fire passed over the thermocouple array on the southeast side of the Burned Stand lysimeter plot during the Rx fire on 22 April 2021.

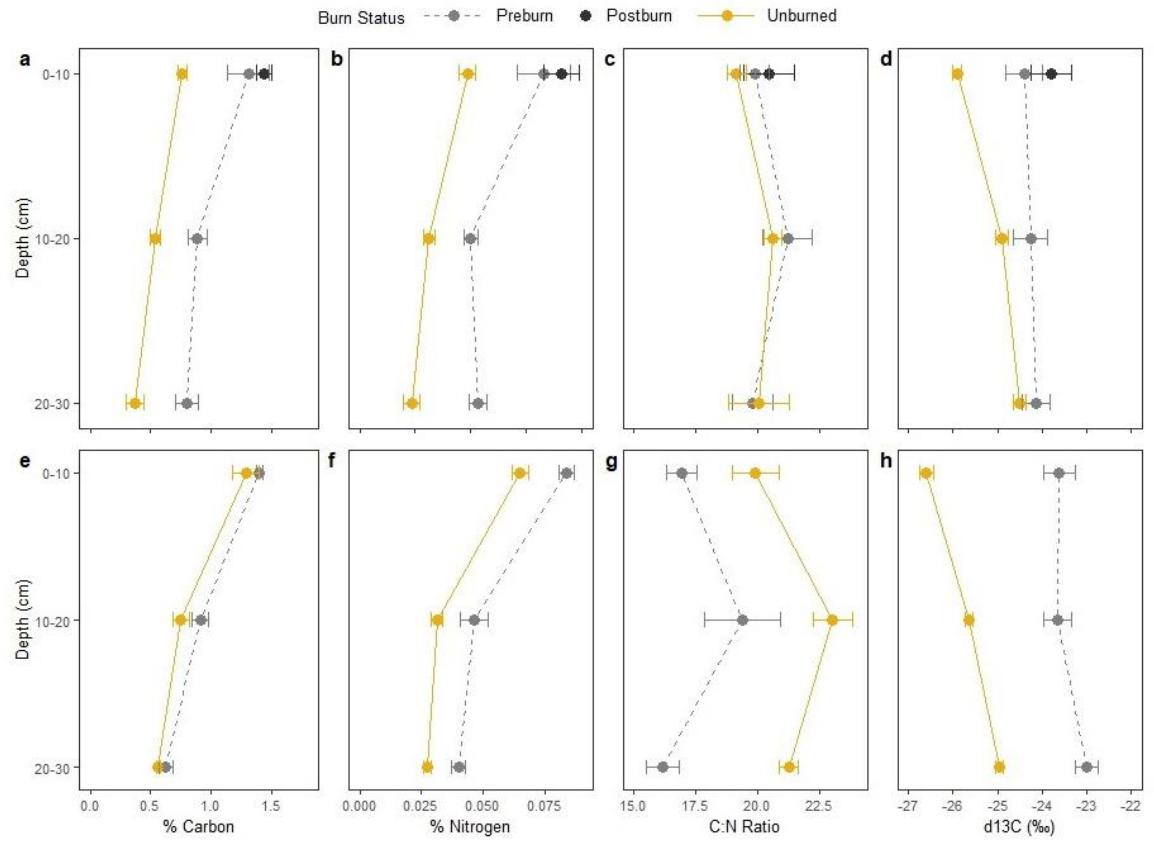


Figure 2.5. Average (a, e) percent carbon, (b, f) percent nitrogen, (c, g) carbon to nitrogen (C:N) ratio, and (d, h) δ^{13} C. Soils were collected in (a-d) April 2021 and (e-h) March 2022 from 0-10, 10-20, and 20-30 cm down the soil profile. Plots were either managed with regular Rx fire (Burned) or without (Unburned). Postburn samples were collected from Burned plots immediately after the 22 April 2021 Rx fire. Values represent the average of all cores (n = 4) across two analytical replicates.

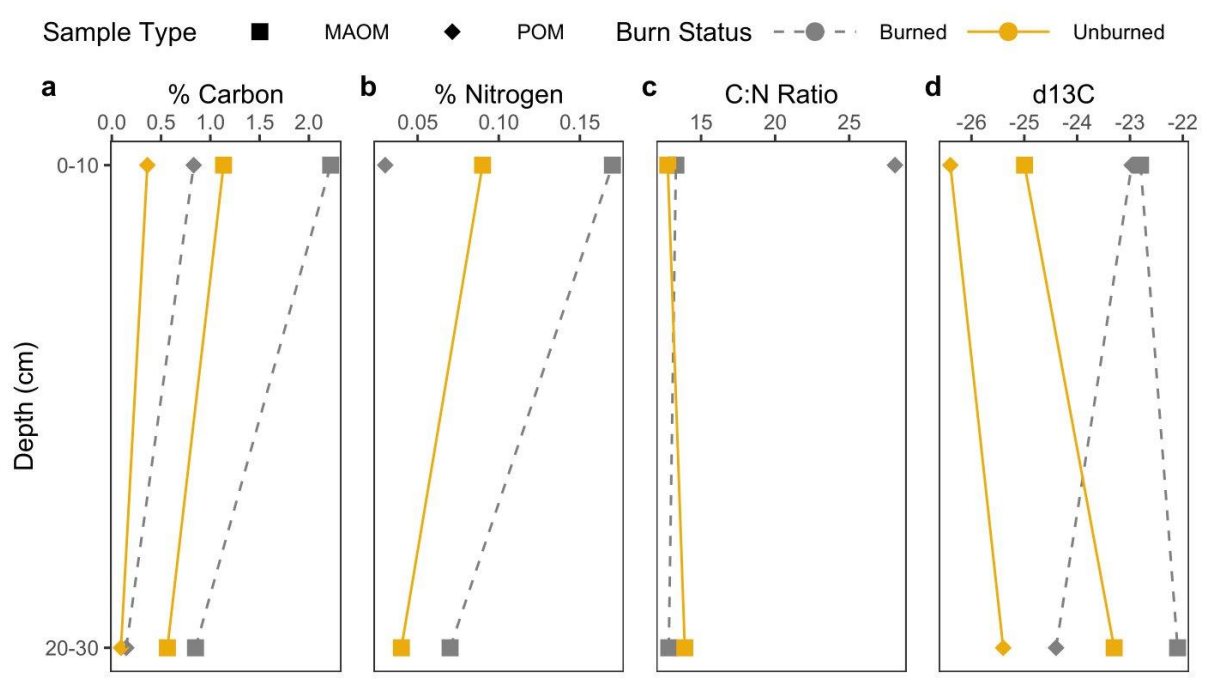


Figure 2.6 Average (a) percent C, (b) percent N, (c) C:N ratio, and (d) δ^{13} C in mineral associated (MAOM) and particulate (POM) organic matter fractions. Fractions were separated from soils (n=4) collected in April 2021 from stands managed with regular Rx fire (Burned) or without (Unburned). Values represent the average of two analytical replicates. Due to low organic matter content of soils, percent N and C:N ratio values are missing for Burned Stand POM from 20-30 cm and Unburned Stand POM for both depths.

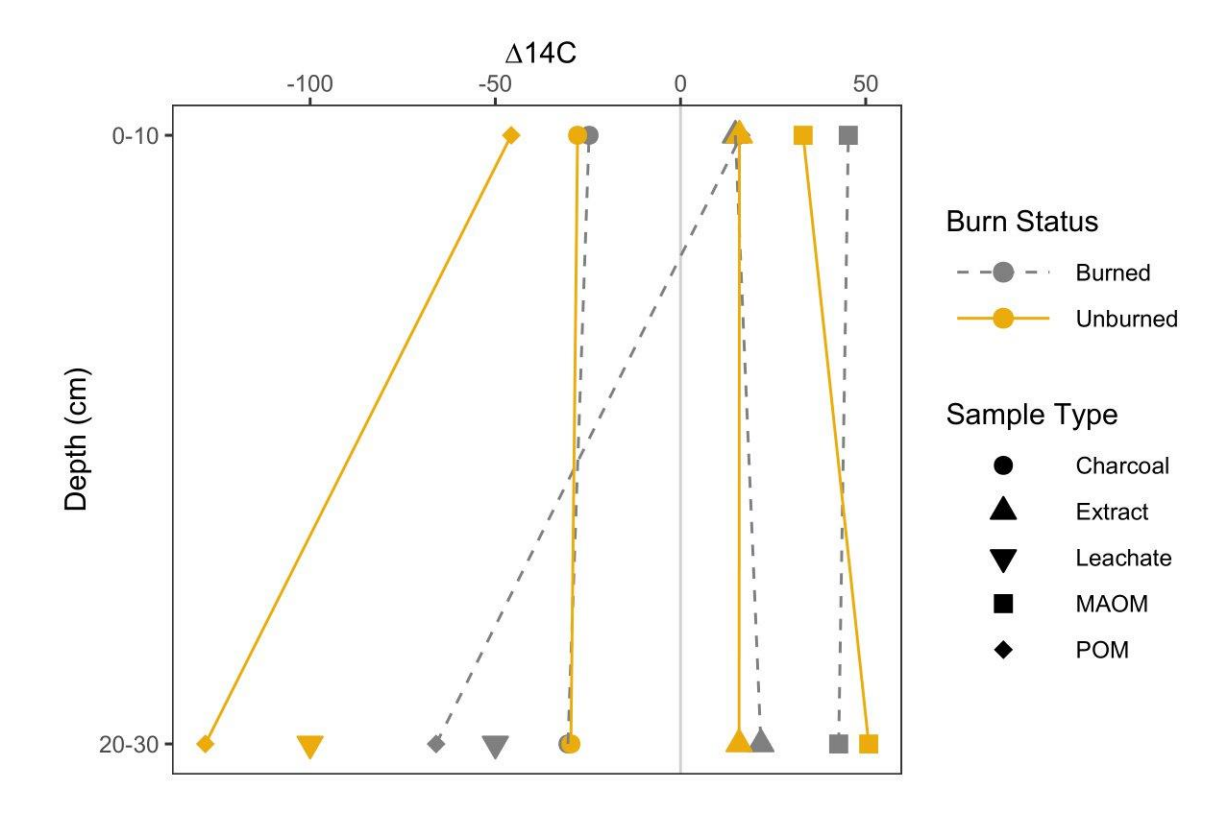


Figure 2.7. Radiocarbon content (Δ^{14} C) of charcoal, mineral-associated organic matter (MAOM), particulate organic matter (POM), and soil-water extract dissolved organic matter (DOM) samples collected from 0-10 and 20-30 cm in the soil profile. Leachate DOM samples were collected from lysimeters installed to 30 cm. The solid grey line indicates the separation between modern (Δ^{14} C>0) and premodern (Δ^{14} C<0) values. No standard error was calculated as each value was derived from one sample.

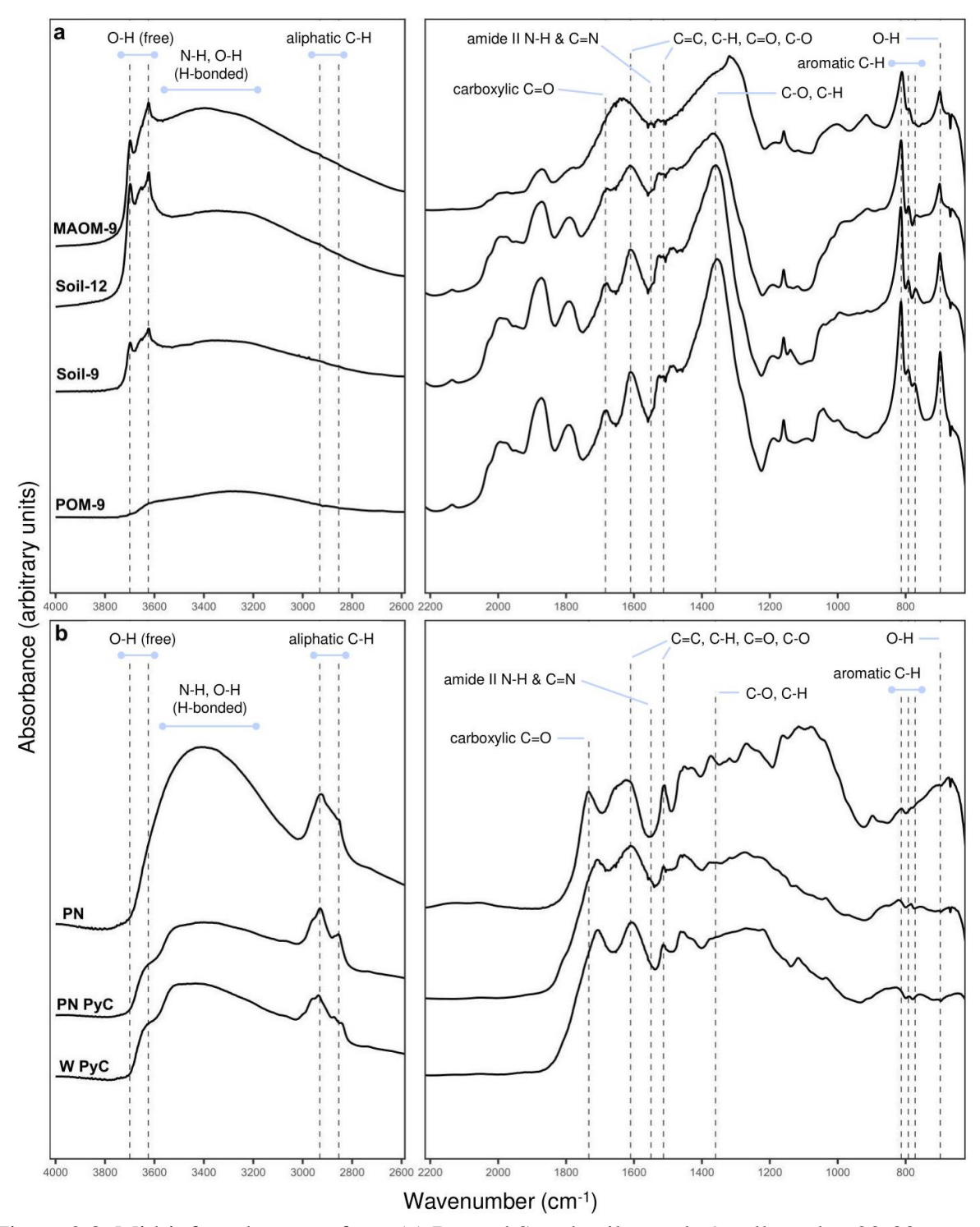


Figure 2.8. Mid-infrared spectra from (a) Burned Stand soil sample 9 collected at 20-30 cm with 16.2% clay, mineral associated organic matter (MAOM), and particulate organic matter (POM) separated from that core. Soil sample 12 has 28.2% clay content. Organic matter reference spectra (b) are longleaf pine needle (PN) and pyrogenic carbon made by pyrolyzing pine needles (PN PyC) and birch popsicle sticks (W PyC) at 350°C.

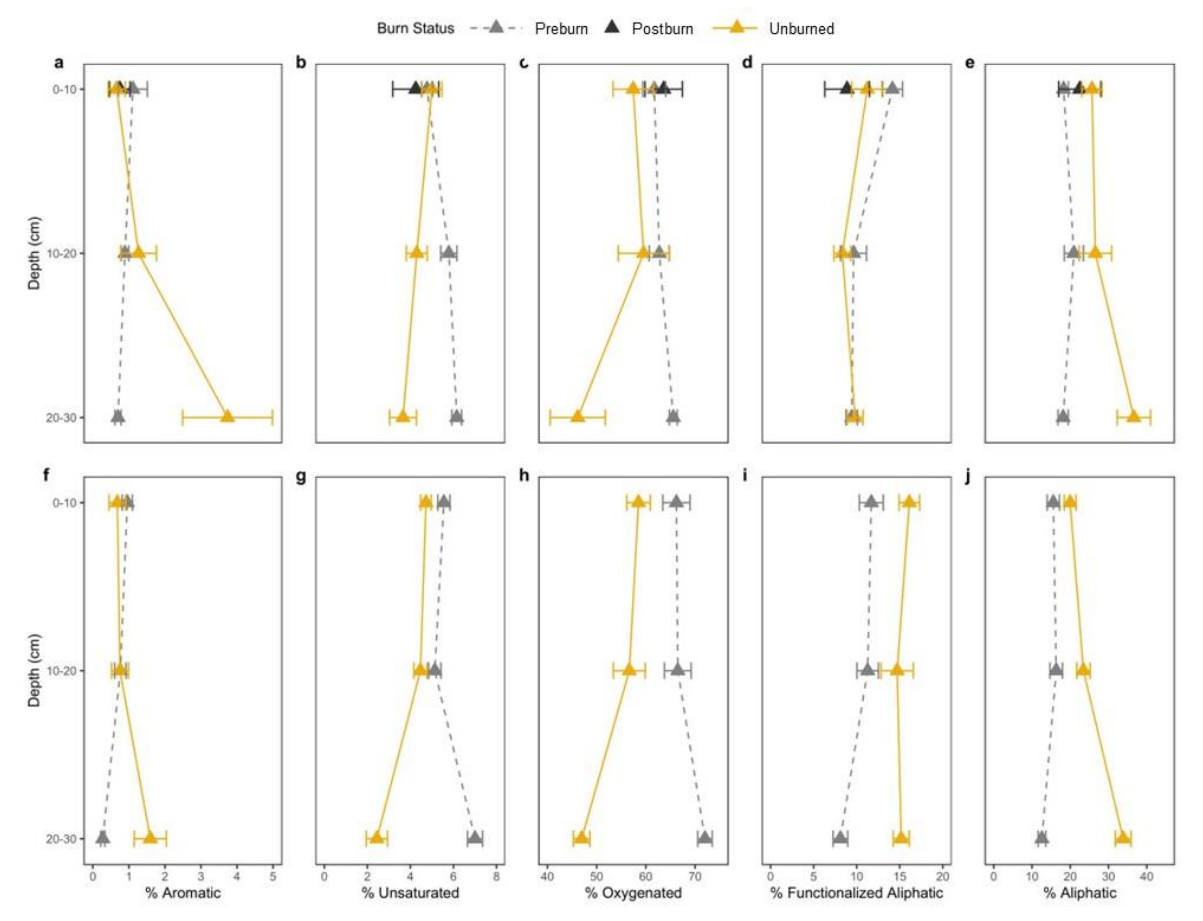


Figure 2.9. ¹H-NMR data depicting the average proportion of DOM which is composed of (a, f) aromatic, (b, g) unsaturated, (c, h) oxygenated, (d, i) functionalized aliphatic, and (e, j) aliphatic functional groups. Extracts were obtained from soils collected in (a-e) April 2021 and (f-j) March 2022 from 0-10, 10-20, and 20-30 cm down the soil profile. Plots were either managed with regular Rx fire (Burned) or without (Unburned). Postburn samples were collected from Burned plots immediately after the 22 April 2021 Rx fire.

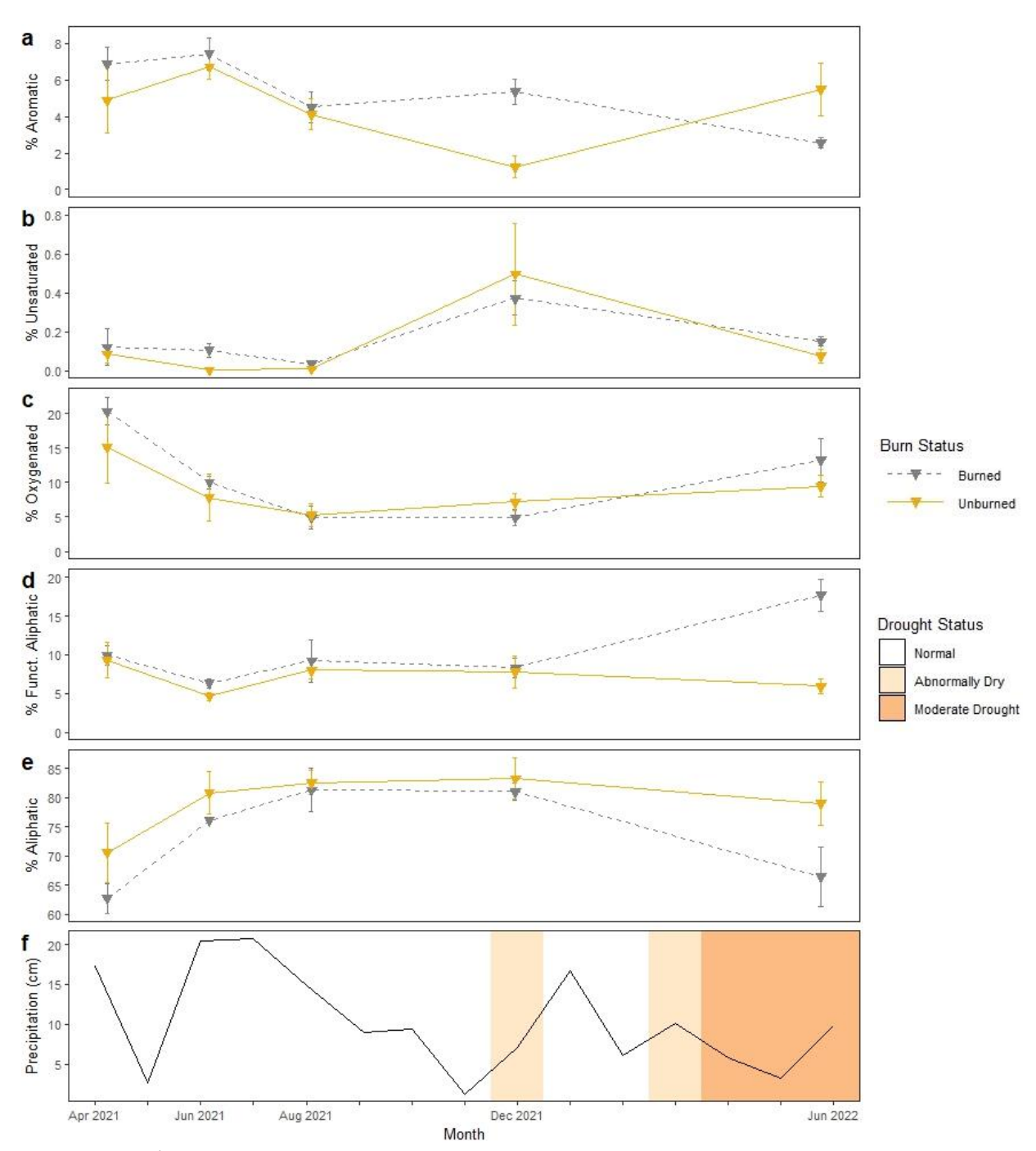


Figure 2.10. ¹H-NMR data showing changes in DOM functional group composition over the course of a 14-month sampling period. Values represent the average proportion of DOM which is composed of (a) aromatic, (b) unsaturated, (c) oxygenated, (d) functionalized aliphatic, and (e) aliphatic functional groups. Leachate samples were collected from lysimeters installed at 30 cm in forested stands managed with regular Rx fire (Burned) or without (Unburned). Precipitation data (f) are from the Coastal Plain Experimental Station (Georgia Automated Environmental Monitoring Network, 2023). Drought data (f) for Tift County are from the National Drought Mitigation Center's U.S. Drought Monitor tool.

CHAPTER 3

STABILITY OF CARBON IN STANDS MANAGED WITH AND WITHOUT PRESCRIBED FIRE

² Moss, A., Clabo, D., and Abney, R.B. 2023. To be submitted to *Journal of Geophysical Research: Biogeosciences*

3.1 Abstract

Prescribed (Rx) fire is widely employed in southeastern U.S. forests creating pyrogenic carbon (PyC), a relatively stable material that may be an important persistent (C) pool. Recent PyC incubation experiments have challenged the previous characterization of PyC as resistant to microbial decomposition; however, incubation experiments may overestimate degradability, highlighting the need to study PyC decomposition in-situ. We placed litterbags filled with pyrolyzed pine needles (PN PyC) and popsicle sticks (W PyC) on soils of longleaf pine stands managed with (Burned) and without (Unburned) regular Rx fire. We used a LI-COR soil flux analyzer to measure carbon dioxide respiration (R_s) from the forest floor every two months for one year. Soil cores collected at 0-10 cm and 10-20 cm were analyzed for total C, total nitrogen (N), δ^{13} C, and soil organic matter (OM) quality using mid-infrared spectroscopy. Fungal colonization of PyC was observed in litterbags collected at 7-months from both Burned and Unburned stands. R_s in the Burned and Unburned stands followed the same annual pattern, generally increasing along with annual temperature cycles. Overall, R_s was significantly higher in the Burned than the Unburned stands and was more variable. Annual harvest of pine needles coupled with soil OM loss during previous agricultural tillage likely contributed to lower soil C and N concentrations in Unburned than Burned stands. Soil C and N were higher in Burned than Unburned stands at 0-10 cm but not at 10-20 cm, indicating that OM is rapidly utilized.

3.2 Introduction

3.2.1 Forest Soil Carbon Cycling

Forests are an important global carbon (C) sink, storing about 45% of terrestrial carbon (Bonan, 2008). In general, within forested ecosystems about half of C is stored in soils, while the rest is split between various pools of live and dead plant material (Samuelson et al., 2014; Turner et al., 1995). Like all organic matter, soil carbon compounds originate from autotrophic organisms that use photosynthesis to convert atmospheric CO2 into biomass. In forest systems, this plant material makes its way into the soil through myriad processes, including leaf/needle abscission, bark shedding, root senescence, and transformation by microorganisms such as mycorrhizal fungi and rhizosphere associated bacteria (Baldock & Broos, 2011). Roots secrete carbon compounds to protect themselves from desiccation and entice microbes into mutualistic relationship (Sasse et al., 2018). Macrofauna carry organic matter through the soil via bioturbation, alter soil structure with aggregate-inducing compounds like glucans (Wolters, 2000), and themselves become soil organic matter. Once in the soil, organic matter may become stabilized through processes like aggregation and mineral association (Cotrufo et al., 2019), decomposed by heterotrophic organisms (Sanderman & Amundson, 2014), or transported offsite through erosion and leaching (Abney et al., 2017; Hagedorn & Machwitz, 2007).

3.2.2 Pyrogenic Carbon Formation Post-Fire

There has been considerable interest in planting and managing longleaf pine as a climate mitigation strategy (Susaeta, 2023) due to higher potential for C-sequestration when compared to other southern pines (Meldahl & Kush, 2006). In longleaf forests, the soil C can be the largest C pool, in some stands containing more carbon than above and belowground plant biomass combined (Samuelson et al., 2014). Many longleaf plantings occur on marginal, post-agricultural

lands with relatively low SOM (Markewitz et al., 2002), however there is potential for persistent C storage in these soils through the production of pyrogenic carbon (PyC) during Rx fires (Puhlick et al., 2023), which are necessary for maintaining longleaf dominant forest types (Loudermilk et al., 2011). Rx fire represents a loss of carbon dioxide (CO₂) as biomass is combusted (Starr et al., 2014), however the PyC, uncombusted material left behind, is often more resistant to decomposition than unburned OM (Glaser et al., 2000). PyC residence times can range from years to millennia and the controls on this variability are not well understood (Bird et al., 2015).

3.2.3 Decomposition of Pyrogenic Carbon in Soils

The chemical nature of PyC is influenced by the starting materials from which it is formed, as well as the temperature and duration of heating (Masiello, 2004). This range of materials formed under low to progressively higher temperatures is conceptualized as the combustion continuum (Hedges et al., 2000). The heterogeneity of these materials has implications for the fate of PyC in soil. For example, a low intensity prescribed fire which pyrolyzes mostly herbaceous understory material will produce PyC with less highly ordered structures than a crown fire which burns entire trees (Czimczik & Masiello, 2007; Hedges et al., 2000). PyC produced in the low intensity scenario may be more chemically reactive and thus susceptible to transformative processes in soils such as decomposition, chemical oxidation, physical fragmentation, and leaching (Hobley, 2019). Conversely, the crown fire PyC created at higher temperatures may be composed of more condensed aromatic structures, and thus be more chemically inert, with larger pore spaces which could increase its potential for adsorption.

Adsorbed compounds may provide PyC protection from degradation by intercepting microbial enzymes, but can also result in supramolecular structures that are more hydrophilic and thus

susceptible to leaching (Keiluweit et al., 2010; Masiello, 2004). The frequency with which fire is applied to the landscape can influence the soil microbial community, potentially shaping its ability to break down PyC (Brown et al., 2013). Recent PyC incubation experiments have challenged the previous characterization of PyC as resistant to microbial decomposition (Whitman et al., 2014b); however incubation experiments may overestimate degradability (Bird et al., 2015), highlighting the need to study PyC decomposition *in-situ*.

3.2.4 Impact of Rx Fire on Soil Respiration

Forest ecosystem properties likely recover quickly after Rx fire, however long-term changes to C cycling may also occur. (Flanagan et al., 2019). Starr et al. (2014) estimated that Rx fire constituted a loss of 408 and 153 g C m⁻² yr⁻¹ from fuel combusted during Rx fire in mesic longleaf pine and xeric longleaf pine-turkey oak stands, respectively. Factored into net ecosystem exchange, with a 2-year fire return interval these C losses transformed sites from a C-sink and C-neutral, respectively, into C-sources. There is interest in determining whether Rx-fire induced changes to soil C mineralization, through PyC production and changes to microbial community function, could offset C losses from combustion.

Soil respiration (R_s) is the total amount of carbon dioxide emitted from soils through a combination of autotrophic (R_a) and heterotrophic (R_h) respiration. R_a is produced by roots and R_s is released from soil organisms, especially microbes, during C mineralization (Bahn et al., 2010). R_a provides information about root density and plant photosynthetic activity, while R_h is often used as a proxy for microbial decomposition, however separating the two poses a significant methodological challenge due to the near impossibility of removing or excluding roots without altering microbial activity through soil disruption.

Rx fire has the potential to impact R_s through a variety of mechanisms. In the short term, the heating from Rx fire may cause microbial or fine root mortality in the upper soil layers. This is highly dependent on the extent of soil heating, but mortality of fine roots could lead to a reduction in R_a followed by a spike in R_h as soil microorganisms process the flux of senesced roots (Guo et al., 2004). Depending on the relative extent of this reallocation, it may or may not result in a net change to R_s . An immediate postfire flux of nutrients from deposited ash may stimulate R_h as microbes, particularly bacteria, rapidly utilize the available nutrients (Poth et al., 1995). During the postfire recovery phase, there could be an increase in R_a as plants regrow fine roots. In the long term, Rx fire can maintain a reduced litter layer, slowing carbon and nitrogen cycling and thus reducing R_h as less OM is available to decomposers (Gonzalez-Benecke et al., 2015). Rx fire-induced changes to plant composition, which may reduce lower overall biomass via reductions in the shrub layer and thinning of tree density, could influence R_a (Flanagan et al., 2019).

In general, it appears that Rx fire may impact R_s but not dramatically. White (1986) recorded a significant drop in R_s (measured as CO₂ g⁻¹ OM) in a ponderosa pine (*Pinus ponderosa*) stand after a low intensity Rx fire, but no significant difference in R_s between this stand and an unburned control. Concilio et al. (2005) found that a mixed-conifer stand managed with Rx fire did not produce R_s values that differed from unburned controls. Plaza-Álvarez et al. (2017) found no difference in R_s after a low intensity Rx fire in a Spanish black pine (*Pinus nigra* Arn. spp. *Salzmannii*) dominated forest. There is much left to be determined to quantify how site and Rx fire conditions influence R_s not only immediately post-fire but on annual scales.

3.2.5 Study Objectives and Hypotheses

The objective of our study was to use litterbags installed on the forest floor to compare *in-situ* decomposition of PyC in stands managed with (Burned) and without (Unburned) regular broadcast fire. We also used soil respiration monitoring to compare the loss of C to the atmosphere as R_s in Burned versus Unburned stands over a one year period. We hypothesized that 1) there would be a relative increase in aromatic functional groups in litterbag PyC over time as more labile material was preferentially decomposed 2) more rapid decomposition would be found in the Burned versus the Unburned stand due to a microbial community better adapted to utilize PyC.

3.3 Materials & Methods

3.3.1 Southeastern Plains

See Section 2.3.2 'Study Location."

3.3.2 Study Location

See Section 2.3.2 'Study Location."

3.3.3 Stand Descriptions

Burned Stand 1: This 4.3 ha, 90-year-old naturally-regenerated longleaf pine stand was never in agricultural production, as indicated by the presence of wiregrass and gopher tortoise (*Gopherus polyphemus*) burrows. The canopy was open with an understory characteristic of oldgrowth longleaf pine savannas; in addition to wiregrass there was a diversity of forbs such as sensitive briar (*Mimosa quadrivalvis*), ironweeds (*Vernonia spp.*) and goldenrods (*Solidago spp.*). The shrub layer (when present) was dominated by gallberry (*Ilex glabra*) and wax myrtle (*Morella cerifera*). The stand had been burned on a 3-year fire return interval since the mid-1980's and thinned three times during that period. Before that, fire was suppressed for an

unknown amount of time. When last inventoried in 2011, the basal area (excluding hardwoods) was 7.0 m² ha⁻¹. The stand was last burned April 22, 2021 (*see Section 2.3.4 "Prescribed Fire in the Burned Stand"*). Soils were primarily Cowarts loamy sand. Cowarts series are fine-loamy, kaolinitic, thermic Typic Kanhapludults.

Burned Stand 2: Stand composition, management history, and dominant soils in this stand were the same as Burned Stand 1. This stand consisted of 13.6 ha. It was burned during the study period in April 2022 (not part of the experimental plan) and was last burned approximately 3 years before that.

Burned Stand 3: Stand was planted during 1989 through the USDA FSA Conservation Reserve Program (CRP) with mostly slash, and some mature, volunteer loblolly pine. Previously, the stand was planted in peanuts. There was a higher stand basal area than Burned Stands 1 and 2, but the canopy was not closed, allowing for herbaceous understory. The stand was thinned twice, and when last inventoried in 2011, average basal area (excluding hardwoods) was 18.9 m² ha⁻¹. Due to its history of agriculture tillage, this stand did not have wiregrass. The stand was burned on a 3- to 4-year return interval since establishment. The stand was burned in 2015, then 2019, and was burned during the study period in February 2022 (not part of the experimental plan). Soils were primarily Cowarts loamy sand.

<u>Unburned Stand 1:</u> See "Unburned Stand" in Section 2.3.3..

<u>Unburned Stand 2:</u> This longleaf pine stand was planted in 2003 through CRP at 1,495 trees ha⁻¹. Before reforestation, the stand was in agricultural production with a crop rotation of peanuts and cotton. The stand was raked annually for pine straw in the winter to early spring. Small, randomly-spaced slash piles were burned as part of the raking process. Soils were

primarily Tifton loamy sand. Tifton series are fine-loamy, kaolinitic, thermic Plinthic Kandiudults (Soil Survey Staff).

<u>Unburned Stand 3:</u> Stand history and conditions were the same as Unburned Stand 2. Soils were primarily Stilson loamy sand. Stilson series are loamy, siliceous, subactive, thermic Oxyaquic Paleudults (Soil Survey Staff).

3.3.4 Production of Pyrogenic Carbon Litterbags

Pyrogenic carbon was produced to assess PyC decomposition *in-situ*. Longleaf pine needles and birch wood popsicle sticks were trimmed to ~2 cm pieces. Wide-form porcelain crucibles (Fisher Scientific, Waltham, MA, USA) were filled to approximately two-thirds of 250 mL capacity with either 60 g wood or 15 g pine needle pieces. Crucibles were tightly enclosed with aluminum foil to minimize airflow and pyrolyzed in a muffle furnace at 350 °C for 1 hour to simulate a low-intensity fire (Abney et al., 2019a; Majidzadeh et al., 2015). Ten-centimeter square litterbags were constructed out of 1 mm black fiberglass window screen mesh stapled together to form a pouch. The mesh material was double-layered to minimize loss of PyC while allowing access to fungal hyphae, soil microfauna, and smaller mesofauna. Litterbags were filled with either 1.5 g pine needle PyC or 3 g wood PyC. The two weights reflect an attempt to standardize the volume of PyC in the bag despite a difference in densities. Each litterbag was assigned a unique ID and labeled with an aluminum tag.

3.3.5 Plot Establishment, Soil Sampling, & Soil Preparation

In each of the six stands, one 5 x 5 m plot was established (Fig. 3.2) on 17 August 2021. One 20 x, 11 cm PCV collar was installed in each corner of the plot using a rubber mallet and wooden board to evenly distribute force (n=4 per plot). Aboveground vegetation was excluded

by using pruners to gently clip all plants growing within the collar as close as possible to the ground without disturbing the soil.

Eight paired PyC litterbags (four each PyC type) were deposited at the soil surface in a grid in the center of the plot, with the middle square of the grid empty (this is where soil core B was collected). In Unburned stands, the canopy is closed resulting in a relatively empty understory. Herbaceous plants in these stands are considered weeds and often treated with herbicide to prepare the stands for pine straw raking, so litterbags were placed onto a relatively exposed soil surface with a light covering of longleaf pine needles. Burned Stands have lower basal area and an understory dominated by grasses and forbs; litterbags were placed as close as possible to the soil surface where bare spots could be found between bunch grasses.

To collect soils, the organic layer was brushed aside and a hand auger was used to remove soil cores at two depths (0-10 cm and 10-20 cm) in three replicates down the center of each plot (Fig. 3.2), with adjacent bulk density cores at 0-10 cm. *See section 2.3.5 "Soil Sampling & Preparation" for further details*.

3.3.6 Bulk Soil Analysis

See section 2.3.10 "Bulk Soil Analysis" for details.

3.3.7 Soil Organic Matter Characterization

Ground soil samples (n=36) were sent to University of New Mexico Center for Stable Isotopes for total C, total N, and δ^{13} C analysis. *See section 2.3.11 "Soil Organic Matter Characterization" for further details.*

Organic matter composition of all soil samples (*n*=36), PyC (*n*=2), and unburned longleaf pine needle was spectroscopically characterized using a Thermo Scientific Nicolet iS10 FT-IR Spectrometer (ThermoFisher Scientific, Waltham, MA, USA) operated with OMNIC Series

Software (ThermoFisher Scientific, Waltham, MA, USA). See section 2.3.11 "Soil Organic Matter Characterization" for further details.

3.3.8 Litterbag Collection

Litterbags were collected on 20 September 2021, 23 November 2021, 29 March 2022, and 24 October 2022—approximately one-, three-, seven-, and fourteen months after they were installed at the soil surface. The initial sampling plan was to collect one litterbag of each PyC type from each plot for every sampling event (except for the one-month sampling, when two of each type were collected). However, due to miscommunication with the landowner, two Rx fires were conducted—one in Burned Stand 3 in February 2022 and another in Burned Stand 2 in April 2022—without our knowledge. These fires burned through the plots, compromising our initial plan to assess PyC mass loss over time. We adjusted our strategy to focus on culturing fungi growing on litterbag PyC. Litterbags collected in March and October 2022 were stored in a walk-in refrigerator at 4 °C for approximately one week until they were transferred to the lab of Dr. Anny Chung for fungal culturing. Michelle Henderson, Shafat Zaman, and Dr. Anny Chung will be spearheading a pyrophilic fungi metabolism project, which is outside the scope of this thesis.

3.3.9 Soil Carbon Dioxide Flux Sampling

Soil CO₂ flux was recorded approximately every two months for one year using a LI-870 CO₂/H₂O analyzer fitted with an 8200-01S Smart Chamber and 6000-09TC Soil Probe (LI-COR Biosciences, Lincoln, NE, USA). Sampling dates were 27 September 2021, 23 November 2021, 12 January 2022, 29 March 2022, 8 May 2022, and 20 July 2022. Before each reading was taken, a ruler was used to record collar height and hand pruners were used to gently trim any vegetation growing within the PVC collar back to the soil surface. Trimming was done to minimize the

analyzer reading any leaf-derived gas emissions. Any material external to the collar which would interfere with the chamber's ability to form a seal was also trimmed back. Soil CO_2 flux (R_s), recorded as μ mol m⁻² s⁻¹, was measured for one minute across three replicates. Measurements were between 10:00 and 16:00 h to minimize effects of diurnal fluctuation. The probe was inserted into soil adjacent to the collarr and used to record soil moisture and temperature readings.

3.3.10 Statistical Analysis

Total carbon, total nitrogen, C:N ratio, δ^{13} C, and pH were analyzed for differences across treatment groups using mixed linear effects models run with the lmer() function as described previously (see section 2.3.12 "Statistical Analysis"). We included burn status and depth as fixed effects with and without an interaction. Models were selected using AIC as described previously. Site and soil core ID were included in the model as random effects. The effect of burn status on bulk density was analyzed using a one-way ANOVA and the Anova() function, with pairwise comparisons as described previously.

The effect of burn status and sampling date on soil CO₂ flux was analyzed using a mixed linear effects model. We included burn status and sampling date as fixed effects with and without interaction. After calculating AIC for both models, we selected the model without interaction. Site and collar ID were included in the model as random effects.

Data were collected in either a lab notebook (lab experiments) or data sheet (field experiments) then organized and archived in Microsoft Excel. Statistical analyses and data visualizations were completed in R version 4.2.0 (R Core Team, 2020) using the ggplot2 package (Wickham, 2016). For all linear mixed effects models, significance was determined using a likelihood ratio test as described previously.

3.4 Results

3.4.1 Bulk Soil Analysis

Soil physical and chemical characteristics are summarized in Table 3.1. Average topsoil bulk density was significantly ($F_{1,16} = 23.203 p = 0.0002$) higher in the Unburned than in the Burned Stands (for full model results see Appendix B, Figure B.7. Soils at both depths in both Burned and Unburned stands were all determined by particle size distribution to be sandy loam.

Soils were acidic, with pH values ranging from 4.80 to 5.52 in H₂O and 4.11 to 4.83 in CaCl₂. Overall, pH was slightly higher in the Unburned than the Burned stands, but this was not statistically significant when measured in H₂O (χ^2 (1) = 1.190, p = 0.28) or in CaCl₂ (χ^2 (1) = 0.495, p = 0.4). For both Burned and Unburned treatments, pH decreased significantly with depth when measured in H₂O (χ^2 (1) = 11.616, p = 0.0007) and CaCl₂ (χ^2 (1) = 46.288, p < 0.0001). For full model results see Appendix B, Figures B.5 and B.6.

3.4.2 Soil Organic Matter Characterization

Organic matter concentrations were low in both the Burned and Unburned stands, with C ranging from 0.6% to 1.5% and N from ~0.02% to 0.05% (Fig. 3.3). Percent C was significantly higher in Burned stands (χ^2 (2) = 22.537, p < 0.0001) than Unburned, and both C (χ^2 (2) = 46.437, p < 0.0001) and N (χ^2 (1) = 40.328, p < 0.0001) decreased significantly with depth. The C:N ratio was 27.2 in Burned stand 0-10 cm soils and 25.6 at 10-20 cm, which was significantly (χ^2 (1) = 40.328, p < 0.0001) higher than in Unburned stands, where topsoil C:N ratio was 19.1 and increased to 22.1 with depth. Carbon-13 isotope values ranged from -26.1% to ~-24.9%, increasing significantly with depth (χ^2 (1) = 88.168, p = <0.0001) and with no significant difference between Burned and Unburned stands (χ^2 (1) = 1.492, p = 0.23). For full model results see Appendix B, Figures B.1 through B.4.

To facilitate qualitative comparison, absorption spectra of soils from Burned Stand 1 and Unburned Stand 1 were plotted (Fig. 3.4) along with spectra from dried longleaf pine needle (PN), longleaf pine needle PyC (PN PyC), and birch popsicle stick PyC (W PyC). Soils depicted were collected from 0-10 cm and are very similar in texture, though Burned Stand 1 has a slightly higher clay content (13.0%) than the Unburned soil (11.4%). For the purposes of discussion, these soils will be referred to as the Burned and the Unburned soil.

Peaks at 3700 and 3625 cm⁻¹ are associated with stretching of free alcoholic and phenolic hydroxyl O-H (Fig. 2.8), including O-H stretching of hydroxyl groups in clay (Nguyen et al., 1991), in particular kaolinite (Guillou et al., 2015). These peaks are absent in the pine needle sample but present as a small shoulder on the larger intermolecular O-H peak in the PyC. The free O-H peaks are more prominent in the Burned than the Unburned soil. From 3200-3600 cm⁻¹ there is a broad peak created by intermolecularly bonded O-H and N-H stretching (Parikh et al., 2014) which has greatest absorption in the fresh pine needle sample – this can be observed to decrease substantially with charring as O-containing plant materials like cellulose are transformed by dehydration. This peak is larger in the Burned than the Unburned Soil. Peaks at 2931 and 2854 cm⁻¹, which are associated with asymmetric and symmetric aliphatic C-H stretching, respectively, are quite small in soil samples when compared to the OM references (Hall et al., 2018). They are slightly more prominent in the Burned than the Unburned soil. There is a reduction in aliphatic peak absorbance from uncharred to charred pine needles (PN PyC), another indication that cellulose-associated functional groups are destroyed with charring (Keiluweit et al., 2010).

A series of three peaks between 1790 and 2000 cm⁻¹ were observed, and these are commonly associated with quartz overtones from sand (Calderón et al., 2011; Nguyen et al.,

1991). Logically, these quartz peaks are absent in the OM references. The peak presenting at 1684 cm⁻¹ in soil, 1733 cm⁻¹ in pine needles, and 1710 cm⁻¹ in PyC samples was interpreted as carboxylic acid C=O (Calderón et al., 2011; Strakova et al., 2020) with possible contribution from C=O stretching in aldehydes and ketones. A peak at 1610 is interpreted frequently as aromatic C=C, carboxylate C=O, and some combination of the two (Calderón et al., 2011; Kaiser et al., 2012). Some studies also assign conjugated carbonyl C-O, ketone C=O, and aromatic C-H deformations to this peak (Parikh et al., 2014). This peak becomes sharper with charring, most significantly in the wood PyC (e.g., POM, pine needle and wood PyC), suggesting aromatic functional groups are the largest contributors. A second peak associated with aromatic C=C was identified at 1513 cm⁻¹. This peak was sharpest in the pine needle and shrunk with charring, consistent with studies where it has been assigned in particular to lignin (Parikh et al., 2014). In a study by Calderón et al. (2013), charring of corn stover reduced absorbance in this region from a sharp peak in fresh material to none at all for biochar pyrolyzed at 500 °C. Modelling approaches consider a decrease in this area relative to other aromatic regions to indicate increasing PyC content (Chatterjee et al., 2012).

A series of regions associated with amides suggest proteinaceous materials, such as microbial biomass. A very small deformation at 1550 cm⁻¹, is slightly more prominent in the Burned than the Unburned soil, and can be attributed to amide II N-H bending and C-N stretching (Parikh et al., 2014). This may indicate a larger proportion of proteins from microbial biomass. A corresponding peak at 1641 cm⁻¹, which is associated with amide I C=O stretching is obscured by the deformation from clay which occurs in the same region. The amide I peak presents as a shoulder on the larger 1610 cm⁻¹ peak but is quite flat in both the Burned and Unburned soils suggesting no difference in contribution from this functional group.

The large peak at 1360 cm⁻¹ is attributed mainly to C-O from carboxylate and phenolic groups, with contributions from ester C-O and aliphatic C-H. This is the most prominent peak in the soils, larger and sharper in the Unburned soil, but not the OM references. Conversely, the region from about 1190 to 1000 cm⁻¹, frequently associated with C-O-C esters and aliphatic O-H groups indicative of cellulose, hemicellulose, and other polysaccharides, (Keiluweit et al., 2010; Parikh et al., 2014) is prominent in the pine needle sample as a broad and complex series of peaks that do not exist in the soils. This region becomes more flattened in the pine needle PyC as fresh plant components are transformed during pyrolysis. A series of peaks from 885 to 752 cm⁻¹ are associated with aromatic C-H out of plane aromatic deformations, with degree of substitution decreases with decreasing wavenumber (Keiluweit et al., 2010; Parikh et al., 2014). However the sharp, tall peak at 813 cm⁻¹ followed by two smaller peaks at, 792, and 722 cm⁻¹ seen in soil closely resembles an absorbance pattern indicating O-Si-O bonds in quartz (Calderón et al., 2013; Guillou et al., 2015). If the smaller aryl C-H peak we see in pine needle and biochar samples are present in soils, they are obscured by, or incorporated into, the stronger signal from quartz. Keiluweit et al. (2010) speculated that peaks near 815 and 750 cm⁻¹ in biochar spectra indicate O-containing aromatic structures such as quinones. A small, sharp peak at 672 cm⁻¹, which is most prominent in the POM and whole soil, can be attributed to alcohol O-H out of plane bending (Parikh et al., 2014) and is also attributed to O-Si-O bands (Guillou et al., 2015). This peak has also been identified in biochar but is not present in our PyC samples (Parikh et al., 2014).

3.4.3 Soil Carbon Dioxide Flux

Two Rx fires Burned through Stands during our study period, impacting soil CO₂ flux monitoring. The February 2022 Rx fire occurred in Burned Stand 3 and was of sufficiently low

intensity that PVC collars were only lightly impacted and could still be sampled on 29 March 2022. The Rx fire in April 2022 occurred in the Burned Stand 2 during a hotter month and in a stand with higher fuel loading. This fire created deformations in the PVC collars severe enough that CO2 flux could not be read on 8 May 2022, so these values are missing from the analysis. New collars were installed on 16 June 2022 and used during the final reading on 20 July 2022.

Average soil CO₂ flux ranged from a low of 0.24 μ mol m⁻² s⁻¹ in Unburned stands during January 2022 to a high of 1.09 μ mol m⁻² s⁻¹ in Burned stands during September 2021 (Fig. 3.5). Overall, CO₂ flux in the Burned Stands were significantly higher (χ^2 (1) = 4.330, p = 0.04) and more variable than fluxes in the Unburned Stands, though between-treatment differences were not as pronounced for soil respiration values recorded in March and July of 2022. *For full model results see Appendix B, Figure B.8*.

3.5 Discussion

We conducted a comparison of SOM cycling within soils of longleaf pine stands managed with regular Rx fire versus those raked for pine straw. We expected that decomposition of PyC in litterbags would be more rapid in regularly burned than in unburned stands. We were not able to test this hypothesis due to destruction of litterbag OM during two Rx fires unplanned by researchers. Litterbags did experience fungal colonization, and fungi were collected and cultured for future research. R_s was higher in the Burned than the Unburned stands and all stands followed the same seasonal trend. Carbon and nitrogen stocks were lower in the Unburned stands at 0-10 cm but not 10-20 cm, suggesting OM is rapidly utilized.

3.5.1 Soil Carbon Dioxide Flux was Higher in Burned than in Unburned Stands

Both Burned and Unburned Stand R_s followed a seasonal pattern that generally mimicked annual temperature trends. This is consistent with other studies conducted in longleaf and other

ecosystems (McCarthy & Brown, 2006; Plaza-Álvarez et al., 2017; Starr et al., 2014).

ArchMiller and Samuelson (2016) found that R_s in longleaf pine stands was significantly less temperature sensitive during drought. Overall, Burned stands were located in more upland positions, with lower soil moisture, and would have been more impacted by the effects of a moderate drought from spring through summer 2022. This may be a reason why we see higher Rs in Burned stands than Unburned stands throughout the year, except for during March and July 2022 (during the drought period).

Significantly higher R_s was measured in Burned versus Unburned stands. Though studies comparing similar treatments in longleaf pine are not extensive, our results seem to oppose the established trend. (Callaham et al., 2004) measured R_s in a mixed pine (*Pinus taeda* and *Pinus* virginiana) hardwood stand in the South Carolina piedmont found that burning significantly reduced R_s in both burned and thinned and burned plots, but not plots that were thinned only. (Godwin et al., 2017) found that R_s in north Florida burned, open canopy mixed-pine stands had lower monthly mean R_s, and estimated annual soil C fluxes, than closed canopy mixed hardwood stands where fire had been excluded. Soil temperature may be an important contributor to these results. (Samuelson & Whitaker, 2012) found that R_s was more strongly influenced by soil temperature than to basal area and other stand structural characteristics. While soil temperature was not factored into our analysis, the open structure of Burned stands resulted in plots that were less shaded by forest canopy than plots in Unburned stands. Other studies have found that soil temperature explained temporal variation, but not between-treatment characteristics (Godwin et al., 2017). Further analysis of these data factoring soil temperature into the statistical model are required to investigate this phenomenon.

3.5.2 Impact of Stand Management on Soil Organic Matter Quality and Persistence

Bulk density was higher in Unburned than in Burned stands, which is expected given the higher rate of OM inputs to soil in Burned stands, compared to Unburned stands where needle cast is removed annually. A key factor controlling bulk density is tillage history: bulk density is higher in Burned Stand 3, which was formally row cropped, compared to Burned Stands 1 and 2. Agricultural legacy effects may also explain pH dynamics. Contrary to what is generally observed in both longleaf and most other landscapes managed with Rx fire (Alcañiz et al., 2018; McKee, 1982), pH was lower in the Burned than Unburned stands, though not significantly. Looking closer, we see that pH at 10-20 cm is highest in the previously cropped stands. This may be an effect of previous managers adding lime to neutralize naturally acidic Coastal Plain soils for major crops cotton, corn, and peanuts, which all require a soil pH of ~6-6.5 (Gascho & Parker, 2001).

Our models found that C and N stocks were significantly higher in Burned than in Unburned Stands, but this difference narrowed substantially with depth, indicating OM is rapidly utilized by microbes in Burned stand soils. The C:N ratio in Burned stand soils was significantly higher, signaling a greater proportion of fresh plant material, which declined with depth. C:N ratio in the Unburned stands increased with depth, which was somewhat unexpected but may be related to input from pine tree roots at this depth. Prominence of the carboxylate, ester C-O peak compared to peaks indicating fresher OM (e.g. the cellulosic region ~1190 cm⁻¹, aliphatic peaks at 2931 and 2854 cm⁻¹) suggests highly decomposed, fast cycling SOM (Hall et al., 2018). The C/N stocks were low, but within expected concentrations for these soil series (Soil Survey Staff). Due to the complexity of the main OM informational region (1750-1210 cm⁻¹) in mid-IR spectra (Guillou et al., 2015), estimation of PyC proportions will require modelling techniques that are

beyond the scope of this thesis (Chatterjee et al., 2012; Cotrufo et al., 2016; Uhelski et al., 2022). Thus, we are not able to present a comparison of PyC stocks across Burned and Unburned stands at this time. Observationally, there appeared to be some differences between Burned and Unburned stand soils, which indicate the presence of fresher OM in Burned stand soils. This may correspond with differences in total C and N and C:N ratio across stands and is likely controlled by management differences: there is an herbaceous understory and fine roots adding fresh OM, plus PyC addition every ~3 years. Unburned stands also have fresh OM added by fine roots and associated ectomycorrhizal fungi, however the lack of understory vegetation, annual pine needle removal, and a loss of legacy lateral and taproot necromass during the agricultural era (Anderson et al., 2018; Markewitz et al., 2002) likely reduced the contribution of O-H containing functional groups in this stand. Our ability to interpret these O-H regions is complicated as they tend to co-occur with clay-associated spectral regions and clay % is slightly higher in the Burned than the Unburned stand soils.

Our aim of assessing whether regular Rx fire influenced the ability of the soil microbial community to decompose PyC was compromised by external circumstances. Fungi were observed colonizing PyC in litterbags collected at 7 months (Fig. 3.7). Anecdotally, more fungal hyphae were observed growing on litterbags in the Unburned than the Burned stands. This suggests that fungi utilizing PyC could be a generalist strategy, or that legacy PyC in Unburned stand soils persisted in high enough concentrations to maintain a PyC degradation-associated fungal community. Litterbags in the Unburned stands existed in a more fungal-friendly microenvironment (under a bed of fall needlecast, with cooler, moister soils due to closed canopy conditions). Furthermore, fungal growth on PyC does not necessarily mean the substrate is being consumed. Future studies will investigat the metabolic capabilities of these isolated organisms.

3.5.3 Future Directions and Limitations

A primary limitation of this study was the destruction of our decomposition experiment by unexpected Rx fire. As a result, R_s and bulk soil data collected originally to support our *insitu* PyC decomposition experiment, which was to be measured by mass loss and characterized by MIR qualitative description, became our primary data. However, the experimental design of our plots is not sufficient to capture the variability required for an in-depth study of longleaf pine R_s. MIR spectroscopy can help us compare the quality of SOM at two depths across stand management types, and potentially (semi)quantify PyC. Quantitative analysis of this rich and complex data requires sophisticated modelling approaches which are outside the scope of this thesis. Future directions for the mid-IR dataset may include quantifying PyC in a subset of samples using benzene polycarboxylic acid (Brodowski et al., 2005b) or hydrogen pyrolysis (hypy) (Wurster et al., 2013), then using these data to calibrate MIR coupled with partial least squares regression (Cotrufo et al., 2016).

3.6 Conclusion

As a result of unexpected Rx fire, results from this study are shifted away from direct quantification of *in-situ* PyC decomposition and towards a more general assessment of how Rx fire versus pine straw harvesting influences the C dynamics in longleaf and longleaf-slash stands under these management regimes. Total C and N was higher in Burned than Unburned stand 0-10 cm soils, likely due to fresh SOM inputs, but this difference disappeared at 10-20 cm suggesting rapid decomposition. R_s was higher in Burned than in Unburned stands, but because our study design does not allow for partitioning of heterotrophic and autotrophic respiration, we are not able to tie this difference to SOM turnover.

Tables 3.7

Table 3.1. Bulk soil chemical and physical properties

Depth (cm)	Bulk Density	pH in H ₂ O	pH in CaCl ₂	Sand %	Silt %	Clay %	%N	%C	C:N	$\delta^{13}\mathrm{C}$
Burned Stand 1										
0-10	0.99 (0.19)	5.07 (0.05)	4.43 (0.06)	75.5 (0.3)	11.5 (0.3)	13.1 (0.1)	0.06 (0.00)	1.6 (0.1)	25.8 (1.3)	-26.4 (0.0)
10-20	-	4.89 (0.03)	4.42 (0.01)	76.1 (0.9)	10.3 (0.4)	13.7 (0.6)	0.03 (0.00)	0.6 (0.1)	22.8 (1.0)	-25.0 (0.1)
Burned Stand 2										
0-10	0.82 (0.12)	4.80 (0.07)	4.17 (0.06)	76.3 (0.1)	10.9 (0.6)	12.9 (0.1)	0.07 (0.02)	2.3 (0.6)	31.6 (0.9)	-26.2 (0.2)
10-20	-	4.95 (0.02)	4.38 (0.01)	77.1 (0.2)	10.2 (0.2)	12.7 (0.1)	0.03 (0.00)	0.9 (0.1)	30.3 (0.6)	-25.2 (0.2)
Burned Stand 3										
0-10	1.37 (0.10)	5.06 (0.04)	4.24 (0.03)	78.0 (0.4)	9.9 (0.7)	12.2 (0.4)	0.03 (0.00)	0.7 (0.0)	24.4 (0.5)	-25.8 (0.2)
10-20	-	5.31 (0.03)	4.65 (0.01)	77.8 (0.2)	10.3 (0.3)	11.9 (0.4)	0.03 (0.00)*	0.4 (0.0)	23.3 (0.4)*	-24.4 (0.2)
Unburned Stand 1										
0-10	1.55 (0.04)	4.86 (0.05)	4.11 (0.03)	79.7 (0.3)	8.4 (0.2)	12.0 (0.3)	0.04 (0.00)	0.7 (0.0)	19.0 (0.2)	-25.6 (0.1)
10-20	-	5.03 (0.04)	4.42 (0.02)	79.1 (0.3)	8.9 (0.3)	12.0 (0.1)	0.03 (0.00)	0.6 (0.0)	21.0 (0.5)	-25.2 (0.1)
Unburned Stand 2										
0-10	1.60 (0.03)	5.52 (0.02)	4.83 (0.03)	77.1 (0.1)	10.5 (0.1)	12.4 (0.1)	0.03 (0.00)	0.7 (0.1)	19.4 (0.5)	-25.9 (0.1)
10-20	-	5.47 (0.04)	4.76 (0.04)	77.7 (0.1)	9.27 (0.1)	13.0 (0.1)	0.02 (0.00)	0.5 (0.0)	21.8 (0.3)	-24.3 (0.2)
Unburned Stand 3										
0-10	1.61 (0.04)	5.03 (0.04)	4.25 (0.03)	78.8 (0.4)	9.5 (0.4)	11.7 (0.4)	0.04 (0.00)	0.8 (0.0)	18.9 (0.4)	-25.9 (0.3)
10-20	-	5.20 (0.07)	4.51 (0.07)	77.6 (0.2)	10.7 (0.4)	11.7 (0.2)	0.02 (0.00)	0.6 (0.0)	23.5 (0.3)	-24.8 (0.2)

Values are reported as mean (standard error) with n=3 replicates. *missing value, n=2

3.8 Figures

Brumby Property - Tifton, GA Burn Status Unburned 0.38 0.75 1.5 km ZZZ Burned

Figure 3.1. Map of the study location highlighting relevant stands and research plots. The white line indicates property boundaries.

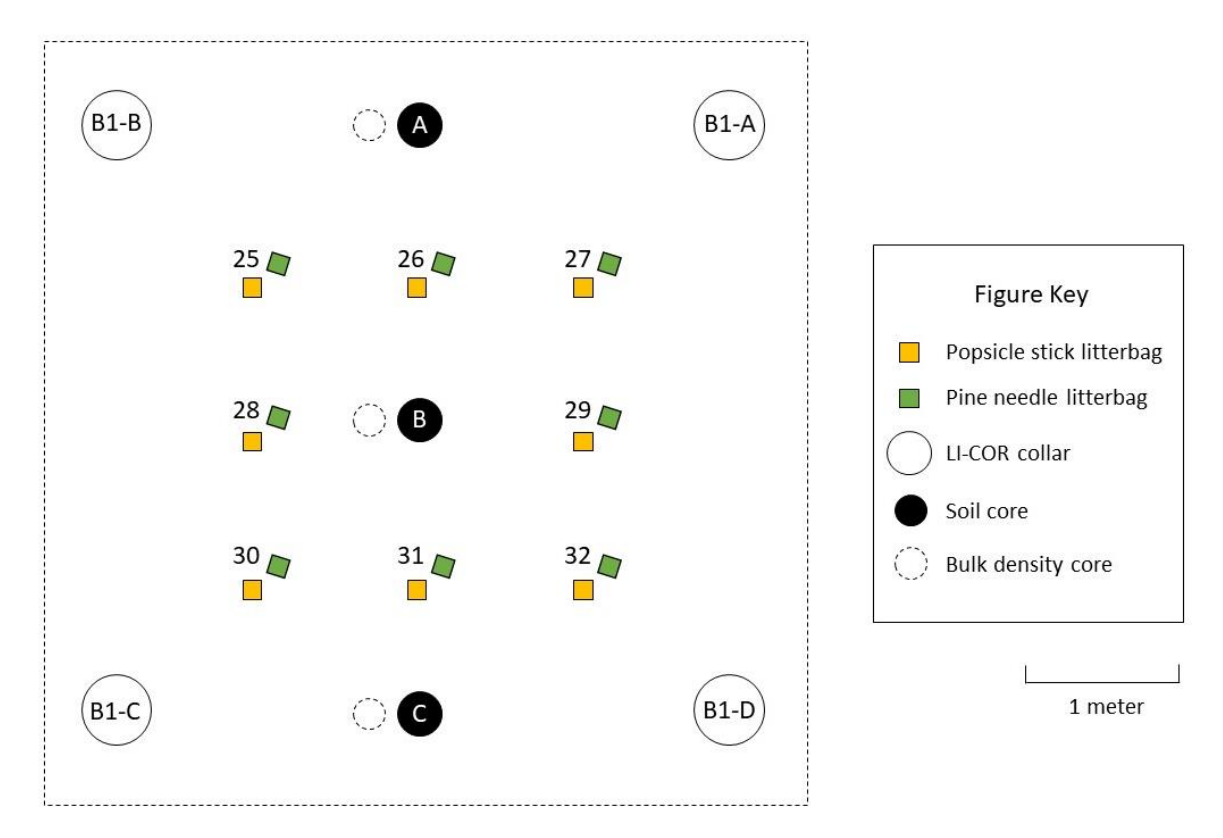


Figure 3.2. Litterbag plot layout using Burned Plot 1 as an example. Image is not to scale.

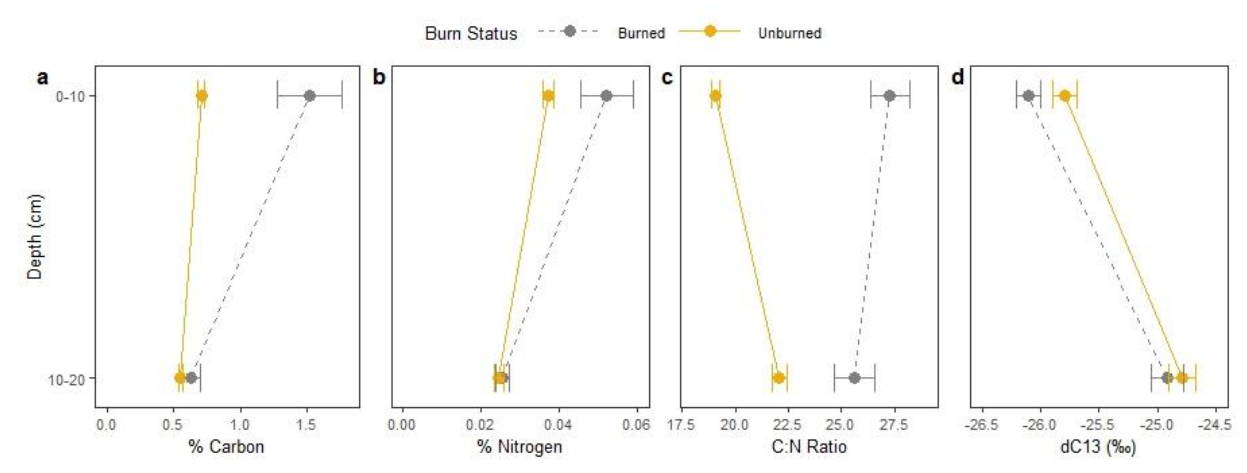


Figure 3.3. Average (a) percent carbon, (b) percent nitrogen, (c) carbon to nitrogen (C:N) ratio, and (d) δ^{13} C. Soils were collected on August 17, 2021 from 0-10 and 10-20 cm depths. Plots were either managed with regular Rx fire (Burned) or without (Unburned). Values represent the average of all cores (n = 3) across two analytical replicates, with the exception of missing N values for one Burned stand 10-20 cm soil sample.

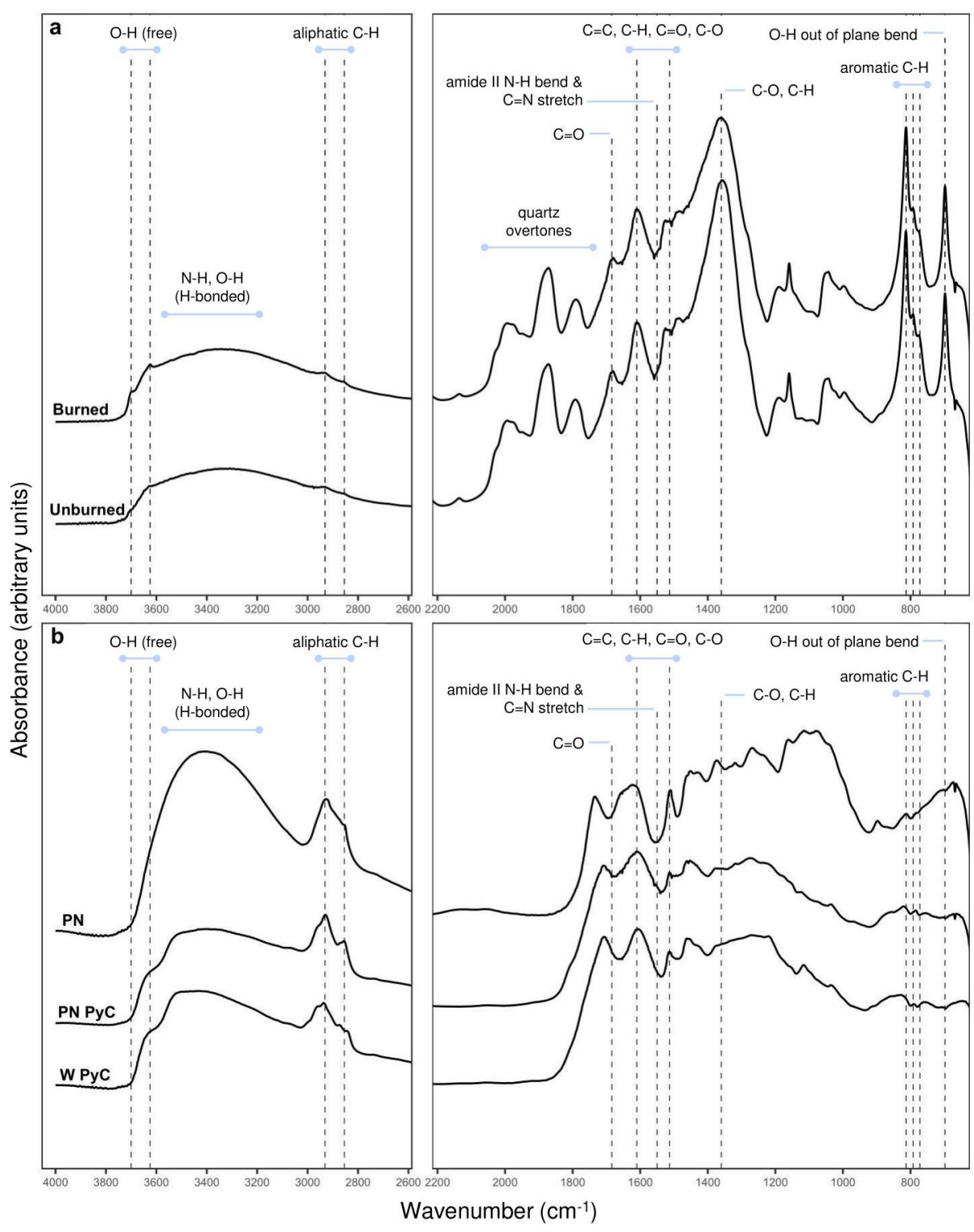


Figure 3.4. Mid-infrared spectra from (a) Burned and Unburned stand soil samples taken at 0-10 cm (b) dried longleaf pine needle and longleaf pine needle PyC references.

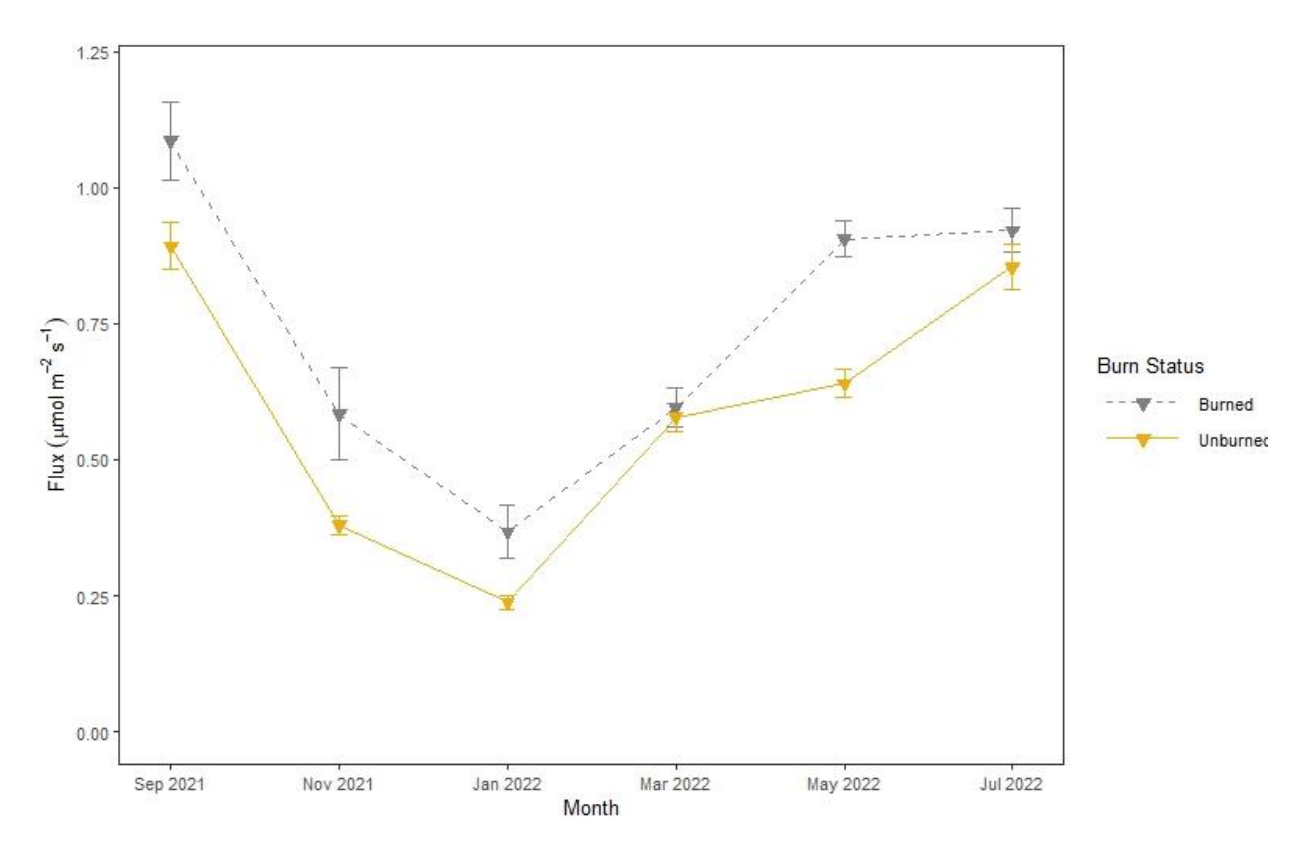


Figure 3.5. Average carbon dioxide flux (μ mol CO₂ m⁻² s⁻¹) from soils of forested stands (n=3) managed with (Burned) and without (Unburned) Rx fire collected every two months over one year. Flux readings were collected from PVC collars installed in the soil surface, using a LI-870 CO₂/H₂O analyzer.



Figure 3.6. Fungal hyphae colonizing wood PyC in a litterbag collected from Unburned Stand 2 on 29 March 2022, approximately 7 months after it was placed on the forest floor.

CHAPTER 4

SUMMARY AND CONCLUSION

We used classical soil physical and chemical characterization, radiocarbon, stable isotope, advanced spectroscopy, and soil carbon dioxide flux (R_s) monitoring to characterize soil organic matter (SOM) pools in longleaf pine stands managed with (Burned) and without (Unburned) regular Rx fire at a private property in the Coastal Plain of Georgia, USA. Overall, Burned stands were characterized by greater spatial heterogeneity, younger SOM pools that reflected higher inputs of pyrogenic carbon and fresh plant litter, and higher R_s. Unburned stands had older SOM pools possibly due to the annual removal of fresh organic matter during pine straw harvest, lower R_s and a greater proportion of microbially processed, persistent carbon (C). Soils also showed evidence of past management practices: higher pH and bulk density were recorded in stands that were previously in agricultural production than in those that were never cultivated.

Extract dissolved organic matter (DOM) was younger and predominantly composed of inherently soluble oxygenated structures, while leachate DOM was older and composed mostly of aliphatic structures reflecting the chemical and microbial processes that allow hydrophobic compounds to enter the soil solution. Soil water extractions are an extremely common technique for simulating soil water, so this finding may present an important consideration for researchers planning soil water studies.

Several lines of evidence indicate that our mineral associated organic matter (MAOM) fraction was a faster cycling, younger pool that was more microbially processed, while

particulate organic matter (POM) included much older C which was resistant to decomposition. This suggests that either mineral association is not a significant mode of SOM protection in our poorly aggregated soils, or that size fractionation did not isolate mineral-stabilized C which could have been adsorbed to larger particles and thus separated into the POM. Given these findings, we suggest that density fractionation may be more appropriate for studying mineral association of organic matter in high sand-content soils.

REFERENCES

- Abella, S. R., & Fornwalt, P. J. (2015). Ten years of vegetation assembly after a North American mega fire [https://doi.org/10.1111/gcb.12722]. *Global Change Biology*, 21(2), 789-802. https://doi.org/https://doi.org/10.1111/gcb.12722
- Abiven, S., Hengartner, P., Schneider, M. P. W., Singh, N., & Schmidt, M. W. I. (2011). Pyrogenic carbon soluble fraction is larger and more aromatic in aged charcoal than in fresh charcoal. *Soil Biology and Biochemistry*, *43*(7), 1615-1617. https://doi.org/10.1016/j.soilbio.2011.03.027
- Abney, R. B., & Berhe, A. A. (2018). Pyrogenic Carbon Erosion: Implications for Stock and Persistence of Pyrogenic Carbon in Soil. *Frontiers in Earth Science*, 6. https://doi.org/10.3389/feart.2018.00026
- Abney, R. B., Jin, L., & Berhe, A. A. (2019a). Soil properties and combustion temperature: Controls on the decomposition rate of pyrogenic organic matter. *Catena*, 182. https://doi.org/10.1016/j.catena.2019.104127
- Abney, R. B., Kuhn, T. J., Chow, A., Hockaday, W., Fogel, M. L., & Berhe, A. A. (2019b). Pyrogenic carbon erosion after the Rim Fire, Yosemite National Park: The Role of Burn Severity and Slope. *Journal of Geophysical Research: Biogeosciences*, *124*(2), 432-449. https://doi.org/10.1029/2018jg004787
- Abney, R. B., Sanderman, J., Johnson, D., Fogel, M. L., & Berhe, A. A. (2017). Post-wildfire Erosion in Mountainous Terrain Leads to Rapid and Major Redistribution of Soil Organic Carbon. *Frontiers in Earth Science*, 5. https://doi.org/10.3389/feart.2017.00099
- Adamczyk, S., Adamczyk, B., Kitunen, V., & Smolander, A. (2015). Monoterpenes and higher terpenes may inhibit enzyme activities in boreal forest soil. *Soil Biology and Biochemistry*, 87, 59-66. https://doi.org/10.1016/j.soilbio.2015.04.006
- Aide, M., Pavich, Z., Lilly, M. E., Thornton, R., & Kingery, W. (2004). Plinthite Formation in the Coastal Plain Region of Mississippi. *Soil Science*, *169*(9). https://journals.lww.com/soilsci/Fulltext/2004/09000/PLINTHITE_FORMATION_IN_THE_COASTAL_PLAIN_REGION_OF.1.aspx
- Alcañiz, M., Outeiro, L., Francos, M., & Ubeda, X. (2018). Effects of prescribed fires on soil properties: A review. *Sci Total Environ*, *613-614*, 944-957. https://doi.org/10.1016/j.scitotenv.2017.09.144

- Anderson, P. H., Johnsen, K. H., Butnor, J. R., Gonzalez-Benecke, C. A., & Samuelson, L. J. (2018). Predicting longleaf pine coarse root decomposition in the southeastern US. *Forest Ecology and Management*, 425, 1-8. https://doi.org/10.1016/j.foreco.2018.05.024
- Anderson, R. C., & Menges, E. S. (1997). Effects of fire on sandhill herbs: nutrients, mycorrhizae, and biomass allocation. *American Journal of Botany*, 84(7), 938-948. https://doi.org/10.2307/2446284
- Andrade, V. S., de Barros Neto, B., Fukushima, K., & de Campos Takaki, G. M. (2004). Effect of medium components and time of cultivation on chitin production by Mucor circinelloides (Mucor javanicus IFO 4570) A factorial study. *Revista iberoamericana de micología*, 20, 149-153.
- ArchMiller, A. A., & Samuelson, L. J. (2016). Intra-annual variation of soil respiration across four heterogeneous longleaf pine forests in the southeastern United States. *Forest Ecology and Management*, 359, 370-380. https://doi.org/10.1016/j.foreco.2015.05.016
- Augustine, D. J., Brewer, P., Blumenthal, D. M., Derner, J. D., & von Fischer, J. C. (2014). Prescribed fire, soil inorganic nitrogen dynamics, and plant responses in a semiarid grassland. *Journal of Arid Environments*, 104, 59-66. https://doi.org/10.1016/j.jaridenv.2014.01.022
- Bahn, M., Janssens, I., Reichstein, M., Smith, P., & Trumbore, S. (2010). Soil respiration across scales: Towards an integration of patterns and processes. *The New phytologist*, *186*, 292-296. https://doi.org/10.1111/j.1469-8137.2010.03237.x
- Baldock, J., & Broos, K. (2011). Soil Organic Matter. In P. M. Huang, Y. Li, & M. E. Sumner (Eds.), *Handbook of Soil Sciences: Properties and Processes* (Second Edition ed., pp. B1-B52). CRC Press Taylor and Francis Group.
- Baldock, J. A., & Skjemstad, J. O. (2000). Role of the soil matrix and minerals in protecting natural organic materials against biological attack. *Organic Geochemistry*, *31*(7), 697-710. https://doi.org/https://doi.org/10.1016/S0146-6380(00)00049-8
- Bastias, B. A., Anderson, I. C., Rangel-Castro, J. I., Parkin, P. I., Prosser, J. I., & Cairney, J. W. G. (2009). Influence of repeated prescribed burning on incorporation of 13C from cellulose by forest soil fungi as determined by RNA stable isotope probing. *Soil Biology and Biochemistry*, *41*(3), 467-472. https://doi.org/10.1016/j.soilbio.2008.11.018
- Bastias, B. A., Xu, Z., & Cairney, J. W. (2006). Influence of long-term repeated prescribed burning on mycelial communities of ectomycorrhizal fungi. *New Phytol*, *172*(1), 149-158. https://doi.org/10.1111/j.1469-8137.2006.01793.x
- Bates, D., Mächler, M., Bolker, B., & Walker, S. (2015). Fitting Linear Mixed-Effects Models Using lme4. *Journal of Statistical Software*, 67(1), 1 48. https://doi.org/10.18637/jss.v067.i01
- Bauer, P., Ransom, M., Frederick, J., & Hardee, G. (2020). Chapter 18: Southern Coastal Plain and Atlantic Coast Flatwoods Case Studies. In J. Bergtold & M. Sailus (Eds.), *Conservation Tillage Systems in the Southeast* (pp. 252-274). Sustainable Agriculture Research and Education (SARE) program.

- Bell, R. L., & Binkley, D. (1989). Soil nitrogen mineralization and immobilization in response to periodic prescribed fire in a loblolly pine plantation. *Canadian Journal of Forest Research*, 19(6), 816-820.
- Bellè, S.-L., Berhe, A. A., Hagedorn, F., Santin, C., Schiedung, M., van Meerveld, I., & Abiven, S. (2021). Key drivers of pyrogenic carbon redistribution during a simulated rainfall event. *Biogeosciences*, *18*(3), 1105-1126. https://doi.org/10.5194/bg-18-1105-2021
- Bird, M. I., Wynn, J. G., Saiz, G., Wurster, C. M., & McBeath, A. (2015). The Pyrogenic Carbon Cycle. *Annual Review of Earth and Planetary Sciences*, 43(1), 273-298. https://doi.org/10.1146/annurev-earth-060614-105038
- Bonan, G. B. (2008). Forests and climate change: forcings, feedbacks, and the climate benefits of forests. *Science*, *320*(5882), 1444-1449.
- Bonner, S. R., Hoffman, C. M., Kane, J. M., Varner, J. M., Hiers, J. K., O'Brien, J. J., Rickard, H. D., Tinkham, W. T., Linn, R. R., Skowronski, N., Parsons, R. A., & Sieg, C. H. (2021). Invigorating Prescribed Fire Science Through Improved Reporting Practices. *Frontiers in Forests and Global Change*, 4. https://doi.org/10.3389/ffgc.2021.750699
- Boom, A., Sinninge Damsté, J. S., & de Leeuw, J. W. (2005). Cutan, a common aliphatic biopolymer in cuticles of drought-adapted plants. *Organic Geochemistry*, *36*(4), 595-601. https://doi.org/10.1016/j.orggeochem.2004.10.017
- Bouyoucos, G. J. (1962). Hydrometer Method Improved for Making Particle Size Analyses of Soils1 [https://doi.org/10.2134/agronj1962.00021962005400050028x]. *Agronomy Journal*, *54*(5), 464-465. https://doi.org/https://doi.org/10.2134/agronj1962.00021962005400050028x
- Brenner, J., & Wade, D. (2003). Florida's Revised Prescribed Fire Law: Protection For Responsible Burners. https://www.fs.usda.gov/treesearch/pubs/6208
- Brockway, D. G. (1997). Long-term effects of dormant-season prescribed fire on plant community diversity, structure and productivity in a longleaf pine wiregrass ecosystem. *Forest ecology and management.*, *96*(1/2), 167.
- Brodowski, S., Amelung, W., Haumaier, L., Abetz, C., & Zech, W. (2005a). Morphological and chemical properties of black carbon in physical soil fractions as revealed by scanning electron microscopy and energy-dispersive X-ray spectroscopy. *Geoderma*, *128*(1-2), 116-129. https://doi.org/10.1016/j.geoderma.2004.12.019
- Brodowski, S., John, B., Flessa, H., & Amelung, W. (2006). Aggregate-occluded black carbon in soil. *European Journal of Soil Science*, *57*(4), 539-546. https://doi.org/10.1111/j.1365-2389.2006.00807.x
- Brodowski, S., Rodionov, A., Haumaier, L., Glaser, B., & Amelung, W. (2005b). Revised black carbon assessment using benzene polycarboxylic acids. *Organic Geochemistry*, *36*(9), 1299-1310. https://doi.org/10.1016/j.orggeochem.2005.03.011
- Broek, T. A. B., Ognibene, T. J., McFarlane, K. J., Moreland, K. C., Brown, T. A., & Bench, G. (2021). Conversion of the LLNL/CAMS 1 MV biomedical AMS system to a semi-automated natural abundance 14C spectrometer: system optimization and performance

- evaluation. *Nuclear Instruments and Methods in Physics Research Section B: Beam Interactions with Materials and Atoms*, 499, 124-132. https://doi.org/https://doi.org/10.1016/j.nimb.2021.01.022
- Brown, S. P., Callaham, J., M. A., Oliver, A. K., & Jumpponen, A. (2013). Deep Ion Torrent sequencing identifies soil fungal community shifts after frequent prescribed fires in a southeastern US forest ecosystem. *FEMS Microbiol Ecol*, 86(3), 557-566. https://doi.org/10.1111/1574-6941.12181
- Brown, T. J., Hall, B. L., & Westerling, A. L. (2004). The Impact of Twenty-First Century Climate Change on Wildland Fire Danger in the Western United States: An Applications Perspective. *Climatic Change*, 62(1), 365-388. https://doi.org/10.1023/B:CLIM.0000013680.07783.de
- Butnor, J. R., Samuelson, L. J., Johnsen, K. H., Anderson, P. H., González Benecke, C. A., Boot, C. M., Cotrufo, M. F., Heckman, K. A., Jackson, J. A., Stokes, T. A., & Zarnoch, S. J. (2017). Vertical distribution and persistence of soil organic carbon in fire-adapted longleaf pine forests. *Forest Ecology and Management*, *390*, 15-26. https://doi.org/10.1016/j.foreco.2017.01.014
- Calderón, F., Haddix, M., Conant, R., Magrini-Bair, K., & Paul, E. (2013). Diffuse-Reflectance Fourier-Transform Mid-Infrared Spectroscopy as a Method of Characterizing Changes in Soil Organic Matter. *Soil Science Society of America Journal*, 77(5), 1591-1600. https://doi.org/10.2136/sssaj2013.04.0131
- Calderón, F. J., Reeves, J. B., Collins, H. P., & Paul, E. A. (2011). Chemical Differences in Soil Organic Matter Fractions Determined by Diffuse-Reflectance Mid-Infrared Spectroscopy. *Soil Science Society of America Journal*, 75(2), 568-579. https://doi.org/10.2136/sssaj2009.0375
- Callaham, J., Mac A., Anderson, P., Waldrop, T., Lione, D., & Shelburne, V. (2004). Litter decomposition and soil respiration responses to fuel reduction treatments in piedmont loblolly pine forests.
- Callaham, J., Mac A., Scott, D. A., O'Brien, J. J., & Stanturf, J., A. (2012). *Cumulative effects of fuel management on the soils of eastern U.S. watersheds* (Cumulative watershed effects of fuel management in the eastern United States, Issue. S. R. S. Forest Service. https://www.fs.usda.gov/research/treesearch/41099
- Cerling, T., Harris, J., Macfadden, B., Lea-key, M., Quade, J., Eisenmann, V., & Eh-leringer, J. (1997). Global vegetation change through the Miocene/Pliocene boundary: Nature. *Nature*, 389.
- Chatterjee, S., Santos, F., Abiven, S., Itin, B., Stark, R. E., & Bird, J. A. (2012). Elucidating the chemical structure of pyrogenic organic matter by combining magnetic resonance, midinfrared spectroscopy and mass spectrometry. *Organic Geochemistry*, *51*, 35-44. https://doi.org/10.1016/j.orggeochem.2012.07.006
- Cheng, C.-H., Lehmann, J., Thies, J. E., Burton, S. D., & Engelhard, M. H. (2006). Oxidation of black carbon by biotic and abiotic processes. *Organic Geochemistry*, *37*(11), 1477-1488. https://doi.org/10.1016/j.orggeochem.2006.06.022

- Choromanska, U., & DeLuca, T. H. (2001). Prescribed Fire Alters the Impact of Wildfire on Soil Biochemical Properties in a Ponderosa Pine Forest. *Soil Science Society of America Journal*, 65(1), 232-238. https://doi.org/10.2136/sssaj2001.651232x
- Civil liability: prescribed burning operations: gross negligence., 332, California Legislature (2021).
- Concilio, A., Ma, S., Li, Q., LeMoine, J., Chen, J., North, M., Moorhead, D., & Jensen, R. (2005). Soil respiration response to prescribed burning and thinning in mixed-conifer and hardwood forests. *Canadian Journal of Forest Research*, *35*(7), 1581-1591. https://doi.org/10.1139/x05-091
- Coppola, A. I., Ziolkowski, L. A., Masiello, C. A., & Druffel, E. R. M. (2014). Aged black carbon in marine sediments and sinking particles [https://doi.org/10.1002/2013GL059068]. *Geophysical Research Letters*, 41(7), 2427-2433. https://doi.org/https://doi.org/10.1002/2013GL059068
- Cotrufo, M. F., Boot, C., Abiven, S., Foster, E. J., Haddix, M., Reisser, M., Wurster, C. M., Bird, M. I., & Schmidt, M. W. I. (2016). Quantification of pyrogenic carbon in the environment: An integration of analytical approaches. *Organic Geochemistry*, *100*, 42-50. https://doi.org/10.1016/j.orggeochem.2016.07.007
- Cotrufo, M. F., Ranalli, M. G., Haddix, M. L., Six, J., & Lugato, E. (2019). Soil carbon storage informed by particulate and mineral-associated organic matter. *Nature Geoscience*, 12(12), 989-994. https://doi.org/10.1038/s41561-019-0484-6
- Coyle, D. R., Nagendra, U. J., Taylor, M. K., Campbell, J. H., Cunard, C. E., Joslin, A. H., Mundepi, A., Phillips, C. A., & Callaham, J., Mac A. (2017). Soil fauna responses to natural disturbances, invasive species, and global climate change: Current state of the science and a call to action. *Soil Biology and Biochemistry*, *110*, 116-133. https://doi.org/10.1016/j.soilbio.2017.03.008
- Czimczik, C. I., & Masiello, C. A. (2007). Controls on black carbon storage in soils. *Global Biogeochemical Cycles*, 21(3), Article Gb3005. https://doi.org/10.1029/2006gb002798
- da Silva Rodrigues-Corrêa, K. C., de Lima, J. C., & Fett-Neto, A. G. (2013). Oleoresins from Pine: Production and Industrial Uses. In *Natural Products* (pp. 4037-4060). https://doi.org/10.1007/978-3-642-22144-6 175
- Dickens, D., Morris, L., Clabo, D., & Ogden, L. (2020). Pine Straw Raking and Growth of Southern Pine: Review and Recommendations. *Forests*, *11*(8). https://doi.org/10.3390/f11080799
- Diemer, J. E. (1986). The Ecology and Management of the Gopher Tortoise in the Southeastern United States. *Herpetologica*, 42(1), 125-133. https://www.jstor.org/stable/3892243
- Eberhardt, T. L., Sheridan, P. M., & Mahfouz, J. M. (2009). Monoterpene persistence in the sapwood and heartwood of longleaf pine stumps: assessment of differences in composition and stability under field conditions. *Canadian Journal of Forest Research*, 39(7), 1357-1365. https://doi.org/10.1139/X09-063

- Fischer, M. S., Stark, F. G., Berry, T. D., Zeba, N., Whitman, T., & Traxler, M. F. (2021). Pyrolyzed substrates induce aromatic compound metabolism in the post-fire fungus, Pyronema domesticum. *bioRxiv*, 2021.2003.2015.435558. https://doi.org/10.1101/2021.03.15.435558
- Flanagan, S. A., Bhotika, S., Hawley, C., Starr, G., Wiesner, S., Hiers, J. K., O'Brien, J. J., Goodrick, S., Callaham Jr., M. A., Scheller, R. M., Klepzig, K. D., Taylor, R. S., & Loudermilk, E. L. (2019). Quantifying carbon and species dynamics under different fire regimes in a southeastern U.S. pineland. *Ecosphere*, 10(6).
- Fontúrbel, T., Carrera, N., Vega, J. A., & Fernández, C. (2021). The Effect of Repeated Prescribed Burning on Soil Properties: A Review. *Forests*, *12*(6). https://doi.org/10.3390/f12060767
- Forest Service Research & Development. (2021). Research improves climate-smart management of America's forests and grasslands. U. F. Service.
- Fowler, C., & Konopik, E. (2007). The history of fire in the southern United States. *HUMAN ECOLOGY REVIEW*, 14(2), 165-176.
- Fox, J., & Weisberg, S. (2019). *An R Companion to Applied Regression*. In Sage. https://socialsciences.mcmaster.ca/jfox/Books/Companion/
- Gascho, G. J., & Parker, M. (2001). Long-Term Liming Effects on Coastal Plain Soils and Crops. *Agronomy Journal AGRON J*, 93. https://doi.org/10.2134/agronj2001.1305
- Georgia Automated Environmental Monitoring Network. (2023, 05/01/2023). *Historical Data*. Coastal Plain Experimental Station. http://weather.uga.edu/index.php?variable=HI&site=TIFTON
- Gill, R. A., & Jackson, R. B. (2000). Global patterns of root turnover for terrestrial ecosystems [https://doi.org/10.1046/j.1469-8137.2000.00681.x]. *New Phytologist*, *147*(1), 13-31. https://doi.org/https://doi.org/10.1046/j.1469-8137.2000.00681.x
- Gilliam, F. S. (1991). The significance of fire in an oligotrophic ecosystem.
- Glaser, B. (2007). Prehistorically modified soils of central Amazonia: a model for sustainable agriculture in the twenty-first century. *Philosophical Transactions of the Royal Society B: Biological Sciences*, 362(1478), 187-196. https://doi.org/doi:10.1098/rstb.2006.1978
- Glaser, B., Balashov, E., Haumaier, L., Guggenberger, G., & Zech, W. (2000). Black carbon in density fractions of anthropogenic soils of the Brazilian Amazon region. *Organic Geochemistry*, *31*(7), 669-678. https://doi.org/https://doi.org/10.1016/S0146-6380(00)00044-9
- Glaser, B., Haumaier, L., Guggenberger, G., & Zech, W. (2001). The 'Terra Preta' phenomenon: a model for sustainable agriculture in the humid tropics. *Naturwissenschaften*, 88(1), 37-41. https://doi.org/10.1007/s001140000193
- Glassman, S. I., Levine, C. R., DiRocco, A. M., Battles, J. J., & Bruns, T. D. (2016). Ectomycorrhizal fungal spore bank recovery after a severe forest fire: some like it hot. *ISME J*, 10(5), 1228-1239. https://doi.org/10.1038/ismej.2015.182

- Godwin, D., Kobziar, L., & Robertson, K. (2017). Effects of Fire Frequency and Soil Temperature on Soil CO2 Efflux Rates in Old-Field Pine-Grassland Forests. *Forests*, 8(8). https://doi.org/10.3390/f8080274
- Gonzalez-Benecke, C. A., Samuelson, L. J., Martin, T. A., Cropper, W. P., Johnsen, K. H., Stokes, T. A., Butnor, J. R., & Anderson, P. H. (2015). Modeling the effects of forest management on in situ and ex situ longleaf pine forest carbon stocks. *Forest Ecology and Management*, 355, 24-36. https://doi.org/10.1016/j.foreco.2015.02.029
- Gonzalez-Perez, J. A., Gonzalez-Vila, F. J., Almendros, G., & Knicker, H. (2004). The effect of fire on soil organic matter--a review. *Environ Int*, *30*(6), 855-870. https://doi.org/10.1016/j.envint.2004.02.003
- Griffith, G. E., Omernik, J. N., Comstock, J. A., Lawrence, & Foster, T. (2001). *Ecoregions of Georgia*. Corvallis, OR, U.S. Environmental Protection Agency.
- Guillou, F. L., Wetterlind, W., Viscarra Rossel, R. A., Hicks, W., Grundy, M., & Tuomi, S. (2015). How does grinding affect the mid-infrared spectra of soil and their multivariate calibrations to texture and organic carbon? *Soil Research*, *53*(8). https://doi.org/10.1071/sr15019
- Guinto, D., Xu, Z., House, A., & Saffigna, P. (2001). Soil chemical properties and forest floor nutrients under repeated prescribed-burning in eucalypt forests of south-east Queensland, Australia. *New Zealand Journal of Forestry Science*, 31(2), 170-187.
- Guo, D., Mitchell, R. J., Withington, J. M., Fan, P.-P., & Hendricks, J. J. (2008). Endogenous and exogenous controls of root life span, mortality and nitrogen flux in a longleaf pine forest: root branch order predominates. *Journal of Ecology*, *96*(4), 737-745. https://doi.org/10.1111/j.1365-2745.2008.01385.x
- Guo, D. L., Mitchell, R. J., & Hendricks, J. J. (2004). Fine root branch orders respond differentially to carbon source-sink manipulations in a longleaf pine forest. *Oecologia*, 140(3), 450-457. https://doi.org/10.1007/s00442-004-1596-1
- Hagedorn, F., & Machwitz, M. (2007). Controls on dissolved organic matter leaching from forest litter grown under elevated atmospheric CO2. *Soil Biology and Biochemistry*, *39*(7), 1759-1769. https://doi.org/10.1016/j.soilbio.2007.01.038
- Hall, S., Berhe, A., & Thompson, A. (2018). Order from disorder: do soil organic matter composition and turnover co-vary with iron phase crystallinity? *Biogeochemistry*, *140*. https://doi.org/10.1007/s10533-018-0476-4
- Halofsky, J. E., Peterson, D. L., & Harvey, B. J. (2020). Changing wildfire, changing forests: the effects of climate change on fire regimes and vegetation in the Pacific Northwest, USA. *Fire Ecology*, *16*(1). https://doi.org/10.1186/s42408-019-0062-8
- Hargrove, W. W., & Pickering, J. (1992). Pseudoreplication: a sine qua non for regional ecology. *Landscape Ecology*, 6(4), 251-258. https://doi.org/10.1007/BF00129703
- Harman-Ware, A. E., Sparks, S., Addison, B., & Kalluri, U. C. (2021). Importance of suberin biopolymer in plant function, contributions to soil organic carbon and in the production

- of bio-derived energy and materials. *Biotechnol Biofuels*, *14*(1), 75. https://doi.org/10.1186/s13068-021-01892-3
- Hart, S. C., DeLuca, T. H., Newman, G. S., MacKenzie, M. D., & Boyle, S. I. (2005). Post-fire vegetative dynamics as drivers of microbial community structure and function in forest soils. Forest Ecology and Management, 220(1-3), 166-184. https://doi.org/10.1016/j.foreco.2005.08.012
- Hedges, J. I., Eglinton, G., Hatcher, P. G., Kirchman, D. L., Arnosti, C., Derenne, S., Evershed, R. P., Kögel-Knabner, I., De Leeuw, J. W., Littke, R., Michaelis, W., & Rullkötter, J. (2000). The molecularly-uncharacterized component of nonliving organic matter in natural environments. *Organic Geochemistry*, *31*(10), 945-958. https://doi.org/10.1016/s0146-6380(00)00096-6
- Hendricks, J. J., Mitchell, R. J., Kuehn, K. A., & Pecot, S. D. (2016). Ectomycorrhizal fungal mycelia turnover in a longleaf pine forest. *New Phytol*, 209(4), 1693-1704. https://doi.org/10.1111/nph.13729
- Hiers, J. K., O'Brien, J. J., Varner, J. M., Butler, B. W., Dickinson, M., Furman, J., Gallagher, M., Godwin, D., Goodrick, S. L., Hood, S. M., Hudak, A., Kobziar, L. N., Linn, R., Loudermilk, E. L., McCaffrey, S., Robertson, K., Rowell, E. M., Skowronski, N., Watts, A. C., & Yedinak, K. M. (2020). Prescribed fire science: the case for a refined research agenda. *Fire Ecology*, 16(1). https://doi.org/10.1186/s42408-020-0070-8
- Hilscher, A., & Knicker, H. (2011). Degradation of grass-derived pyrogenic organic material, transport of the residues within a soil column and distribution in soil organic matter fractions during a 28 month microcosm experiment. *Organic Geochemistry*, 42(1), 42-54. https://doi.org/10.1016/j.orggeochem.2010.10.005
- Hobley, E. (2019). Vertical Distribution of Soil Pyrogenic Matter: A Review. *Pedosphere*, 29(2), 137-149. https://doi.org/10.1016/s1002-0160(19)60795-2
- Hobley, E., Zoor, L. C., Shrestha, H. R., Bennett, L. T., Weston, C. J., & Baker, T. G. (2019). Prescribed fire affects the concentration and aromaticity of soluble soil organic matter in forest soils. *Geoderma*, *341*, 138-147. https://doi.org/10.1016/j.geoderma.2019.01.035
- Hoover, K., & Riddle, A. A. (2021). *U.S. Forest Ownership and Managment: Bacground and Issues for Congress* [CRS Report Prepared for Members and Committees of Congress](R46976). (CRS Report, Issue. https://crsreports.congress.gov/product/pdf/R/R46976
- Hunt, S., & Simpson, J. (1985). Effects of low intensity prescribed fire on the growth and nutrition of a slash pine plantation. *Australian Forest Research (Australia)*.
- Hurlbert, S. H. (1984). Pseudoreplication and the Design of Ecological Field Experiments [https://doi.org/10.2307/1942661]. *Ecological Monographs*, *54*(2), 187-211. https://doi.org/https://doi.org/10.2307/1942661
- Jacobs, K. A., Nix, B., & Scharenbroch, B. C. (2015). The Effects of Prescribed Burning on Soil and Litter Invertebrate Diversity and Abundance in an Illinois Oak Woodland. *Natural Areas Journal*, *35*(2), 318-327. https://doi.org/10.3375/043.035.0214

- Jaffé, R., Ding, Y., Niggemann, J., Vähätalo, A. V., Stubbins, A., Spencer, R. G., Campbell, J., & Dittmar, T. (2013). Global charcoal mobilization from soils via dissolution and riverine transport to the oceans. *Science*, *340*(6130), 345-347.
- Jian, M., Berhe, A. A., Berli, M., & Ghezzehei, T. A. (2018). Vulnerability of Physically Protected Soil Organic Carbon to Loss Under Low Severity Fires. *Frontiers in Environmental Science*, 6. https://doi.org/10.3389/fenvs.2018.00066
- Johnson, A. S., & Hale, P. E. (2002). The historical foundations of prescribed burning for wildlife: a southeastern perspective. https://www.fs.usda.gov/treesearch/pubs/19091
- Kaiser, M., Ellerbrock, R. H., Wulf, M., Dultz, S., Hierath, C., & Sommer, M. (2012). The influence of mineral characteristics on organic matter content, composition, and stability of topsoils under long-term arable and forest land use. *Journal of Geophysical Research: Biogeosciences*, 117(G2), n/a-n/a. https://doi.org/10.1029/2011jg001712
- Keiluweit, M., Nico, P. S., Johnson, M. G., & Kleber, M. (2010). Dynamic Molecular Structure of Plant Biomass-Derived Black Carbon (Biochar). *Environmental Science & Technology*, 44(4), 1247-1253. https://doi.org/10.1021/es9031419
- Kelly, L. A., Wentworth, T. R., & Brownie, C. (2000). Short-term effects of pine straw raking on plant species richness and composition of longleaf pine communities. *Forest Ecology and Management*, 127(1), 233-247. https://doi.org/https://doi.org/10.1016/S0378-1127(99)00133-4
- Kelly, L. T., Giljohann, K. M., Duane, A., Aquilue, N., Archibald, S., Batllori, E., Bennett, A. F., Buckland, S. T., Canelles, Q., Clarke, M. F., Fortin, M. J., Hermoso, V., Herrando, S., Keane, R. E., Lake, F. K., McCarthy, M. A., Moran-Ordonez, A., Parr, C. L., Pausas, J. G., . . . Brotons, L. (2020). Fire and biodiversity in the Anthropocene. *Science*, 370(6519). https://doi.org/10.1126/science.abb0355
- Kimmerer, R. W., & Lake, F. K. (2001). The Role of Indigenous Burning in Land Management. *Journal of Forestry*, 99(11), 36-41. https://doi.org/https://doi.org/10.1093/jof/99.11.36
- Kleber, M. (2010). What is recalcitrant soil organic matter? *Environmental Chemistry*, 7(4). https://doi.org/10.1071/en10006
- Kleber, M., Eusterhues, K., Keiluweit, M., Mikutta, C., Mikutta, R., & Nico, P. S. (2015). Mineral–Organic Associations: Formation, Properties, and Relevance in Soil Environments. In (pp. 1-140). https://doi.org/10.1016/bs.agron.2014.10.005
- Kleber, M., & Johnson, M. G. (2010). Advances in Understanding the Molecular Structure of Soil Organic Matter. In *Advances in Agronomy v106* (pp. 77-142). https://doi.org/10.1016/s0065-2113(10)06003-7
- Kögel-Knabner, I., & Amelung, W. (2014). Dynamics, Chemistry, and Preservation of Organic Matter in Soils. In *Treatise on Geochemistry* (pp. 157-215). https://doi.org/10.1016/b978-0-08-095975-7.01012-3
- Kolden, C. A. (2019). We're Not Doing Enough Prescribed Fire in the Western United States to Mitigate Wildfire Risk. *Fire*, 2(2). https://doi.org/10.3390/fire2020030

- Kranz, C., & Whitman, T. (2019). Short communication: Surface charring from prescribed burning has minimal effects on soil bacterial community composition two weeks post-fire in jack pine barrens. *Applied Soil Ecology*, *144*, 134-138. https://doi.org/10.1016/j.apsoil.2019.07.004
- Laird, D. A., Chappell, M. A., Martens, D. A., Wershaw, R. L., & Thompson, M. (2008). Distinguishing black carbon from biogenic humic substances in soil clay fractions. *Geoderma*, 143(1-2), 115-122. https://doi.org/10.1016/j.geoderma.2007.10.025
- Lake, F. K., & Christianson, A. C. (2019). Indigenous Fire Stewardship. In *Encyclopedia of Wildfires and Wildland-Urban Interface (WUI) Fires* (pp. 1-9). https://doi.org/10.1007/978-3-319-51727-8_225-1
- Lavallee, J. M., Conant, R. T., Haddix, M. L., Follett, R. F., Bird, M. I., & Paul, E. A. (2019). Selective preservation of pyrogenic carbon across soil organic matter fractions and its influence on calculations of carbon mean residence times. *Geoderma*, *354*. https://doi.org/10.1016/j.geoderma.2019.07.024
- Lavallee, J. M., Soong, J. L., & Cotrufo, M. F. (2020). Conceptualizing soil organic matter into particulate and mineral-associated forms to address global change in the 21st century. *Glob Chang Biol*, 26(1), 261-273. https://doi.org/10.1111/gcb.14859
- Lavoie, M., Starr, G., Mack, M. C., Martin, T. A., & Gholz, H. L. (2010). Effects of a Prescribed Fire on Understory Vegetation, Carbon Pools, and Soil Nutrients in a Longleaf Pine-Slash Pine Forest in Florida. *Natural Areas Journal*, *30*(1), 82-94. https://doi.org/10.3375/043.030.0109
- Lawton, D. E., Moye, F. J., Murray, J. B., O'Connor, B. J., Penley, H. M., Sandrock, G. S., Marsalis, W. E., Friddell, M. S., Hetrick, J. H., Huddlestun, P. F., Hunter, R. E., Mann, W. R., Martin, B. F., Pickering, S. M., Schneeberger, F. J., & Wilson, J. D. (1976). Geologic map of Georgia. Envronmental Protection Division, Georgia Department of Natural Resources. https://epd.georgia.gov/document/publication/sm-3-geologic-map-georgia-1500000-1976/download
- Lehmann, J., Hansel, C. M., Kaiser, C., Kleber, M., Maher, K., Manzoni, S., Nunan, N., Reichstein, M., Schimel, J. P., Torn, M. S., Wieder, W. R., & Kögel-Knabner, I. (2020). Persistence of soil organic carbon caused by functional complexity. *Nature Geoscience*, 13(8), 529-534. https://doi.org/10.1038/s41561-020-0612-3
- Lehmann, J., & Joseph, S. (2009). Biochar for environmental management: An introduction. Biochar for Environmental Management: Science and Technology, 1-12.
- Lehmann, J., & Kleber, M. (2015). The contentious nature of soil organic matter. *Nature*, 528(7580), 60-68. https://doi.org/10.1038/nature16069
- Lenth, R. V. (2022). *emmeans: Estimated Marginal Means, aka Least-Squares Means*. In (Version R package version 1.7.2.) https://CRAN.R-project.org/package=emmeans
- Levy, S. (2022). The Return of Intentional Forest Fires: Scientists look to Indigenous practices. *BioScience*, 72(4), 324-330. https://doi.org/10.1093/biosci/biac016

- Loudermilk, E. L., Cropper, W. P., Mitchell, R. J., & Lee, H. (2011). Longleaf pine (Pinus palustris) and hardwood dynamics in a fire-maintained ecosystem: A simulation approach. *Ecological Modelling*, 222(15), 2733-2750. https://doi.org/https://doi.org/10.1016/j.ecolmodel.2011.05.004
- Lussenhop, J. (1976). Soil Arthropod Response to Prairie Burning [https://doi.org/10.2307/1936400]. *Ecology*, *57*(1), 88-98. https://doi.org/https://doi.org/10.2307/1936400
- Majidzadeh, H., Wang, J.-J., & Chow, A. T. (2015). Prescribed Fire Alters Dissolved Organic Matter and Disinfection By-Product Precursors in Forested Watersheds Part I. A Controlled Laboratory Study. In *Recent Advances in Disinfection By-Products* (Vol. 1190, pp. 271-292). American Chemical Society. https://doi.org/doi:10.1021/bk-2015-1190.ch015
- Major, J., Lehmann, J., Rondon, M., & Goodale, C. (2010). Fate of soil-applied black carbon: downward migration, leaching and soil respiration. *Global Change Biology*, *16*(4), 1366-1379. https://doi.org/10.1111/j.1365-2486.2009.02044.x
- Malmström, A., Persson, T., & Ahlström, K. (2008). Effects of fire intensity on survival and recovery of soil microarthropods after a clearcut burning. *Canadian Journal of Forest Research*, 38(9), 2465-2475. https://doi.org/10.1139/X08-094
- Markewitz, D., Sartori, F., & Craft, C. (2002). Soil Change and Carbon Storage in Longleaf Pine Stands Planted on Marginal Agricultural Lands. *Ecological Applications*, *12*(5), 1276-1285. https://doi.org/10.1890/1051-0761(2002)012[1276:Scacsi]2.0.Co;2
- Masiello, C. A. (2004). New directions in black carbon organic geochemistry. *Marine Chemistry*, 92(1-4), 201-213. https://doi.org/10.1016/j.marchem.2004.06.043
- Masyita, A., Mustika Sari, R., Dwi Astuti, A., Yasir, B., Rahma Rumata, N., Emran, T. B., Nainu, F., & Simal-Gandara, J. (2022). Terpenes and terpenoids as main bioactive compounds of essential oils, their roles in human health and potential application as natural food preservatives. *Food Chem X*, *13*, 100217. https://doi.org/10.1016/j.fochx.2022.100217
- Matamala, R., Gonzalez-Meler, M. A., Jastrow, J. D., Norby, R. J., & Schlesinger, W. H. (2003). Impacts of fine root turnover on forest NPP and soil C sequestration potential. *Science*, 302(5649), 1385-1387.
- Mazerolle, M. J. (2023). *Model selection and multimodel inference based on (Q)AIC(c)*. In https://cran.r-project.org/package=AICcmodavg
- McCarthy, D. R., & Brown, K. J. (2006). Soil respiration responses to topography, canopy cover, and prescribed burning in an oak-hickory forest in southeastern Ohio. *Forest Ecology and Management*, 237(1-3), 94-102. https://doi.org/10.1016/j.foreco.2006.09.030
- McKee, W. H. (1982). *Changes in soil fertility following prescribed burning on Coastal Plain pine sites*. http://dx.doi.org/10.2737/SE-RP-234
- McLauchlan, K. K., Higuera, P. E., Miesel, J., Rogers, B. M., Schweitzer, J., Shuman, J. K., Tepley, A. J., Varner, J. M., Veblen, T. T., Adalsteinsson, S. A., Balch, J. K., Baker, P.,

- Batllori, E., Bigio, E., Brando, P., Cattau, M., Chipman, M. L., Coen, J., Crandall, R., . . . Durigan, G. (2020). Fire as a fundamental ecological process: Research advances and frontiers. *Journal of Ecology*, *108*(5), 2047-2069. https://doi.org/10.1111/1365-2745.13403
- Meldahl, R. S., & Kush, J. S. (2006). *Carbon sequestration and natural longleaf pine ecosystems*. [Gen. Tech. Rep.]. S. R. S. Forest Service. https://www.fs.usda.gov/research/treesearch/23352
- Metz, L. J., & Farrier, M. H. (1973). Prescribed Burning and Populations of Soil Mesofauna. *Environmental Entomology*, 2(3), 433-440. https://doi.org/10.1093/ee/2.3.433
- Miller, R. F., & Rose, J. A. (1999). Fire history and western juniper encroachment in sagebrush steppe. In (Vol. 52, pp. 550-559): Society for Range Management.
- Mitchell, R. J., Hiers, J. K., O'Brien, J., & Starr, G. (2009). Ecological Forestry in the Southeast: Understanding the Ecology of Fuels. *Journal of Forestry*, *107*(8), 391-397. Go to ISI>://WOS:000272987700005
- Mitchell, R. J., Hiers, J. K., O'Brien, J. J., Jack, S. B., & Engstrom, R. T. (2006). Silviculture that sustains: the nexus between silviculture, frequent prescribed fire, and conservation of biodiversity in longleaf pine forests of the southeastern United States. *Canadian Journal of Forest Research*, *36*(11), 2724-2736. https://doi.org/10.1139/x06-100
- Mitchener, L. J., & Parker, A. J. (2005). Climate, Lightning, and Wildfire in the National Forests of the Southeastern United States: 1989-1998. *Physical Geography*, 26(2), 147-162. https://doi.org/10.2747/0272-3646.26.2.147
- Munoz, S. E., Mladenoff, D. J., Schroeder, S., Williams, J. W., & Bush, M. (2014). Defining the spatial patterns of historical land use associated with the indigenous societies of eastern North America. *Journal of Biogeography*, 41(12), 2195-2210. https://doi.org/10.1111/jbi.12386
- National Prescribed Fire Act of 2020, S.4625, U.S. Senate (2020).
- Nguyen, T. T., Janik, L. J., & Raupach, M. (1991). Diffuse reflectance infrared fourier transform (DRIFT) spectroscopy in soil studies. *Soil Research*, 29(1), 49-67. https://doi.org/10.1071/SR9910049
- North, M. P., York, R. A., Collins, B. M., Hurteau, M. D., Jones, G. M., Knapp, E. E., Kobziar, L., McCann, H., Meyer, M. D., Stephens, S. L., Tompkins, R. E., & Tubbesing, C. L. (2021). Pyrosilviculture Needed for Landscape Resilience of Dry Western United States Forests. *Journal of Forestry*. https://doi.org/10.1093/jofore/fvab026
- Noss, R. F. (1988). The longleaf pine landscape of the southeast: almost gone and almost forgotten
- Endanger Species Update, 5(5), 1–8.
- Nzila, A. (2018). Current Status of the Degradation of Aliphatic and Aromatic Petroleum Hydrocarbons by Thermophilic Microbes and Future Perspectives. *Int J Environ Res Public Health*, *15*(12). https://doi.org/10.3390/ijerph15122782

- Oliver, A. K., Callaham, J., Mac A., & Jumpponen, A. (2015). Soil fungal communities respond compositionally to recurring frequent prescribed burning in a managed southeastern US forest ecosystem. *Forest Ecology and Management*, 345, 1-9.
- Ormeño, E., Céspedes, B., Sánchez, I. A., Velasco-García, A., Moreno, J. M., Fernandez, C., & Baldy, V. (2009). The relationship between terpenes and flammability of leaf litter. *Forest Ecology and Management*, 257(2), 471-482. https://doi.org/10.1016/j.foreco.2008.09.019
- Parikh, S. J., Goyne, K. W., Margenot, A. J., Mukome, F. N. D., & Calderón, F. J. (2014). Soil Chemical Insights Provided through Vibrational Spectroscopy. In (pp. 1-148). https://doi.org/10.1016/b978-0-12-800132-5.00001-8
- Pellegrini, A. F. A., Harden, J., Georgiou, K., Hemes, K. S., Malhotra, A., Nolan, C. J., & Jackson, R. B. (2021). Fire effects on the persistence of soil organic matter and long-term carbon storage. *Nature Geoscience*. https://doi.org/10.1038/s41561-021-00867-1
- Pellegrini, A. F. A., Hobbie, S. E., Reich, P. B., Jumpponen, A., Brookshire, E. N. J., Caprio, A. C., Coetsee, C., & Jackson, R. B. (2020). Repeated fire shifts carbon and nitrogen cycling by changing plant inputs and soil decomposition across ecosystems. *Ecological Monographs*, 90(4). https://doi.org/10.1002/ecm.1409
- Plaza-Álvarez, P., Lucas-Borja, M., Sagra, J., Moya, D., Fontúrbel, T., & de las Heras, J. (2017). Soil Respiration Changes after Prescribed Fires in Spanish Black Pine (Pinus nigra Arn. ssp. salzmannii) Monospecific and Mixed Forest Stands. *Forests*, 8(7). https://doi.org/10.3390/f8070248
- Poth, M., Anderson, I. C., Miranda, H. S., Miranda, A. C., & Riggan, P. J. (1995). The magnitude and persistence of soil NO, N2O, CH4, and CO2 fluxes from burned tropical savanna in Brazil [https://doi.org/10.1029/95GB02086]. *Global Biogeochemical Cycles*, 9(4), 503-513. https://doi.org/https://doi.org/10.1029/95GB02086
- Prescribed Fire Liability Pilot Program: Prescribed Fire Claims Fund, CA SB926, California State Senate (2022).

 https://leginfo.legislature.ca.gov/faces/billCompareClient.xhtml?bill_id=202120220SB92
 6&showamends=false
- Puhlick, J. J., O'Halloran, T. L., Starr, G., Abney, R. B., Pile Knapp, L. S., McCleery, R. A., Klepzig, K. D., Brantley, S. T., McIntyre, R. K., & Song, B. (2023). Opportunities for Research on Carbon Management in Longleaf Pine Ecosystems. *Forests*, *14*(5). https://doi.org/10.3390/f14050874
- R Core Team. (2020). *R: A language and environment for statistical computing*. In R Foundation for Statistical Computing. https://www.R-project.org/.
- Ratcliff, A. W., Busse, M. D., & Shestak, C. J. (2006). Changes in microbial community structure following herbicide (glyphosate) additions to forest soils. *Applied Soil Ecology*, 34(2-3), 114-124. https://doi.org/10.1016/j.apsoil.2006.03.002
- Rebollo, N. R., Cohen-Ofri, I., Popovitz-Biro, R., Bar-Yosef, O., Meignen, L., Goldberg, P., Weiner, S., & Boaretto, E. (2016). Structural Characterization of Charcoal Exposed to

- High and Low Ph: Implications for 14C Sample Preparation and Charcoal Preservation. *Radiocarbon*, 50(2), 289-307. https://doi.org/10.1017/s0033822200033592
- Reisser, M., Purves, R. S., Schmidt, M. W. I., & Abiven, S. (2016). Pyrogenic Carbon in Soils: A Literature-Based Inventory and a Global Estimation of Its Content in Soil Organic Carbon and Stocks. *Frontiers in Earth Science*, 4. https://doi.org/10.3389/feart.2016.00080
- Richter, D. D., Ralston, C. W., & Harms, W. R. (1982). Prescribed Fire: Effects on Water Quality and Forest Nutrient Cycling. *Science*, 215(4533), 661-663. https://doi.org/10.1126/science.215.4533.661
- Rojo, F. (2009). Degradation of alkanes by bacteria. *Environ Microbiol*, *11*(10), 2477-2490. https://doi.org/10.1111/j.1462-2920.2009.01948.x
- Ryan, K. C., Knapp, E. E., & Varner, J. M. (2013). Prescribed fire in North American forests and woodlands: history, current practice, and challenges. *Frontiers in Ecology and the Environment*, 11(s1). https://doi.org/10.1890/120329
- Samuelson, L., Stokes, T., Butnor, J., Johnsen, K., Anderson, P., Jackson, J., Ferrari, L., Martin, T., & Cropper, W. (2014). Ecosystem carbon stocks in Pinus palustris forests. *Canadian Journal of Forest Research*, 44, 476-486. https://doi.org/10.1139/cjfr-2013-0446
- Samuelson, L. J., Stokes, T. A., Butnor, J. R., Johnsen, K. H., Gonzalez-Benecke, C. A., Martin, T. A., Cropper, W. P., Jr., Anderson, P. H., Ramirez, M. R., & Lewis, J. C. (2017). Ecosystem carbon density and allocation across a chronosequence of longleaf pine forests. *Ecol Appl*, 27(1), 244-259. https://doi.org/10.1002/eap.1439
- Samuelson, L. J., & Whitaker, W. B. (2012). Relationships between Soil CO2 Efflux and Forest Structure in 50-Year-Old Longleaf Pine. *Forest Science*, *58*(5), 472-484. https://doi.org/10.5849/forsci.11-049
- Sanderman, J., & Amundson, R. (2014). Biogeochemistry of Decomposition and Detrital Processing. In *Treatise on Geochemistry* (pp. 217-272). https://doi.org/10.1016/b978-0-08-095975-7.00807-x
- Santín, C., Doerr, S. H., Kane, E. S., Masiello, C. A., Ohlson, M., de la Rosa, J. M., Preston, C. M., & Dittmar, T. (2016). Towards a global assessment of pyrogenic carbon from vegetation fires. *Glob Chang Biol*, 22(1), 76-91. https://doi.org/10.1111/gcb.12985
- Santín, C., Doerr, S. H., Preston, C. M., & Gonzalez-Rodriguez, G. (2015). Pyrogenic organic matter production from wildfires: a missing sink in the global carbon cycle. *Glob Chang Biol*, 21(4), 1621-1633. https://doi.org/10.1111/gcb.12800
- Santos, F., Bird, J. A., & Asefaw Berhe, A. (2022). Dissolved pyrogenic carbon leaching in soil: Effects of soil depth and pyrolysis temperature. *Geoderma*, 424. https://doi.org/10.1016/j.geoderma.2022.116011
- Santos, F., Russell, D., & Berhe, A. A. (2016). Thermal alteration of water extractable organic matter in climosequence soils from the Sierra Nevada, California. *Journal of Geophysical Research: Biogeosciences*, 121(11), 2877-2885. https://doi.org/10.1002/2016jg003597

- Santos, F., Torn, M. S., & Bird, J. A. (2012). Biological degradation of pyrogenic organic matter in temperate forest soils. *Soil Biology and Biochemistry*, *51*, 115-124. https://doi.org/10.1016/j.soilbio.2012.04.005
- Santos, F., Wagner, S., Rothstein, D., Jaffe, R., & Miesel, J. R. (2017). Impact of a Historical Fire Event on Pyrogenic Carbon Stocks and Dissolved Pyrogenic Carbon in Spodosols in Northern Michigan. *Frontiers in Earth Science*, 5. https://doi.org/10.3389/feart.2017.00080
- Sasse, J., Martinoia, E., & Northen, T. (2018). Feed Your Friends: Do Plant Exudates Shape the Root Microbiome? *Trends Plant Sci*, 23(1), 25-41. https://doi.org/10.1016/j.tplants.2017.09.003
- Saterson, K. A., & Vitousek, P. M. (1984). Fine-root biomass and nutrient cycling in Aristida stricta in a North Carolina coastal plain savanna. *Canadian Journal of Botany*, 62(4), 823-829. https://doi.org/10.1139/b84-120
- Schiedung, M., Bellè, S.-L., Sigmund, G., Kalbitz, K., & Abiven, S. (2020). Vertical mobility of pyrogenic organic matter in soils: a column experiment. *Biogeosciences*, *17*(24), 6457-6474. https://doi.org/10.5194/bg-17-6457-2020
- Schmidt, M. W., Torn, M. S., Abiven, S., Dittmar, T., Guggenberger, G., Janssens, I. A., Kleber, M., Kogel-Knabner, I., Lehmann, J., Manning, D. A., Nannipieri, P., Rasse, D. P., Weiner, S., & Trumbore, S. E. (2011). Persistence of soil organic matter as an ecosystem property. *Nature*, 478(7367), 49-56. https://doi.org/10.1038/nature10386
- Scholl, A. E., & Taylor, A. H. (2010). Fire regimes, forest change, and self-organization in an old-growth mixed-conifer forest, Yosemite National Park, USA. *Ecol Appl*, 20(2), 362-380. https://doi.org/10.1890/08-2324.1
- Singh, N., Abiven, S., Maestrini, B., Bird, J., Torn, M., & Schmidt, M. (2014). Transformation and stabilization of pyrogenic organic matter in a temperate forest field experiment. *Global Change Biology*, 20. https://doi.org/10.1111/gcb.12459
- Soil Survey Staff. Web Soil Survey. Natural Resources Conservation Service, United States Department of Agriculture. Retrieved 05/01/2023 from http://websoilsurvey.sc.egov.usda.gov/
- Starr, G., Staudhammer, C. L., Loescher, H. W., Mitchell, R., Whelan, A., Hiers, J. K., & O'Brien, J. J. (2014). Time series analysis of forest carbon dynamics: recovery of Pinus palustris physiology following a prescribed fire. *New Forests*, 46(1), 63-90. https://doi.org/10.1007/s11056-014-9447-3
- Stephenson, L. W., Veatch, J. O., & Dole, R. B. (1915). *Underground waters of the coastal plain of Georgia* [Report](341). (Water Supply Paper, Issue. U. S. G. Survey. http://pubs.er.usgs.gov/publication/wsp341
- Strakova, P., Larmola, T., Andres, J., Ilola, N., Launiainen, P., Edwards, K., Minkkinen, K., & Laiho, R. (2020). Quantification of Plant Root Species Composition in Peatlands Using FTIR Spectroscopy. *Front Plant Sci*, *11*, 597. https://doi.org/10.3389/fpls.2020.00597

- Stuiver, M., & Polach, H. (1977). Discussion Reporting of 14C Data. *Radiocarbon*, 19(3), 355-363. https://doi.org/doi:10.1017/S0033822200003672
- Susaeta, A. (2023). Optimal Forest Management of Even-Aged Longleaf Pine Stands with Nontimber Benefits. *Journal of Agricultural and Applied Economics*, 55(1), 1-12. https://doi.org/10.1017/aae.2022.41
- Susaeta, A. I., Gonzalez-Benecke, C. A., Carter, D. R., Jokela, E. J., & Martin, T. A. (2012). Economical sustainability of pinestraw raking in slash pine stands in the southeastern United States. *Ecological Economics*, 80, 89-100. https://doi.org/https://doi.org/10.1016/j.ecolecon.2012.05.010
- Turner, D. P., Koerper, G. J., Harmon, M. E., & Lee, J. J. (1995). A Carbon Budget for Forests of the Conterminous United States. *Ecological Applications*, *5*(2), 421-436. https://doi.org/10.2307/1942033
- Uchytil, R. J. (1992). Aristida Stricta. *Fire Effects Information System*. https://www.fs.usda.gov/database/feis/plants/graminoid/aristr/all.html
- Uhelski, D. M., Kane, E. S., Chimner, R. A., Heckman, K. A., Miesel, J., & Xie, L. (2022). Pyrogenic carbon content of Sphagnum peat soils estimated using diffuse reflectance FTIR spectrometry. *Mires & Peat*(28).
- van der Werf, G. R., Randerson, J. T., Giglio, L., Collatz, G. J., Mu, M., Kasibhatla, P. S., Morton, D. C., DeFries, R. S., Jin, Y., & van Leeuwen, T. T. (2010). Global fire emissions and the contribution of deforestation, savanna, forest, agricultural, and peat fires (1997–2009). *Atmospheric Chemistry and Physics*, *10*(23), 11707-11735. https://doi.org/10.5194/acp-10-11707-2010
- Van Lear, D. H., Carroll, W. D., Kapeluck, P. R., & Johnson, R. (2005). History and restoration of the longleaf pine-grassland ecosystem: Implications for species at risk. *Forest Ecology and Management*, 211(1-2), 150-165. https://doi.org/10.1016/j.foreco.2005.02.014
- Vasilyeva, N. A., Abiven, S., Milanovskiy, E. Y., Hilf, M., Rizhkov, O. V., & Schmidt, M. W. I. (2011). Pyrogenic carbon quantity and quality unchanged after 55 years of organic matter depletion in a Chernozem. *Soil Biology and Biochemistry*, *43*(9), 1985-1988. https://doi.org/10.1016/j.soilbio.2011.05.015
- Vogel, J. S., Southon, J. R., Nelson, D. E., & Brown, T. A. (1984). Performance of catalytically condensed carbon for use in accelerator mass spectrometry. *Nuclear Instruments and Methods in Physics Research Section B: Beam Interactions with Materials and Atoms*, 5(2), 289-293. https://doi.org/https://doi.org/https://doi.org/10.1016/0168-583X(84)90529-9
- Wagner, S., Brantley, S., Stuber, S., Van Stan, J., Whitetree, A., & Stubbins, A. (2019). Dissolved black carbon in throughfall and stemflow in a fire-managed longleaf pine woodland. *Biogeochemistry*, 146(2), 191-207. https://doi.org/10.1007/s10533-019-00620-2
- Wagner, S., Ding, Y., & Jaffé, R. (2017). A New Perspective on the Apparent Solubility of Dissolved Black Carbon. *Frontiers in Earth Science*, 5. https://doi.org/10.3389/feart.2017.00075

- Wagner, S., & Jaffé, R. (2015). Effect of photodegradation on molecular size distribution and quality of dissolved black carbon. *Organic Geochemistry*, 86, 1-4. https://doi.org/10.1016/j.orggeochem.2015.05.005
- Wagner, S., Jaffé, R., & Stubbins, A. (2018). Dissolved black carbon in aquatic ecosystems. Limnology and Oceanography Letters, 3(3), 168-185. https://doi.org/10.1002/lol2.10076
- Wang, J., Xiong, Z., & Kuzyakov, Y. (2015). Biochar stability in soil: meta-analysis of decomposition and priming effects. *GCB Bioenergy*, 8(3), 512-523. https://doi.org/10.1111/gcbb.12266
- Wardle, D. A., & Parkinson, D. (1990). Influence of the herbicide glyphosate on soil microbial community structure. *Plant and Soil*, *122*(1), 29-37. https://doi.org/10.1007/BF02851907
- Weete, J. D. (1972). Aliphatic hydrocarbons of the fungi. *Phytochemistry*, *11*(4), 1201-1205. https://doi.org/https://doi.org/10.1016/S0031-9422(00)90066-9
- Wershaw, R. L. (2004). Evaluation of conceptual models of natural organic matter (humus) from a consideration of the chemical and biochemical processes of humification [Report](2004-5121). (Scientific Investigations Report, Issue. http://pubs.er.usgs.gov/publication/sir20045121
- Wershaw, R. L., Leenheer, J. A., & Cox, L. G. (2005). *Characterization of dissolved and particulate natural organic matter (NOM) in Neversink Reservoir, New York* [Report](2005-5108). (Scientific Investigations Report, Issue. http://pubs.er.usgs.gov/publication/sir20055108
- White, C. s. (1986). Effects of prescribed fire on rates of decomposition and nitrogen mineralization in a Ponderosa Pine Ecosystem. *Biology and Fertility of Soils*, 2, 87-95. https://doi.org/10.1007/BF00257585
- White, C. S. (1991). The interaction of prescribed fire, monoterpenes, and soil N-cycling processes in a stand of ponderosa pine (Pinus ponderosa). Fire and the environment: ecological and cultural perspectives.,
- Whitman, T., Enders, A., & Lehmann, J. (2014a). Pyrogenic carbon additions to soil counteract positive priming of soil carbon mineralization by plants. *Soil Biology and Biochemistry*, 73, 33-41. https://doi.org/10.1016/j.soilbio.2014.02.009
- Whitman, T., Whitman, E., Woolet, J., Flannigan, M. D., Thompson, D. K., & Parisien, M.-A. (2019). Soil bacterial and fungal response to wildfires in the Canadian boreal forest across a burn severity gradient. *Soil Biology and Biochemistry*, *138*. https://doi.org/10.1016/j.soilbio.2019.107571
- Whitman, T., Zhu, Z., & Lehmann, J. (2014b). Carbon mineralizability determines interactive effects on mineralization of pyrogenic organic matter and soil organic carbon. *Environ Sci Technol*, 48(23), 13727-13734. https://doi.org/10.1021/es503331y
- Wickham, H. (2016). ggplot2: Elegant Graphics for Data Analysis. In Springer-Verlag.

- Wiedinmyer, C., & Hurteau, M. D. (2010). Prescribed Fire As a Means of Reducing Forest Carbon Emissions in the Western United States. *Environmental Science & Technology*, 44(6), 1926-1932. https://doi.org/10.1021/es902455e
- Wikars, L.-O., & Schimmel, J. (2001). Immediate effects of fire-severity on soil invertebrates in cut and uncut pine forests. *Forest Ecology and Management*, *141*(3), 189-200. https://doi.org/https://doi.org/10.1016/S0378-1127(00)00328-5
- Williford, S. (2022). Natural Resources Conservation Service Resource Soil Scientist. Tifton Service Center, Tifton, GA.
- Wolters, V. (2000). Invertebrate control of soil organic matter stability. *Biology and Fertility of Soils*, 31(1), 1-19. https://doi.org/10.1007/s003740050618
- Wood, J., & Varner, M. (2023). Burn Back Better: How Wester States Can Encourage Prescribed Fire on Private Lands. P. a. E. R. Center. https://www.perc.org/2023/01/10/burn-back-better/
- Wozniak, A. S., Goranov, A. I., Mitra, S., Bostick, K. W., Zimmerman, A. R., Schlesinger, D. R., Myneni, S., & Hatcher, P. G. (2020). Molecular heterogeneity in pyrogenic dissolved organic matter from a thermal series of oak and grass chars. *Organic Geochemistry*, *148*, Article 104065. https://doi.org/10.1016/j.orggeochem.2020.104065
- Wurster, C. M., Saiz, G., Schneider, M. P. W., Schmidt, M. W. I., & Bird, M. I. (2013). Quantifying pyrogenic carbon from thermosequences of wood and grass using hydrogen pyrolysis. *Organic Geochemistry*, 62, 28-32. https://doi.org/10.1016/j.orggeochem.2013.06.009
- Xu, R., Yu, P., Abramson, M. J., Johnston, F. H., Samet, J. M., Bell, M. L., Haines, A., Ebi, K. L., Li, S., & Guo, Y. (2020). Wildfires, Global Climate Change, and Human Health. *New England Journal of Medicine*, 383(22), 2173-2181. https://doi.org/10.1056/NEJMsr2028985
- Yoder, J. (2008). Liability, Regulation, and Endogenous Risk: The Incidence and Severity of Escaped Prescribed Fires in the United States. *The Journal of Law and Economics*, *51*(2), 297-325. https://doi.org/10.1086/589661
- Zaller, J. G., Heigl, F., Ruess, L., & Grabmaier, A. (2014). Glyphosate herbicide affects belowground interactions between earthworms and symbiotic mycorrhizal fungi in a model ecosystem. *Scientific Reports*, 4(2045-2322 (Electronic)). https://doi.org/https://doi.org/10.1038/srep05634
- Zhang, X., & Wang, W. (2015). The decomposition of fine and coarse roots: their global patterns and controlling factors. *Sci Rep*, *5*, 9940. https://doi.org/10.1038/srep09940

APPENDIX A

CHAPTER 2 FULL MODEL RESULTS

```
MODEL INFO:
Observations: 96
Dependent Variable: Percent_C
Type: Mixed effects linear regression
MODEL FIT:
AIC = 8.86, BIC = 26.81
Pseudo-R^2 (fixed effects) = 0.53
Pseudo-R^2 (total) = 0.78
FIXED EFFECTS:
                        Est. S.E. t val. d.f.
(Intercept)
                         1.45
                                                   -0.00
                         -0.28 -0.00
-0.30 0.02 -12.74 79.00 0.00
BurnStatusUnburned
Depth
Collection
                            0.07 0.05 1.44 13.00
                                                             0.17
RANDOM EFFECTS:
   Group Parameter Std. Dev.
 Core:Site (Intercept) 0.18
Site (Intercept) 0.09
Residual 0.19
                             0.19
<u>Grouping variables:</u>
 -----
            # groups ICC
   Group
 Core:Site 16
Site 2
                       0.43
                      0.10
Data: lys.soils
Models:
lys.C.null1: Percent_C ~ Depth + Collection + (1 | Site/Core)
lys.C.full: Percent_C ~ BurnStatus + Depth + Collection + (1 | Site/Co
npar AIC BIC logLik deviance Chisq Df Pr(>Chisq)
lys.C.null1 6 -5.2549 10.1311 8.6275 -17.255
lys.C.full 7 -8.2821 9.6683 11.1411 -22.282 5.0272 1 0.02495
Signif. codes: 0 '*** 0.001 '** 0.01 '* 0.05 '.' 0.1 ' '1
c
```

```
# test depth effect
 anova(lys.C.full, lys.C.null2)
Data: lys.soils
Models:
lys.C.null2: Percent_C ~ BurnStatus + Collection + (1 | Site/Core)
lys.C.full: Percent_C ~ BurnStatus + Depth + Collection + (1 | Site/Co
                          BIC logLik deviance Chisq Df Pr(>Chisq)
                   AIC
            npar
lys.C.null2
               6 79.084 94.470 -33.542
                                         67.084
lys.C.full
               7 -8.282 9.668 11.141 -22.282 89.366 1 < 2.2e-16 *
Signif. codes: 0 '***' 0.001 '**' 0.01 '*' 0.05 '.' 0.1 ' ' 1
   test collection effect
> anova(lys.C.full, lys.C.null3)
Data: lys.soils
Models:
lys.C.null3: Percent_C ~ BurnStatus + Depth + (1 | Site/Core)
lys.C.full: Percent_C ~ BurnStatus + Depth + Collection + (1 | Site/Co
                     AIC
                            BIC logLik deviance Chisq Df Pr(>Chisq)
            npar
               6 -7.8640 7.5221
lys.C.null3
                                9.932
                                        -19.864
lys.C.full
               7 -8.2821 9.6683 11.141
                                       -22.282 2.4182 1
                                                              0.1199
```

Figure A.1. Model results from a) mixed linear effects model testing the influence of burn status, depth, and collection date on percent carbon in soils. Significance was tested by constructing null models that excluded b) burn status, c) depth, or d) collection date and running an ANOVA to compare the null model for each variable in question to the full model. Soil core ID was included as a random variable.

Total Nitrogen Mixed Linear Effects Model Results

```
MODEL FIT:
AIC = -507.67, BIC = -489.72
Pseudo-R^2 (fixed effects) = 0.51
 Pseudo-R^2 (total) = 0.73
FIXED EFFECTS:
                         Est. S.E. t val. d.f.
                                                           р
                      0.07 0.04 2.11 -0.00
-0.02 0.04 -0.45 -0.00
-0.02 0.00 -10.52 79.00
 (Intercept)
BurnStatusUnburned
Depth
                                                          0.00
Collection
                          0.01 0.00 2.70 13.00
                                                          0.02
RANDOM EFFECTS:
          Parameter Std. Dev.
 Core:Site (Intercept) 0.01
   Site
             (Intercept)
                           0.01
                          0.01
 Residual
Grouping variables:
   Group # groups ICC
 Core:Site 16
                      0.14
               2
   Site
                        0.31
b
Data: lys.soils
Models:
lys.N.null1: Percent_N ~ Depth + Collection + (1 | Site/Core)
lys.N.full: Percent_N ~ BurnStatus + Depth + Collection + (1 | Site/Co
           npar AIC BIC logLik deviance Chisq Df Pr(>Chisq)
lys.N.null1 6 -544.47 -529.08 278.24 -556.47
lys.N.full 7 -549.58 -531.63 281.79 -563.58 7.1118 1 0.007658
Signif. codes: 0 '*** 0.001 '** 0.01 '* 0.05 '.' 0.1 ' 1
c
```

```
> # test depth effect
> anova(lys.N.full, lys.N.null2)
Data: lys.soils
Models:
lys.N.null2: Percent_N ~ BurnStatus + Collection + (1 | Site/Core)
lys.N.full: Percent_N ~ BurnStatus + Depth + Collection + (1 | Site/Co
                            BIC logLik deviance Chisq Df Pr(>Chisq)
                    AIC
           npar
lys.N.null2
             6 -483.55 -468.17 247.78 -495.55
              7 -549.58 -531.63 281.79 -563.58 68.029 1 < 2.2e-16
lys.N.full
Signif. codes: 0 '***' 0.001 '**' 0.01 '*' 0.05 '.' 0.1 ' '1
Data: lys.soils
Models:
lys.N.null3: Percent_N ~ BurnStatus + Depth + (1 | Site/Core)
lys.N.full: Percent_N ~ BurnStatus + Depth + Collection + (1 | Site/Co
                            BIC logLik deviance Chisq Df Pr(>Chisq)
            npar
                    AIC
lys.N.null3
               6 -544.77 -529.38 278.38 -556.77
lys.N.full
               7 -549.58 -531.63 281.79 -563.58 6.8101 1
Signif. codes: 0 '*** 0.001 '** 0.01 '*' 0.05 '.' 0.1 ' ' 1
```

Figure A.2. Model results from a) mixed linear effects model testing the influence of burn status, depth, and collection date on percent nitrogen in soils. Significance was tested by constructing null models that excluded b) burn status, c) depth, or d) collection date and running an ANOVA to compare the null model for each variable in question to the full model. Soil core ID was included as a random variable.

C:N Ratio Mixed Linear Effects Model Results

MODEL INFO:

```
Observations: 96
Dependent Variable: CN_Ratio
Type: Mixed effects linear regression
MODEL FIT:
AIC = 442.81, BIC = 463.32
Pseudo-R^2 (fixed effects) = 0.07
Pseudo-R^2 (total) = 0.74
FIXED EFFECTS:
                                      Est. S.E. t val.

    19.98
    2.81
    7.10
    228.42
    0.00

    0.22
    3.65
    0.06
    1340.81
    0.95

    -0.21
    0.35
    -0.61
    78.00
    0.54

    -0.33
    0.56
    -0.60
    13.00
    0.56

    0.78
    0.49
    1.59
    78.00
    0.12

(Intercept)
BurnStatusUnburned
Depth
Collection
BurnStatusUnburned:Depth
RANDOM EFFECTS:
   Group Parameter Std. Dev.
 ----- -----
               (Intercept)
 Core:Site
                                 2.09
   Site (Intercept)
                                 2.36
 Residual
                                  1.96
<u>Grouping variables:</u>
   Group
               # groups ICC
 Core:Site 16
Site 2
                           0.32
                 2
                            0.40
> # test burn status effect
> anova(lys.CN.full, lys.CN.null1)
Data: lys.soils
Models:
lys.CN.null1: CN_Ratio ~ Depth + Collection + (1 | Site/Core)
lys.CN.full: CN_Ratio ~ BurnStatus * Depth + Collection + (1 | Site/Co
               npar AIC BIC logLik deviance Chisq Df Pr(>Chisq)
lys.CN.nulll 6 446.61 461.99 -217.30 434.61
lys.CN.full
                8 445.31 465.83 -214.66 429.31 5.2963 2 0.07078
Signif. codes: 0 '*** 0.001 '** 0.01 '* 0.05 '.' 0.1 ' '1
```

```
C
  # test depth effect
  anova(lys.CN.full, lys.CN.null2)
Data: lys.soils
Models:
 lys.CN.null2: CN_Ratio ~ BurnStatus + Collection + (1 | Site/Core)
 lys.CN.full: CN_Ratio ~ BurnStatus * Depth + Collection + (1 | Site/Co
                             BIC logLik deviance Chisq Df Pr(>Chisq)
                      AIC
              npar
 lys.CN.null2
                 6 444.37 459.75 -216.18
                                           432.37
 lys.CN.full
                 8 445.31 465.83 -214.66
                                           429.31 3.0555
                                                                  0.217
  # test collection effect
  anova(lys.CN.full, lys.CN.null3)
Data: lys.soils
Models:
lys.CN.null3: CN_Ratio ~ BurnStatus * Depth + (1 | Site/Core)
 lys.CN.full: CN_Ratio ~ BurnStatus * Depth + Collection + (1 | Site/Co
                      AIC
                             BIC logLik deviance Chisq Df Pr(>Chisq)
 lys.CN.null3
                 7 443.74 461.69 -214.87
                                           429.74
                 8 445.31 465.83 -214.66
                                           429.31 0.4312
                                                                 0.5114
 lys.CN.full
  # test interaction effect
 > anova(lys.CN.full, lys.CN.null4)
Data: lys.soils
Models:
lys.CN.null4: CN_Ratio ~ BurnStatus + Depth + Collection + (1 | Site/Co
lys.CN.full: CN_Ratio ~ BurnStatus * Depth + Collection + (1 | Site/Col
                                logLik deviance Chisq Df Pr(>Chisq)
                     AIC
                             BIC
lvs.CN.null4
                7 445.85 463.80 -215.93
                                           431.85
                8 445.31 465.83 -214.66
                                           429.31 2.5419 1
                                                                 0.1109
lys.CN.full
```

Figure A.3. Model results from a) mixed linear effects model testing the influence of burn status, depth, and collection date, and the interaction of burn status and depth on carbon to nitrogen ratio in soils. Significance was tested by constructing null models that excluded b) burn status, c) depth, d) collection date, or e) interaction of burn status and depth and running an ANOVA to compare the null model for each variable in question to the full model. Soil core ID was included as a random variable.

$\delta^{13}C$ Mixed Linear Effects Model Results

```
MODEL INFO:
Observations: 96
Dependent Variable: d13C
Type: Mixed effects linear regression
MODEL FIT:
AIC = 131.17, BIC = 151.69
Pseudo-R^2 (fixed effects) = 0.50
Pseudo-R^2 (total) = 0.94
FIXED EFFECTS:
                                 Est. S.E. t val. d.f.
(Intercept)
                               -24.40 0.62 -39.58 <u>31.65</u> <u>0.00</u>
                                -2.66 0.66 -4.03
0.23 0.06 4.03
0.05 0.20 0.27
BurnStatusUnburned
                                                       93.14 0.00
Depth
                                                       78.00 0.00
Collection
                                                       13.00
                                                              0.79
                                        0.08 6.82
BurnStatusUnburned:Depth
                                 0.54
                                                       78.00
                                                             0.00
RANDOM EFFECTS:
   Group Parameter Std. Dev.
 Core:Site (Intercept) 0.80
             (Intercept)
                           0.35
   Site
 Residual
                            0.32
Grouping variables:
   Group # groups ICC
 Core:Site 16
                       0.74
               2
                       0.14
 > anova(lys.d13C.full, lys.d13C.null1)
Data: lys.soils
Models:
lys.d13C.null1: d13C ~ Depth + Collection + (1 | Site/Core)
lys.d13C.full: d13C ~ BurnStatus * Depth + Collection + (1 | Site/Core
               npar AIC BIC logLik deviance Chisq Df Pr(>Chisq
               6 159.99 175.38 -73.996 147.99
lys.d13C.null1
lys.d13C.full
                8 120.24 140.76 -52.121
                                           104.24 43.751 2 3.159e-1
Signif. codes: 0 '***' 0.001 '**' 0.01 '*' 0.05 '.' 0.1 ' ' 1
\mathbf{c}
```

```
# test depth effect
> anova(lys.d13C.full, lys.d13C.null2)
Data: lys.soils
Models:
lys.d13C.null2: d13C ~ BurnStatus + Collection + (1 | Site/Core)
lys.d13C.full: d13C ~ BurnStatus * Depth + Collection + (1 | Site/Core
                              BIC
                                    logLik deviance Chisq Df Pr(>Chisq)
               npar
                       AIC
                  6 218.84 234.23 -103.422
lys.d13C.null2
                                              206.84
lys.d13C.full
                  8 120.24 140.76 -52.121
                                              104.24 102.6 2 < 2.2e-1
Signif. codes: 0 '***' 0.001 '**' 0.01 '*' 0.05 '.' 0.1 ' '1
    test collection effect
  anova(lys.d13C.full, lys.d13C.null3)
Data: lys.soils
Models:
lys.d13C.null3: d13C ~ BurnStatus * Depth + (1 | Site/Core)
lys.d13C.full: d13C ~ BurnStatus * Depth + Collection + (1 | Site/Core)
                              BIC logLik deviance Chisq Df Pr(>Chisq)
                       AIC
               npar
lys.d13C.null3
                  7 118.33 136.28 -52.165
                                            104.33
lys.d13C.full
                  8 120.24 140.76 -52.121
                                            104.24 0.0888 1
                                                                  0.765
Data: lys.soils
Models:
lys.d13C.null4: d13C ~ BurnStatus + Depth + Collection + (1 | Site/Cor
lys.d13C.full: d13C ~ BurnStatus * Depth + Collection + (1 | Site/Core
                              BIC logLik deviance Chisq Df Pr(>Chisq
                       AIC
               npar
lys.d13C.null4
                  7 155.62 173.57 -70.810
                                             141.62
lys.d13C.full
                  8 120.24 140.76 -52.121
                                             104.24 37.378 1 9.733e-1
                0 '***' 0.001 '**' 0.01 '*' 0.05 '.' 0.1 ' ' 1
Signif. codes:
```

Figure A.4. Model results from a) mixed linear effects model testing the influence of burn status, depth, and collection date, and the interaction of burn status and depth on δ ¹³C stable isotope in soils. Significance was tested by constructing null models that excluded b) burn status, c) depth, d) collection date, or e) interaction of burn status and depth and running an ANOVA to compare the null model for each variable in question to the full model. Soil core ID was included as a random variable.

```
MODEL INFO:
Observations: 192
Dependent Variable: pH_H20
Type: Mixed effects linear regression
MODEL FIT:
AIC = -71.64, BIC = -48.83
Pseudo-R^2 (fixed effects) = 0.60
Pseudo-R^2 (total) = 0.73
FIXED EFFECTS:
                          Est. S.E. t val. d.f.
                           4.01
0.40
(Intercept)
                                                     -0.00
BurnStatusUnburned
                                                     -0.00
                           0.09 0.01 9.64 175.10 0.00
0.17 0.06 2.67 13.65 0.02
                                                               0.00
Depth
Collection
RANDOM EFFECTS:
   Group
              Parameter
                           Std. Dev.
 ----- -----
 Core:Site (Intercept) 0.12
Site (Intercept) 0.01
Residual 0.17
Grouping variables:
   Group
            # groups ICC
 Core:Site 16
                         0.33
                 2
   Site
                         0.00
 anova(lys.pH_H2O.full, lys.pH_H2O.null1)
Data: lys.pH
Models:
lys.pH_H20.null1: pH_H20 ~ Depth + Collection + (1 | Site/Core)
lys.pH_H2O.full: pH_H2O ~ BurnStatus + Depth + Collection + (1 | Site/G
npar AIC BIC logLik deviance Chisq Df Pr(>Chi
lys.pH_H2O.null1 6 -86.834 -67.289 49.417 -98.834
lys.pH_H2O.full 7 -92.950 -70.148 53.475 -106.950 8.1168 1 0.004
Signif. codes: 0 '***' 0.001 '**' 0.01 '*' 0.05 '.' 0.1 ' ' 1
\mathbf{c}
```

```
# test depth effect
 anova(lys.pH_H20.full, lys.pH_H20.null2)
Data: lys.pH
Models:
lys.pH_H20.null2: pH_H20 ~ BurnStatus + Collection + (1 | Site/Core)
lys.pH_H2O.full: pH_H2O ~ BurnStatus + Depth + Collection + (1 | Site/Co
                    ar AIC BIC logLik deviance Chisq Df Pr(>Chis
6 -33.105 -13.560 22.553 -45.105
                 npar
lys.pH_H20.null2
                    7 -92.950 -70.148 53.475 -106.950 61.845 1 3.715e-
lys.pH_H2O.full
Signif. codes: 0 '***' 0.001 '**' 0.01 '*' 0.05 '.' 0.1 ' ' 1
    test collection effect
  anova(lys.pH_H20.full, lys.pH_H20.null3)
Data: lys.pH
Models:
lys.pH_H2O.null3: pH_H2O ~ BurnStatus + Depth + (1 | Site/Core)
lys.pH_H2O.full: pH_H2O ~ BurnStatus + Depth + Collection + (1 | Site/Co
                 npar
                          AIC
                                   BIC logLik deviance Chisq Df Pr(>Chis
lys.pH_H2O.null3
                    6 -77.353 -57.808 44.677
                                              -89.353
                     7 -92.950 -70.148 53.475 -106.950 17.597 1
lys.pH_H2O.full
Signif. codes: 0 '***' 0.001 '**' 0.05 '.' 0.1 ' ' 1
```

Figure A.5. Model results from a) mixed linear effects model testing the influence of burn status, depth, and collection date on soil pH when tested in water (H₂O). Significance was tested by constructing null models that excluded b) burn status, c) depth, or d) collection date and running an ANOVA to compare the null model for each variable in question to the full model. Soil core ID was included as a random variable.

```
MODEL INFO:
Observations: 192
Dependent Variable: pH_CaCl2
Type: Mixed effects linear regression
MODEL FIT:
AIC = -46.83, BIC = -20.77
Pseudo-R^2 (fixed effects) = 0.39
Pseudo-R^2 (total) = 0.89
FIXED EFFECTS:
                                 Est.
                                       S.E.
                                               t val.
                                                            d.f.
                                                                      р
(Intercept)
                                 3.83
                                        0.38
                                                10.18
                                                         6297.37
                                                                   0.00
BurnStatusUnburned
                                        0.52
                                                0.60
                                                        51029.22
                                                                   0.55
                                 0.32
                                                -3.78
                                                                   0.00
Depth
                                -0.06
                                        0.01
                                                          177.85
Collection
                                 0.10
                                        0.03
                                                 3.10
                                                          13.67
                                                                   0.01
BurnStatusUnburned:Depth
                                 0.12
                                        0.02
                                                 5.76
                                                          181.33
                                                                   0.00
h
 > # test burn status effect
Data: lys.pH
Models:
lys.pH_CaCl2.null1: pH_CaCl2 ~ Depth + Collection + (1 | Site/Core)
lys.pH_CaCl2.full: pH_CaCl2 ~ BurnStatus * Depth + Collection + (1 | Site
                                  BIC logLik deviance Chisq Df Pr(>Chis
                   npar
                           AIC
                     6 -37.162 -17.617 24.581 -49.162
 lys.pH_CaCl2.null1
 lys.pH_CaCl2.full
                      8 -73.951 -47.891 44.975 -89.951 40.789 2
Signif. codes: 0 '***' 0.001 '**' 0.01 '*' 0.05 '.' 0.1 ' ' 1
  # test depth effect
Data: lys.pH
Models:
lys.pH_CaCl2.null2: pH_CaCl2 ~ BurnStatus + Collection + (1 | Site/Core)
lys.pH_CaCl2.full: pH_CaCl2 ~ BurnStatus * Depth + Collection + (1 | Site/
                                  BIC logLik deviance Chisq Df Pr(>Chis
                   npar AIC
lys.pH_CaCl2.null2
                     6 -47.004 -27.459 29.502 -59.004
lys.pH_CaCl2.full
                      8 -73.951 -47.891 44.975 -89.951 30.947 2 1.905e-
Signif. codes: 0 '***' 0.001 '**' 0.05 '.' 0.1 ' ' 1
```

```
test collection effect
 Data: lys.pH
 Models:
 lys.pH_CaCl2.null3: pH_CaCl2 ~ BurnStatus * Depth + (1 | Site/Core)
lys.pH_CaCl2.full: pH_CaCl2 ~ BurnStatus * Depth + Collection + (1 | Site
                          ar AIC BIC logLik deviance
7 -67.031 -44.228 40.515 -81.031
                                           BIC logLik deviance Chisq Df Pr(>Chi
                       npar
 lys.pH_CaCl2.null3
 lys.pH_CaCl2.full
                          8 -73.951 -47.891 44.975 -89.951 8.9202 1
                                                                                 0.00
 Signif. codes: 0 '***' 0.001 '**' 0.05 '.' 0.1 ' ' 1
  # test interaction effect
Data: lys.pH
Models:
lys.pH_CaCl2.null4: pH_CaCl2 ~ BurnStatus + Depth + Collection + (1 | Site
lys.pH_CaCl2.full: pH_CaCl2 ~ BurnStatus * Depth + Collection + (1 | Site/
```

BIC logLik deviance Chisq Df Pr(>Chis

-89.951 30.818 1 2.834e-

-59.133

Figure A.6. Model results from a) mixed linear effects model testing the influence of burn status, depth, collection date, and the interaction of burn status and depth on soil pH when tested in a 1M calcium chloride solution (CaCl₂). Significance was tested by constructing null models that excluded b) burn status, c) depth, d) collection date, or e) interaction of burn status and depth and running an ANOVA to compare the null model for each variable in question to the full model. Soil core ID was included as a random variable.

AIC

Signif. codes: 0 '***' 0.001 '**' 0.01 '*' 0.05 '.' 0.1 ' ' 1

7 -45.133 -22.331 29.567

8 -73.951 -47.891 44.975

npar

lys.pH_CaCl2.null4

lys.pH_CaCl2.full

Total Carbon 0-10 cm ANOVA Model Results

```
> Anova(top.C.anova)
Anova Table (Type II tests)
Response: Percent_C
          Sum Sq Df F value
                               Pr(>F)
BurnStatus 2.0633 2 11.132 0.0005059 ***
Residuals 1.9463 21
Signif. codes: 0 '***' 0.001 '**' 0.05 '.' 0.1 ' ' 1
  emmeans(top.C.anova, specs=pairwise~BurnStatus, adjust="sidak'
$emmeans
                     SE df lower.CL upper.CL
 BurnStatus emmean
 Burned 1.312 0.108 21
                             1.089
                                       1.536
             1.438 0.108 21
 Postburn
                              1.214
                                       1.661
 Unburned 0.762 0.108 21
                              0.539
                                       0.986
Confidence level used: 0.95
$contrasts
 contrast
                               SE df t.ratio p.value
                    estimate
 Burned - Postburn
                      -0.125 0.152 21 -0.821 0.8057
 Burned - Unburned
                       0.550 0.152 21 3.613 0.0049
                       0.675 0.152 21
                                       4.434 0.0007
 Postburn - Unburned
P value adjustment: sidak method for 3 tests
```

Figure A.7. Model results from a a) one-way ANOVA testing the influence of burn status on percent carbon in soils collected at 0-10 cm. Pairwise significance was tested by b) running a Sidak test.

```
Anova(top.N.anova)
Anova Table (Type II tests)
Response: Percent_N
              Sum Sq Df F value Pr(>F)
BurnStatus 0.0051583 2 6.7492 0.00545 **
Residuals 0.0080250 21
Signif. codes: 0 '*** 0.001 '** 0.01 '* 0.05 '.' 0.1 ' ' 1
> emmeans(top.N.anova, specs=pairwise~BurnStatus, adjust="sidak")
$emmeans
                       SE df lower.CL upper.CL
 BurnStatus emmean
          0.0663 0.00691 21
                               0.0519
 Burned
                                        0.0806
           0.0725 0.00691 21
                                        0.0869
 Postburn
                               0.0581
 Unburned 0.0387 0.00691 21
                               0.0244
                                        0.0531
Confidence level used: 0.95
$contrasts
                                  SE df t.ratio p.value
 contrast
                     estimate
                    -0.00625 0.00977 21 -0.639 0.8958
 Burned - Postburn
 Burned - Unburned
                     0.02750 0.00977 21
                                          2.814
                                                 0.0309
 Postburn - Unburned 0.03375 0.00977 21
                                          3.453
                                                 0.0071
P value adjustment: sidak method for 3 tests
```

Figure A.8. Model results from a a) one-way ANOVA testing the influence of burn status on percent nitrogen in soils collected at 0-10 cm. Pairwise significance was tested by b) running a Sidak test.

C:N Ratio 0-10 cm ANOVA Model Results

```
> Anova(top.CN.anova)
Anova Table (Type II tests)
Response: CN_Ratio
           Sum Sq Df F value Pr(>F)
                      0.826 0.4515
BurnStatus 6.801 2
Residuals 86.452 21
> emmeans(top.CN.anova, specs=pairwise~BurnStatus, adjust="sidak")
$emmeans
 BurnStatus emmean SE df lower.CL upper.CL
              19.9 0.717 21
 Burned
                                18.4
                                         21.4
              20.4 0.717 21
 Postburn
                                18.9
                                         21.9
              19.1 0.717 21
 Unburned
                                17.6
                                         20.6
Confidence level used: 0.95
$contrasts
 contrast
                     estimate
                                SE df t.ratio p.value
 Burned - Postburn
                       -0.562 1.01 21 -0.554
                                               0.9286
 Burned - Unburned
                        0.738 1.01 21
                                        0.727
                                               0.8555
                        1.300 1.01 21
 Postburn - Unburned
                                        1.281 0.5144
P value adjustment: sidak method for 3 tests
```

Figure A.9. Model results from a a) one-way ANOVA testing the influence of burn status on carbon to nitrogen ratio in soils collected at 0-10 cm. Pairwise significance was tested by b) running a Sidak test.

```
> Anova(top.d13C.anova)
Anova Table (Type II tests)
Response: d13C
           Sum Sq Df F value
                              Pr(>F)
BurnStatus 18.961 2 9.0872 0.001435 **
Residuals 21.909 21
Signif. codes: 0 '***' 0.001 '**' 0.01 '*' 0.05 '.' 0.1 ' ' 1
> emmeans(top.d13C.anova, specs=pairwise~BurnStatus, adjust="sidak")
$emmeans
 BurnStatus emmean
                    SE df lower.CL upper.CL
 Burned -24.4 0.361 21
                              -25.2
                                       -23.6
            -23.8 0.361 21
                              -24.6
                                       -23.0
 Postburn
            -25.9 0.361 21
                              -26.7
                                       -25.2
 Unburned
Confidence level used: 0.95
$contrasts
 contrast
                     estimate SE df t.ratio p.value
 Burned - Postburn
                        -0.60 0.511 21 -1.175
                                               0.5835
 Burned - Unburned
                        1.51 0.511 21
                                        2.962
                                               0.0222
 Postburn - Unburned
                        2.11 0.511 21
                                        4.136 0.0014
P value adjustment: sidak method for 3 tests
```

Figure A.10. Model results from a a) one-way ANOVA testing the influence of burn status on δ^{13} C stable isotope in soils collected at 0-10 cm. Pairwise significance was tested by b) running a Sidak test.

```
> Anova(top.pH_H20.anova)
Anova Table (Type II tests)
Response: pH_H2O
          Sum Sq Df F value
BurnStatus 1.3406 2
                    18.78 3.582e-06 ***
Residuals 1.1778 33
Signif. codes: 0 '***' 0.001 '**' 0.01 '*' 0.05 '.' 0.1 ' ' 1
> emmeans(top.pH_H20.anova, specs=pairwise~BurnStatus, adjust="sidak")
$emmeans
BurnStatus emmean
                    SE df lower.CL upper.CL
 Burned
             4.43 0.0545 33
                                4.32
                                        4.54
             4.09 0.0545 33
                                3.98
                                         4.21
 Postburn
             4.55 0.0545 33
                                4.44
                                         4.66
Unburned
Confidence level used: 0.95
$contrasts
contrast
                    estimate
                                 SE df t.ratio p.value
Burned - Postburn
                       0.332 0.0771 33
                                       4.300 0.0004
Burned - Unburned
                      -0.126 0.0771 33
                                       -1.632
                                              0.3005
 Postburn - Unburned -0.458 0.0771 33
                                       -5.932
                                              <.0001
P value adjustment: sidak method for 3 tests
```

Figure A.11. Model results from a a) one-way ANOVA testing the influence of burn status on pH in water (H₂O) for soils collected at 0-10 cm soils collected at 0-10 cm. Pairwise significance was tested by b) running a Sidak test.

```
> Anova(top.pH_H20.anova)
Anova Table (Type II tests)
Response: pH_H2O
          Sum Sq Df F value
BurnStatus 1.3406 2
                    18.78 3.582e-06 ***
Residuals 1.1778 33
Signif. codes: 0 '***' 0.001 '**' 0.05 '.' 0.1 ' ' 1
> emmeans(top.pH_H20.anova, specs=pairwise~BurnStatus, adjust="sidak")
$emmeans
BurnStatus emmean
                    SE df lower.CL upper.CL
             4.43 0.0545 33
                               4.32
                                        4.54
 Burned
             4.09 0.0545 33
                               3.98
                                        4.21
 Postburn
             4.55 0.0545 33
                               4.44
                                        4.66
Unburned
Confidence level used: 0.95
$contrasts
contrast
                    estimate
                                SE df t.ratio p.value
Burned - Postburn
                       0.332 0.0771 33
                                       4.300 0.0004
Burned - Unburned
                      -0.126 0.0771 33
                                      -1.632
                                              0.3005
 Postburn - Unburned -0.458 0.0771 33
                                       -5.932
                                              <.0001
P value adjustment: sidak method for 3 tests
```

Figure A.12. Model results from a a) one-way ANOVA testing the influence of burn status on pH in calcium chloride (CaCl₂) for soils collected at 0-10 cm. Pairwise significance was tested by b) running a Sidak test.

```
> Anova(lys.bd.anova)
Anova Table (Type II tests)
Response: BulkDensity
             Sum Sq Df F value Pr(>F)
BurnStatus 0.17282 2 3.7469 0.06548 .
Residuals 0.20755 9
 Signif. codes: 0 '***' 0.001 '**' 0.01 '*' 0.05 '.' 0.1 ' ' 1
h
$emmeans
 BurnStatus emmean SE df lower.CL upper.CL
 Burned
             1.26 0.0759 9
                                  1.09
 Postburn 1.20 0.0759 9
Unburned 1.48 0.0759 9
                                   1.03
                                            1.37
                                   1.31
                                            1.65
Confidence level used: 0.95
$contrasts
 contrast
                     estimate
                                 SE df t.ratio p.value
 Burned - Postburn 0.0625 0.107 9 0.582 0.9231 Burned - Unburned -0.2175 0.107 9 -2.026 0.2046
 Postburn - Unburned -0.2800 0.107 9 -2.608 0.0828
P value adjustment: sidak method for 3 tests
```

Figure A.13. Model results from a a) one-way ANOVA testing the influence of burn status on bulk density at 0-10 cm. Pairwise significance was tested by b) running a Sidak test.

```
MODEL INFO:
Observations: 40
Dependent Variable: Normalized
Type: Mixed effects linear regression
MODEL FIT:
AIC = 187.71, BIC = 196.15
Pseudo-R<sup>2</sup> (fixed effects) = 0.20
Pseudo-R^2 (total) = 0.20
FIXED EFFECTS:
                                   Est. S.E. t val. d.f. p

      (Intercept)
      7.61
      0.98
      7.80
      28.27
      0.00

      BurnStatusUnburned
      -0.86
      0.74
      -1.16
      32.46
      0.25

      Collection
      -0.75
      0.27
      -2.81
      36.98
      0.01

BurnStatusUnburned
Collection
RANDOM EFFECTS:
                  Parameter Std. Dev.
 LysimeterID (Intercept) 0.00
Residual 2.32
<u>Grouping variables:</u>
     Group # groups ICC
 LysimeterID 8 0.00
 > anova(leach.aro.full, leach.aro.null1)
Data: NMR.leach.aro
Models:
leach.aro.null1: Normalized ~ Collection + (1 | LysimeterID)
leach.aro.full: Normalized ~ BurnStatus + Collection + (1 | LysimeterID)
c
```

Figure A.14. Model results from a) mixed linear effects model testing the influence of burn status and collection date on proportion of carbon structures in leachate DOM that were aromatic. Significance was tested by constructing null models that excluded b) burn status and c) collection date and running an ANOVA to compare the null model for each variable in question to the full model. The response variable "Normalized" refers to aromatic proportion. Lysimeter ID was included as a random variable.

```
MODEL INFO:
Observations: 40
Dependent Variable: Normalized
Type: Mixed effects linear regression
MODEL FIT:
\overline{AIC} = 261.77, BIC = 270.22
Pseudo-R^2 (fixed effects) = 0.13
Pseudo-R^2 (total) = 0.13
FIXED EFFECTS:
                          Est. S.E. t val. d.f.

      (Intercept)
      15.34
      2.65
      5.78
      28.27
      0.00

      BurnStatusUnburned
      -1.70
      2.00
      -0.85
      32.46
      0.40

      Collection
      -1.56
      0.73
      -2.15
      36.98
      0.04

BurnStatusUnburned
Collection
RANDOM EFFECTS:
     Group Parameter Std. Dev.
 LysimeterID (Intercept) 0.00
Residual 6.32
<u>Grouping variables:</u>
     Group # groups ICC
 LysimeterID 8 0.00
 anova(leach.oxy.full, leach.oxy.null1)
Data: NMR.leach.oxy
Models:
leach.oxy.null1: Normalized ~ Collection + (1 | LysimeterID)
leach.oxy.full: Normalized ~ BurnStatus + Collection + (1 | LysimeterIC
                  npar AIC BIC logLik deviance Chisq Df Pr(>Chiso
c
```

```
anova(leach.oxy.full, leach.oxy.null2)
Data: NMR.leach.oxy
Models:
leach.oxy.null2: Normalized ~ BurnStatus + (1 | LysimeterID)
leach.oxy.full: Normalized ~ BurnStatus + Collection + (1 | LysimeterI
                              BIC logLik deviance Chisq Df Pr(>Chis
                       AIC
               npar
leach.oxy.null2
                 4 270.82 277.58 -131.41
                                            262.82
leach.oxy.full
                  5 267.86 276.30 -128.93
                                            257.86 4.9681 1
                                                                0.025
leach.oxy.null2
leach.oxy.full *
Signif. codes: 0 '***' 0.001 '**' 0.05 '.' 0.1 ' ' 1
```

Figure A.15. Model results from a) mixed linear effects model testing the influence of burn status and collection date on proportion of carbon structures in leachate DOM that were oxygenated. Significance was tested by constructing null models that excluded b) burn status and c) collection date and running an ANOVA to compare the null model for each variable in question to the full model. The response variable "Normalized" refers to oxygenated proportion. Lysimeter ID was included as a random variable.

```
MODEL INFO:
Observations: 40
Dependent Variable: Normalized
Type: Mixed effects linear regression
MODEL FIT:
AIC = 231.24, BIC = 239.69
Pseudo-R^2 (fixed effects) = 0.17
Pseudo-R^2 (total) = 0.17
FIXED EFFECTS:
                        Est. S.E. t val. d.f.
(Intercept) 8.20 1.76 4.67 28.27 0.00
BurnStatusUnburned
Collection
                      -3.14 1.32
                                    -2.37 32.46 0.02
                       0.69 0.48 1.44 36.98 0.16
RANDOM EFFECTS:
            Parameter Std. Dev.
 LysimeterID (Intercept) 0.00
Residual 4.18
<u>Grouping variables:</u>
   Group # groups ICC
 LysimeterID 8 0.00
  anova(leach.funct.full, leach.funct.null1)
Data: NMR.leach.funct
Models:
leach.funct.null1: Normalized ~ Collection + (1 | LysimeterID)
leach.funct.full: Normalized ~ BurnStatus + Collection + (1 | Lysimeter
Signif. codes: 0 '*** 0.001 '** 0.01 '* 0.05 '.' 0.1 ' ' 1
\mathbf{c}
```

Figure A.16. Model results from a) mixed linear effects model testing the influence of burn status and collection date on proportion of carbon structures in leachate DOM that were functionalized aliphatic. Significance was tested by constructing null models that excluded b) burn status and c) collection date and running an ANOVA to compare the null model for each variable in question to the full model. The response variable "Normalized" refers to functionalized aliphatic proportion. Lysimeter ID was included as a random variable.

```
MODEL INFO:
Observations: 40
Dependent Variable: Normalized
Type: Mixed effects linear regression
MODEL FIT:
AIC = 285.40, BIC = 293.85
Pseudo-R^2 (fixed effects) = 0.15
Pseudo-R^2 (total) = 0.15
FIXED EFFECTS:
                         Est. S.E. t val. d.f.
                     68.82 3.65 18.84 28.27 0.00
5.71 2.75 2.07 32.46 0.05
(Intercept)
                                      2.07 32.46 0.05
BurnStatusUnburned
Collection
                        1.58 1.00 1.58 36.98 0.12
RANDOM EFFECTS:
             Parameter Std. Dev.
LysimeterID (Intercept) 0.00
Residual 8.69
<u>Grouping variables:</u>
   Group # groups ICC
LysimeterID 8 0.00
> anova(leach.aliph.full, leach.aliph.null1)
Data: NMR.leach.aliph
Models:
leach.aliph.null1: Normalized ~ Collection + (1 | LysimeterID)
leach.aliph.full: Normalized ~ BurnStatus + Collection + (1 | Lysimeter
Signif. codes: 0 '***' 0.001 '**' 0.01 '*' 0.05 '.' 0.1 ' ' 1
```

Figure A.17. Model results from a) mixed linear effects model testing the influence of burn status and collection date on proportion of carbon structures in leachate DOM that were aliphatic. Significance was tested by constructing null models that excluded b) burn status and c) collection date and running an ANOVA to compare the null model for each variable in question to the full model. The response variable "Normalized" refers to aliphatic proportion. Lysimeter ID was included as a random variable.

```
MODEL INFO:
Observations: 48
Dependent Variable: Normalized
Type: Mixed effects linear regression
MODEL FIT:
AIC = 143.63, BIC = 156.73
Pseudo-R^2 (fixed effects) = 0.40
Pseudo-R^2 (total) = 0.46
FIXED EFFECTS:
                                      Est. S.E. t val. d.f.
                                   1128.29 635.78
                                                      1.77
                                                                 7.87
                                                                        \begin{array}{c} 0.11 \\ 0.01 \end{array}
                                                                         0.11
(Intercept)
                                                      1.77 7.87
-2.65 37.39
                                     -1.83
BurnStatusUnburned
                                             0.69
0.22
Depth
                                     -0.27
                                                      -1.23 33.76
                                                                        0.23
Collection
                                     -0.56
                                               0.31
                                                        -1.77
                                                                 7.87
                                                                         0.11
                                                0.31
BurnStatusUnburned:Depth
                                      1.27
                                                         4.05
                                                                 33.76
                                                                        0.00
RANDOM EFFECTS:
  Group Parameter Std. Dev.
             -----
   Core (Intercept) 0.30
                             0.89
 Residual
<u>Grouping variables:</u>
 Group # groups ICC
                     0.10
 Core
             12
> anova(ext.aro.full, ext.aro.null1)
Data: NMR.ext.aro
Models:
ext.aro.null1: Normalized ~ Depth + Collection + (1 | Core)
ext.aro.full: Normalized ~ BurnStatus * Depth + Collection + (1 | Core
npar AIC BIC logLik deviance Chisq Df Pr(>Chisq) ext.aro.null1 5 153.44 162.79 -71.719 143.44 ext.aro.full 7 137.83 150.93 -61.915 123.83 19.609 2 5.52e-05
Signif. codes: 0 '*** 0.001 '** 0.01 '* 0.05 '.' 0.1 ' 1
c
```

```
# test burn status effect
  anova(ext.aro.full, ext.aro.null1)
Data: NMR.ext.aro
Models:
ext.aro.null1: Normalized ~ Depth + Collection + (1 | Core)
ext.aro.full: Normalized ~ BurnStatus * Depth + Collection + (1 | Core
                             BIC logLik deviance Chisq Df Pr(>Chisq)
                      AIC
              npar
ext.aro.null1
               5 153.44 162.79 -71.719
                                           143.44
                7 137.83 150.93 -61.915
                                           123.83 19.609 2
ext.aro.full
Signif. codes: 0 '***' 0.001 '**' 0.01 '*' 0.05 '.' 0.1 ' ' 1
  # test collection effect
 > anova(ext.aro.full, ext.aro.null3)
Data: NMR.ext.aro
Models:
ext.aro.null3: Normalized ~ BurnStatus * Depth + (1 | Core)
ext.aro.full: Normalized ~ BurnStatus * Depth + Collection + (1 | Core
                             BIC logLik deviance Chisq Df Pr(>Chisq)
              npar
                      AIC
ext.aro.null3
                 6 139.21 150.44 -63.605
                                            127.21
ext.aro.full
                 7 137.83 150.93 -61.915
                                           123.83 3.3808 1
                                                               0.06596
Signif. codes: 0 '*** 0.001 '** 0.01 '* 0.05 '.' 0.1 ' 1
e
  # test interaction of burn status and depth effect
 > anova(ext.aro.full, ext.aro.null4)
Data: NMR.ext.aro
Models:
ext.aro.null4: Normalized ~ BurnStatus + Depth + Collection + (1 | Cor
ext.aro.full: Normalized \sim BurnStatus * Depth + Collection + (1 \mid Core
                             BIC logLik deviance Chisq Df Pr(>Chisq)
                      AIC
              npar
ext.aro.null4
                 6 150.60 161.83 -69.300
                                            138.60
                 7 137.83 150.93 -61.915
                                           123.83 14.771 1 0.0001214
ext.aro.full
Signif. codes: 0 '*** 0.001 '** 0.01 '*' 0.05 '.' 0.1 ' ' 1
```

Figure A.18. Model results from a) mixed linear effects model testing the influence of burn status, depth, collection date, and the interaction of burn status and depth on proportion of carbon structures in leachate DOM that were aromatic. Significance was tested by constructing null models that excluded b) burn status, c) depth, d) collection, and e) interaction of burn status and depth and running an ANOVA to compare the null model for each variable in question to the full model. The response variable "Normalized" refers to aromatic proportion. Soil core ID was included as a random variable.

```
MODEL INFO:
Observations: 48
Dependent Variable: Normalized
Type: Mixed effects linear regression
MODEL FIT:
AIC = 134.38, BIC = 147.48
Pseudo-R^2 (fixed effects) = 0.61
Pseudo-R^2 (total) = 0.64
FIXED EFFECTS:
                                   Est. S.E. t val. d.f.
                                 119.69 550.97 0.22 7.86 0.83
1.63 0.62 2.62 37.45 0.01
0.71 0.20 3.52 33.88 0.00
(Intercept)
BurnStatusUnburned
Depth
Collection
                                   -0.06 0.27
                                                    -0.21
                                                              7.86 0.84
BurnStatusUnburned:Depth
                                  -1.61
                                            0.28 -5.67 33.88 0.00
RANDOM EFFECTS:
  Group Parameter Std. Dev.
                          0.23
0.80
 Core (Intercept)
Residual
<u>Grouping variables:</u>
 Group # groups ICC
 Core 12 0.08
b
  # test burn status effect
 > anova(ext.unsat.full, ext.unsat.null1)
Data: NMR.ext.unsat
Models:
ext.unsat.null1: Normalized ~ Depth + Collection + (1 | Core)
ext.unsat.full: Normalized ~ BurnStatus * Depth + Collection + (1 | Co
                 npar AIC BIC logLik deviance Chisq Df Pr(>Chise
ext.unsat.null1 5 171.51 180.86 -80.753 161.51
ext.unsat.full 7 127.34 140.44 -56.669 113.34 48.167 2 3.472e-
Signif. codes: 0 '***' 0.001 '**' 0.01 '*' 0.05 '.' 0.1 ' ' 1
\mathbf{c}
```

```
# test depth effect
  anova(ext.unsat.full, ext.unsat.null2)
Data: NMR.ext.unsat
Models:
ext.unsat.null2: Normalized ~ BurnStatus + Collection + (1 | Core)
ext.unsat.full: Normalized ~ BurnStatus * Depth + Collection + (1 | Co
                               BIC logLik deviance Chisq Df Pr(>Chis
                npar
                        AIC
                  5 149.09 158.45 -69.546
ext.unsat.null2
                                              139.09
ext.unsat.full
                   7 127.34 140.44 -56.669
                                              113.34 25.753 2 2.557e-
Signif. codes: 0 '***' 0.001 '**' 0.01 '*' 0.05 '.' 0.1 ' ' 1
d
  # test collection effect
Data: NMR.ext.unsat
Models:
ext.unsat.null3: Normalized ~ BurnStatus * Depth + (1 | Core)
ext.unsat.full: Normalized ~ BurnStatus * Depth + Collection + (1 | Col
                        AIC
                               BIC logLik deviance Chisq Df Pr(>Chiso
                npar
ext.unsat.null3
                   6 125.39 136.62 -56.698
                                             113.39
                   7 127.34 140.44 -56.669
                                             113.34 0.0566 1
                                                                   0.81
ext.unsat.full
  # test interaction of burn status and depth effect
  anova(ext.unsat.full, ext.unsat.null4)
Data: NMR.ext.unsat
Models:
ext.unsat.null4: Normalized ~ BurnStatus + Depth + Collection + (1 | C
ext.unsat.full: Normalized ~ BurnStatus * Depth + Collection + (1 | Co
                               BIC logLik deviance Chisq Df Pr(>Chis
                npar
                        AIC
ext.unsat.null4
                   6 150.79 162.02 -69.397
                                              138.79
                   7 127.34 140.44 -56.669
                                              113.34 25.455 1 4.529e-
ext.unsat.full
Signif. codes:
                0 '***' 0.001 '**' 0.01 '*' 0.05 '.' 0.1 ' ' 1
```

Figure A.19. Model results from a) mixed linear effects model testing the influence of burn status, depth, collection date, and the interaction of burn status and depth on proportion of carbon structures in leachate DOM that were unsaturated. Significance was tested by constructing null models that excluded b) burn status, c) depth, d) collection, and e) interaction of burn status and depth and running an ANOVA to compare the null model for each variable in question to the full model. The response variable "Normalized" refers to unsaturated proportion. Soil core ID was included as a random variable.

```
MODEL INFO:
Observations: 48
Dependent Variable: Normalized
Type: Mixed effects linear regression
MODEL FIT:
AIC = 308.74, BIC = 321.83
Pseudo-R^2 (fixed effects) = 0.52
Pseudo-R^2 (total) = 0.60
FIXED EFFECTS:
                                    Est. S.E. t val. d.f.
                               -4539.93 4692.61 -0.97 7.94 0.36
5.23 4.64 1.13 37.22 0.27
(Intercept)
BurnStatusUnburned
                                                    1.63
0.98
                                   2.42
Depth
                                            1.48
                                                             33.56
                                                                    0.11
Collection
                                   2.28
                                            2.32
                                                             7.94
                                                                    0.36
BurnStatusUnburned:Depth
                                             2.10
                                                     -3.87
                                                             33.56
                                                                    0.00
                                   -8.12
RANDOM EFFECTS:
  Group Parameter Std. Dev.
   Core
           (Intercept) 2.56
                           5.94
 Residual
<u>Grouping variables:</u>
 Group # groups ICC
         12
                  0.16
 Core
 > anova(ext.oxy.full, ext.oxy.null1)
Data: NMR.ext.oxy
Models:
ext.oxy.null1: Normalized ~ Depth + Collection + (1 | Core)
ext.oxy.full: Normalized ~ BurnStatus * Depth + Collection + (1 | Core
npar AIC BIC logLik deviance Chisq Df Pr(>Chisq) ext.oxy.null1 5 354.51 363.86 -172.25 344.51
                7 322.34 335.44 -154.17
                                            308.34 36.163 2 1.404e-08
ext.oxy.full
Signif. codes: 0 '***' 0.001 '**' 0.01 '*' 0.05 '.' 0.1 ' ' 1
\mathbf{c}
```

```
# test depth effect
  anova(ext.oxy.full, ext.oxy.null2)
Data: NMR.ext.oxy
Models:
ext.oxy.null2: Normalized ~ BurnStatus + Collection + (1 | Core)
ext.oxy.full: Normalized ~ BurnStatus * Depth + Collection + (1 | Core)
                             BIC logLik deviance Chisq Df Pr(>Chisq)
              npar
                      AIC
ext.oxv.null2
                 5 333.48 342.83 -161.74
                                           323.48
                 7 322.34 335.44 -154.17
ext.oxy.full
                                           308.34 15.135 2 0.0005171
                0 '***' 0.001 '**' 0.01 '*' 0.05 '.' 0.1 ' ' 1
Signif. codes:
> # test collection effect
Data: NMR.ext.oxy
Models:
ext.oxy.null3: Normalized ~ BurnStatus * Depth + (1 | Core)
ext.oxy.full: Normalized ~ BurnStatus * Depth + Collection + (1 | Core
                      AIC
                                  logLik deviance Chisq Df Pr(>Chisq)
              npar
                             BIC
ext.oxy.null3
                 6 321.51 332.73 -154.75
                                            309.51
ext.oxy.full
                                           308.34 1.1627
                 7 322.34 335.44 -154.17
                                                                 0.2809
  # test interaction of burn status and depth effect
> anova(ext.oxy.full, ext.oxy.null4)
Data: NMR.ext.oxy
Models:
ext.oxy.null4: Normalized ~ BurnStatus + Depth + Collection + (1 | Cor
ext.oxy.full: Normalized ~ BurnStatus * Depth + Collection + (1 | Core
                             BIC logLik deviance Chisq Df Pr(>Chisq)
                      AIC
              npar
ext.oxy.null4
                 6 333.69 344.91 -160.84
                                            321.69
                 7 322.34 335.44 -154.17
                                           308.34 13.341 1 0.0002596
ext.oxy.full
Signif. codes: 0 '***' 0.001 '**' 0.01 '*' 0.05 '.' 0.1 ' ' 1
```

Figure A.20. Model results from a) mixed linear effects model testing the influence of burn status, depth, collection date, and the interaction of burn status and depth on proportion of carbon structures in leachate DOM that were oxygenated. Significance was tested by constructing null models that excluded b) burn status, c) depth, d) collection, and e) interaction of burn status and depth and running an ANOVA to compare the null model for each variable in question to the full model. The response variable "Normalized" refers to oxygenated proportion. Soil core ID was included as a random variable.

```
MODEL INFO:
Observations: 48
Dependent Variable: Normalized
Type: Mixed effects linear regression
MODEL FIT:
\overline{AIC} = 241.38, BIC = 254.47
Pseudo-R^2 (fixed effects) = 0.22
Pseudo-R^2 (total) = 0.56
FIXED EFFECTS:
                                    Est. S.E. t val. d.f.
(Intercept)
                                -4856.96 3025.09 -1.61 8.67
                                                                      0.14
BurnStatusUnburned
                                   -2.78 1.98
                                                     -1.40
                                                              36.11 0.17
                                   -2.08
                                            0.62
                                                     -3.36
                                                              33.13
                                                                      0.00
Depth
Collection
                                            1.50
                                                     1.61
                                    2.41
                                                              8.67
                                                                      0.14
BurnStatusUnburned:Depth
                                    1.49
                                              0.88
                                                      1.70
                                                              33.13
                                                                      0.10
RANDOM EFFECTS:
  Group Parameter Std. Dev.
           (Intercept) 2.15
 Residual
                           2.48
<u>Grouping variables:</u>
 Group # groups ICC
           12
 Core
                  0.43
 Data: NMR.ext.funct
 Models:
 ext.funct.null1: Normalized ~ Depth + Collection + (1 | Core)
 ext.funct.full: Normalized ~ BurnStatus * Depth + Collection + (1 | Co
npar AIC BIC logLik deviance Chisq Df Pr(>Chis ext.funct.null1 5 247.34 256.70 -118.67 237.34
 ext.funct.full 7 248.11 261.21 -117.06 234.11 3.2274 2
                                                                      0.19
\mathbf{c}
```

```
anova(ext.funct.full, ext.funct.null2)
Data: NMR.ext.funct
Models:
ext.funct.null2: Normalized ~ BurnStatus + Collection + (1 | Core)
ext.funct.full: Normalized ~ BurnStatus * Depth + Collection + (1 | Col
                                    logLik deviance Chisq Df Pr(>Chisq
                        ATC
                               BIC
                npar
ext.funct.null2
                   5 254.21 263.56 -122.10
                                             244.21
ext.funct.full
                   7 248.11 261.21 -117.06
                                             234.11 10.095 2
Signif. codes: 0 '***' 0.001 '**' 0.01 '*' 0.05 '.' 0.1 ' ' 1
  anova(ext.funct.full, ext.funct.null3)
Data: NMR.ext.funct
Models:
ext.funct.null3: Normalized ~ BurnStatus * Depth + (1 | Core)
ext.funct.full: Normalized ~ BurnStatus * Depth + Collection + (1 | Col
                npar
                               BIC logLik deviance Chisq Df Pr(>Chiso
                        AIC
                   6 248.99 260.21 -118.49
ext.funct.null3
                                             236.99
ext.funct.full
                   7 248.11 261.21 -117.06
                                             234.11 2.8746 1
                                                                 0.0899
Signif. codes: 0 '***' 0.001 '**' 0.01 '*' 0.05 '.' 0.1 ' ' 1
  # test interaction of burn status and depth effect
Data: NMR.ext.funct
Models:
ext.funct.null4: Normalized ~ BurnStatus + Depth + Collection + (1 | C
ext.funct.full: Normalized ~ BurnStatus * Depth + Collection + (1 | Co
                               BIC logLik deviance Chisq Df Pr(>Chis
                npar
                        AIC
ext.funct.null4
                   6 248.95 260.18 -118.47
                                              236.95
ext.funct.full
                   7 248.11 261.21 -117.06
                                             234.11 2.8349 1
                                                                  0.092
Signif. codes: 0 '***' 0.001 '**' 0.01 '*' 0.05 '.' 0.1 ' ' 1
```

Figure A.21. Model results from a) mixed linear effects model testing the influence of burn status, depth, collection date, and the interaction of burn status and depth on proportion of carbon structures in leachate DOM that were functionalized aliphatic. Significance was tested by constructing null models that excluded b) burn status, c) depth, d) collection, and e) interaction of burn status and depth and running an ANOVA to compare the null model for each variable in question to the full model. The response variable "Normalized" refers to functionalized aliphatic proportion. Soil core ID was included as a random variable.

```
MODEL INFO:
Observations: 48
Dependent Variable: Normalized
 Type: Mixed effects linear regression
MODEL FIT:
AIC = 284.18, BIC = 297.28
Pseudo-R^2 (fixed effects) = 0.67
Pseudo-R^2 (total) = 0.70
FIXED EFFECTS:
                                    Est.
                                            S.E. t val.
                                                             d.f.
                                 8251.94 3145.74
 (Intercept)
                                                      2.62
                                                             7.86
                                                                     0.03
                                                             37.45
                                                                     0.36
BurnStatusUnburned
                                  -3.27
                                           3.56
                                                     -0.92
Depth
                                   -0.77
                                             1.15
                                                     -0.67
                                                            33.88
                                                                     0.50
Collection
                                   -4.07
                                              1.56
                                                      -2.62
                                                              7.86
                                                                     0.03
BurnStatusUnburned:Depth
                                                      4.30
                                                                     0.00
                                    6.98
                                              1.62
                                                             33.88
RANDOM EFFECTS:
             Parameter Std. Dev.
  Group
   Core
                            1.33
            (Intercept)
 Residual
                           4.59
<u>Grouping variables:</u>
 Group
         # groups ICC
 Core
            12
                    0.08
 Data: NMR.ext.funct
 Models:
 ext.funct.null1: Normalized ~ Depth + Collection + (1 | Core)
 ext.funct.full: Normalized ~ BurnStatus * Depth + Collection + (1 | Co
                         AIC
                                 BIC logLik deviance Chisq Df Pr(>Chis
                 npar
 ext.funct.null1
                    5 247.34 256.70 -118.67
                                               237.34
 ext.funct.full
                    7 248.11 261.21 -117.06
                                               234.11 3.2274 2
                                                                      0.19
c
```

```
anova(ext.funct.full, ext.funct.null2)
Data: NMR.ext.funct
Models:
ext.funct.null2: Normalized ~ BurnStatus + Collection + (1 | Core)
ext.funct.full: Normalized ~ BurnStatus * Depth + Collection + (1 | Col
                                    logLik deviance Chisq Df Pr(>Chisq
                        AIC
                               BIC
                npar
ext.funct.null2
                   5 254.21 263.56 -122.10
                                             244.21
ext.funct.full
                   7 248.11 261.21 -117.06
                                             234.11 10.095 2
Signif. codes: 0 '***' 0.001 '**' 0.01 '*' 0.05 '.' 0.1 ' ' 1
  anova(ext.funct.full, ext.funct.null3)
Data: NMR.ext.funct
Models:
ext.funct.null3: Normalized ~ BurnStatus * Depth + (1 | Core)
ext.funct.full: Normalized ~ BurnStatus * Depth + Collection + (1 | Col
                npar
                               BIC logLik deviance Chisq Df Pr(>Chiso
                        AIC
                   6 248.99 260.21 -118.49
ext.funct.null3
                                             236.99
ext.funct.full
                   7 248.11 261.21 -117.06
                                             234.11 2.8746 1
                                                                 0.0899
Signif. codes: 0 '***' 0.001 '**' 0.01 '*' 0.05 '.' 0.1 ' ' 1
  # test interaction of burn status and depth effect
> anova(ext.funct.full, ext.funct.null4)
Data: NMR.ext.funct
Models:
ext.funct.null4: Normalized ~ BurnStatus + Depth + Collection + (1 | C
ext.funct.full: Normalized ~ BurnStatus * Depth + Collection + (1 | Co
                               BIC logLik deviance Chisq Df Pr(>Chis
                npar
                        AIC
ext.funct.null4
                   6 248.95 260.18 -118.47
                                              236.95
ext.funct.full
                   7 248.11 261.21 -117.06
                                             234.11 2.8349 1
                                                                  0.092
Signif. codes: 0 '***' 0.001 '**' 0.01 '*' 0.05 '.' 0.1 ' ' 1
```

Figure A.22. Model results from a) mixed linear effects model testing the influence of burn status, depth, collection date, and the interaction of burn status and depth on proportion of carbon structures in leachate DOM that were aliphatic. Significance was tested by constructing null models that excluded b) burn status, c) depth, d) collection, and e) interaction of burn status and depth and running an ANOVA to compare the null model for each variable in question to the full model. The response variable "Normalized" refers to aliphatic proportion. Soil core ID was included as a random variable.

Extract Aromatic Proportion 0-10 cm ANOVA Model Results

```
Anova Table (Type II tests)
Response: Normalized
Sum Sq Df F value Pr(>F)
BurnStatus 0.4554 2 0.567 0.5862
Residuals 3.6143 9
$emmeans
 BurnStatus emmean
                        SE df lower.CL upper.CL
              1.110 0.317 9 0.3932
0.748 0.317 9 0.0307
                                             1.83
 Burned
 Postburn
                                             1.46
              0.660 0.317 9 -0.0568
 Unburned
                                             1.38
Confidence level used: 0.95
$contrasts
                                    SE df t.ratio p.value
 contrast
                       estimate
                        0.3625 0.448 9
 Burned - Postburn
                                             0.809 0.8238
 Burned - Unburned
                         0.4500 0.448 9
                                             1.004
                                                     0.7145
 Postburn - Unburned
                         0.0875 0.448 9
                                             0.195
                                                     0.9966
```

Figure A.23. Model results from a a) one-way ANOVA testing the influence of burn status on aromatic proportion of extract DOM from soils collected at 0-10 cm. The response variable "Normalized" refers to aromatic proportion. Pairwise significance was tested by b) running a Sidak test.

Extract Unsaturated Proportion 0-10 cm ANOVA Model Results

```
Anova Table (Type II tests)
Response: Normalized
Sum Sq Df F value Pr(>F)
BurnStatus 1.1895 2 0.3131 0.7388
                     0.3131 0.7388
Residuals 17.0971 9
b
   emmeans(top.unsat.anova, specs=pairwise~BurnStatus, adjust="sidak'
                         SE df lower.CL upper.CL
 BurnStatus emmean
               4.77 0.689 9
                                    3.21
                                              6.33
 Burned
                                    2.69
                                              5.81
 Postburn
                4.25 0.689 9
 Unburned
                5.00 0.689 9
                                    3.44
                                              6.56
Confidence level used: 0.95
$contrasts
                                     SE df t.ratio p.value
 contrast
                        estimate
                          0.522 0.975 9 0.536 0.9383
-0.230 0.975 9 -0.236 0.9940
 Burned - Postburn
 Burned - Unburned
                          -0.230 0.975
 Postburn - Unburned
                          -0.752 0.975 9 -0.772
                                                      0.8424
```

Figure A.24. Model results from a a) one-way ANOVA testing the influence of burn status on unsaturated proportion of extract DOM from soils collected at 0-10 cm. The response variable "Normalized" refers to unsaturated proportion. Pairwise significance was tested by b) running a Sidak test.

Extract Oxygenated Proportion 0-10 cm ANOVA Model Results

```
Anova Table (Type II tests)
Response: Normalized
Sum Sq Df F value Pr(>F)
BurnStatus 80.43 2 0.8215 0.4702
Residuals 440.58 9
b
    emmeans(top.oxy.anova, specs=pairwise~BurnStatus, adjust="sidak"
$emmeans
 BurnStatus emmean SE df lower.CL upper.CL
Burned 61.7 3.5 9 53.8 69.6
Postburn 63.6 3.5 9 55.7 71.5
                                         53.8
55.7
49.5
                   57.4 3.5 9
  Unburned
                                                      65.3
 Confidence level used: 0.95
$contrasts
                             estimate SE df t.ratio p.value
  contrast
                                -1.91 4.95 9 -0.387 0.9751
4.28 4.95 9 0.865 0.7940
6.19 4.95 9 1.252 0.5649
  Burned - Postburn
  Burned - Unburned
  Postburn - Unburned
P value adjustment: sidak method for 3 tests
```

Figure A.25. Model results from a a) one-way ANOVA testing the influence of burn status on oxygenated proportion of extract DOM from soils collected at 0-10 cm. The response variable "Normalized" refers to unsaturated proportion. Pairwise significance was tested by b) running a Sidak test.

```
Anova Table (Type II tests)
Response: Normalized
          Sum Sq Df F value Pr(>F)
BurnStatus 55.49 2 1.8302 0.2153
Residuals 136.44 9
$emmeans
BurnStatus emmean SE df lower.CL upper.CL
             14.14 1.95 9
8.89 1.95 9
                                        18.5
Burned
                               9.74
Postburn
                               4.48
                                        13.3
             11.24 1.95
                               6.83
                                        15.6
Unburned
                        9
Confidence level used: 0.95
$contrasts
                                SE df t.ratio p.value
contrast
                     estimate
                         5.26 2.75 9
                                        1.910 0.2427
Burned - Postburn
                         2.91 2.75
                                    9
Burned - Unburned
                                        1.056
                                               0.6834
 Postburn - Unburned
                        -2.35 2.75 9 -0.854
                                               0.8003
```

Figure A.26. Model results from a a) one-way ANOVA testing the influence of burn status on functionalized aliphatic proportion of extract DOM from soils collected at 0-10 cm. The response variable "Normalized" refers to functionalized aliphatic proportion. Pairwise significance was tested by b) running a Sidak test.

Extract Aliphatic Proportion 0-10 cm ANOVA Model Results

```
Anova Table (Type II tests)
Response: Normalized
Sum Sq Df F value Pr(>F)
BurnStatus 110.47 2 1.0628 0.3851
Residuals 467.74
                  9
 BurnStatus emmean SE df lower.CL upper.CL
                18.3 3.6 9
22.5 3.6 9
25.7 3.6 9
                                            26.4
 Burned
                                  10.1
                                  14.3
17.5
                                             30.6
 Postburn
 Unburned
                                             33.8
Confidence level used: 0.95
$contrasts
 contrast
                        estimate SE df t.ratio p.value
                            -4.23 5.1 9 -0.829 0.8132
 Burned - Postburn
                            -7.41 5.1 9
                                          -1.453 0.4489
 Burned - Unburned
                           -3.18 5.1 9 -0.624 0.9078
 Postburn - Unburned
```

Figure A.27. Model results from a a) one-way ANOVA testing the influence of burn status on aliphatic proportion of extract DOM from soils collected at 0-10 cm. The response variable "Normalized" refers to aliphatic proportion. Pairwise significance was tested by b) running a Sidak test.

```
Anova(aro.anova)
Anova Table (Type II tests)
Response: Normalized
                      Sum Sq Df F value
                                          Pr(>F)
BurnStatus
                       1.092
                             1 0.1964 0.665500
                      54.096
                             1 9.7308 0.008864 **
SampleType
BurnStatus:SampleType 25.402 1
                                 4.5692 0.053823 .
                      66.711 12
Residuals
Signif. codes: 0 '***' 0.001 '**' 0.01 '*' 0.05 '.' 0.1 ' ' 1
> emmeans(aro.anova, specs=pairwise~BurnStatus*SampleType, adjust="sid
$emmeans
 BurnStatus SampleType emmean
                                SE df lower.CL upper.CL
                        0.698 1.18 12
                                         -1.87
                                                    3.27
 Burned
            Extract
                        3.740 1.18 12
                                          1.17
                                                    6.31
 Unburned
            Extract
                        6.895 1.18 12
                                          4.33
 Burned
            Leachate
                                                    9.46
                        4.897 1.18 12
 Unburned
            Leachate
                                          2.33
                                                    7.47
Confidence level used: 0.95
$contrasts
                                                 SE df t.ratio p.value
 contrast
                                      estimate
 Burned Extract - Unburned Extract
                                         -3.04 1.67 12
                                                         -1.825
                                                                 0.4433
 Burned Extract - Burned Leachate
                                         -6.20 1.67 12
                                                         -3.717
                                                                 0.0175
 Burned Extract - Unburned Leachate
                                         -4.20 1.67 12
                                                         -2.519
                                                                 0.1512
                                         -3.15 1.67 12
 Unburned Extract - Burned Leachate
                                                                 0.4047
                                                         -1.892
                                                         -0.694
 Unburned Extract - Unburned Leachate
                                         -1.16 1.67 12
                                                                 0.9845
 Burned Leachate - Unburned Leachate
                                          2.00 1.67 12
                                                          1.198
                                                                 0.8277
P value adjustment: sidak method for 6 tests
```

Figure A.28. Model results from a a) two-way ANOVA testing the influence of burn status, sample type, and the interaction of burn status and sample type on aromatic proportion of DOM from leachate (30 cm) and extracts (20-30 cm) collected during April 2021. The response variable "Normalized" refers to aromatic proportion. Pairwise significance was tested by b) running a Sidak test.

```
Anova(oxy.anova)
Anova Table (Type II tests)
Response: Normalized
                      Sum Sq Df F value
                                           Pr(>F)
                       605.3 1 9.5429 0.009377 **
BurnStatus
SampleType
                      5828.2 1 91.8872 5.646e-07 ***
BurnStatus:SampleType 202.4 1
                                3.1914 0.099296 .
                       761.1 12
Residuals
Signif. codes: 0 '***' 0.001 '**' 0.01 '*' 0.05 '.' 0.1 ' '
> emmeans(oxy.anova, specs=pairwise~BurnStatus*SampleType, adjust="sid
$emmeans
 BurnStatus SampleType emmean
                               SE df lower.CL upper.CL
                         65.6 3.98 12
 Burned
            Extract
                                         56.90
                                                   74.3
                         46.2 3.98 12
 Unburned
            Extract
                                         37.49
                                                   54.8
                         20.3 3.98 12
                                         11.62
                                                   29.0
 Burned
            Leachate
                        15.1 3.98 12
                                          6.43
 Unburned
           Leachate
                                                   23.8
Confidence level used: 0.95
$contrasts
 contrast
                                      estimate
                                                 SE df t.ratio p.value
 Burned Extract - Unburned Extract
                                         19.41 5.63 12
                                                         3.448 0.0286
 Burned Extract - Burned Leachate
                                         45.28 5.63 12
                                                         8.041
                                                                <.0001
 Burned Extract - Unburned Leachate
                                         50.47 5.63 12
                                                         8.963
                                                               <.0001
 Unburned Extract - Burned Leachate
                                         25.87 5.63 12
                                                         4.594
                                                                0.0037
 Unburned Extract - Unburned Leachate
                                         31.06 5.63 12
                                                         5.515
                                                                0.0008
 Burned Leachate - Unburned Leachate
                                          5.19 5.63 12
                                                         0.921
                                                                0.9405
P value adjustment: sidak method for 6 tests
```

Figure A.29. Model results from a a) two-way ANOVA testing the influence of burn status, sample type, and the interaction of burn status and sample type on oxygenated proportion of DOM from leachate (30 cm) and extracts (20-30 cm) collected during April 2021. The response variable "Normalized" refers to oxygenated proportion. Pairwise significance was tested by b) running a Sidak test.

Leachate versus Extract Functionalized Aliphatic Proportion ANOVA Model Results

```
> Anova(funct.anova)
Anova Table (Type II tests)

Response: Normalized
Sum Sq Df F value Pr(>F)
BurnStatus
0.045 1 0.0054 0.9425
SampleType
0.000 1 0.0000 0.9993
BurnStatus:SampleType
0.995 1 0.1194 0.7356
Residuals
99.966 12
```

Figure A.30. Model results from a two-way ANOVA testing the influence of burn status, sample type, and the interaction of burn status and sample type on functionalized aliphatic proportion of DOM from leachate (30 cm) and extracts (20-30 cm) collected during April 2021. The response variable "Normalized" refers to functionalized aliphatic proportion.

```
Anova(aliph.anova)
Anova Table (Type II tests)
Response: Normalized
                      Sum Sq Df F value
                       692.0 1
                                13.1636
                                          0.003462 **
BurnStatus
SampleType
                      6178.0 1 117.5288 1.487e-07 ***
BurnStatus:SampleType 113.4 1
                                  2.1577 0.167575
Residuals
                       630.8 12
Signif. codes: 0 '***' 0.001 '**' 0.01 '*' 0.05 '.' 0.1 ''
 emmeans(aliph.anova, specs=pairwise~BurnStatus*SampleType, adjust="s
Semmeans
                                SE df lower.CL upper.CL
 BurnStatus SampleType emmean
                         18.1 3.63 12
                                          10.2
                                                    26.0
 Burned
            Extract
                         36.6 3.63 12
                                          28.7
                                                    44.5
 Unburned
            Extract
                         62.8 3.63 12
 Burned
            Leachate
                                          54.9
                                                    70.7
                         70.6 3.63 12
                                          62.7
 Unburned
            Leachate
                                                    78.5
Confidence level used: 0.95
$contrasts
 contrast
                                      estimate
                                                 SE df t.ratio p.value
                                                                0.0215
 Burned Extract - Unburned Extract
                                        -18.48 5.13 12
                                                        -3.604
 Burned Extract - Burned Leachate
                                        -44.62 5.13 12
                                                        -8.704
                                                                 <.0001
 Burned Extract - Unburned Leachate
                                        -52.45 5.13 12 -10.231
                                                                <.0001
                                        -26.15 5.13 12
 Unburned Extract - Burned Leachate
                                                        -5.100
                                                                0.0016
 Unburned Extract - Unburned Leachate
                                        -33.98 5.13 12
                                                        -6.627
                                                                 0.0001
 Burned Leachate - Unburned Leachate
                                         -7.83 5.13 12
                                                         -1.527
                                                                 0.6300
P value adjustment: sidak method for 6 tests
```

Figure A.31. Model results from a a) two-way ANOVA testing the influence of burn status, sample type, and the interaction of burn status and sample type on aliphatic proportion of DOM from leachate (30 cm) and extracts (20-30 cm) collected during April 2021. The response variable "Normalized" refers to aliphatic proportion. Pairwise significance was tested by b) running a Sidak test.

APPENDIX B

CHAPTER 3 FULL MODEL RESULTS

```
> anova(lit.C.full, lit.C.null1)
Data: lit.soils
Models:
lit.C.null1: Percent_C ~ Depth + (1 | Site/Core) + (1 | Site)
lit.C.full: Percent_C ~ BurnStatus * Depth + (1 | Site/Core) + (1 | Si
                             BIC logLik deviance Chisq Df Pr(>Chisq)
                      AIC
            npar
lit.C.null1
                6 109.930 123.59 -48.965
                                            97.930
lit.C.full
                8 91.394 109.61 -37.697
                                            75.394 22.537 2 1.277e-05
Signif. codes: 0 '***' 0.001 '**' 0.01 '*' 0.05 '.' 0.1 ' ' 1
 # test depth effect
> anova(lit.C.full, lit.C.null2)
Data: lit.soils
Models:
lit.C.null2: Percent_C ~ BurnStatus + (1 | Site/Core) + (1 | Site)
lit.C.full: Percent_C ~ BurnStatus * Depth + (1 | Site/Core) + (1 | Si
                             BIC
                                  logLik deviance Chisq Df Pr(>Chisq)
                      AIC
            npar
lit.C.null2
               6 133.831 147.49 -60.915
                                          121.831
                8 91.394 109.61 -37.697
                                            75.394 46.437 2 8.249e-11
lit.C.full
                0 '***' 0.001 '**' 0.01 '*' 0.05 '.' 0.1 ' ' 1
Signif. codes:
> # test interaction effect
Data: lit.soils
Models:
lit.C.null3: Percent_C ~ BurnStatus + Depth + (1 | Site/Core) + (1 | S
lit.C.full: Percent_C ~ BurnStatus * Depth + (1 | Site/Core) + (1 | Si
                             BIC logLik deviance Chisq Df Pr(>Chisq)
                      AIC
lit.C.null3
              7 109.610 125.55 -47.805
                                            95.610
lit.C.full
                8 91.394 109.61 -37.697
                                            75.394 20.216 1 6.916e-06
```

Figure B.1. Model results from a a) mixed linear effects model testing the influence of burn status, depth, and the interaction of burn status and depth on percent carbon in soils. Significance was tested by constructing null models that excluded b) burn status, c) depth, or d) the interaction of burn status and depth and running an ANOVA to compare the null model for each variable in question to the full model. Soil core ID and plot (called "Site" in the model" were included as random effects.

Signif. codes: 0 '***' 0.001 '**' 0.01 '*' 0.05 '.' 0.1 ' ' 1

Signif. codes:

```
> anova(lit.N.full, lit.N.null1)
Data: lit.soils
Models:
lit.N.null1: Percent_N ~ Depth + (1 | Site/Core) + (1 | Site)
lit.N.full: Percent_N ~ BurnStatus + Depth + (1 | Site/Core) + (1 | Si
            npar
                    AIC
                             BIC logLik deviance Chisq Df Pr(>Chisq)
               6 -398.77 -385.19 205.38
lit.N.null1
                                       -410.77
lit.N.full
               7 -397.74 -381.90 205.87
                                         -411.74 0.972 1
                                                              0.3242
 # test depth effect
> anova(lit.N.full, lit.N.null2)
Data: lit.soils
Models:
lit.N.null2: Percent_N ~ BurnStatus + (1 | Site/Core) + (1 | Site)
lit.N.full: Percent_N ~ BurnStatus + Depth + (1 | Site/Core) + (1 | Si
                             BIC logLik deviance Chisq Df Pr(>Chisq)
            npar
                     AIC
lit.N.null2
               6 -359.41 -345.84 185.71
                                         -371.41
               7 -397.74 -381.90 205.87
                                        -411.74 40.328 1 2.147e-10
lit.N.full
                0 "*** 0.001 "** 0.01 "* 0.05 ". 0.1 " 1
```

Figure B.2. Model results from a a) mixed linear effects model testing the influence of burn status and depth on percent nitrogen in soils. Significance was tested by constructing null models that excluded b) burn status or c) depth and running an ANOVA to compare the null model for each variable in question to the full model. Soil core ID and plot (called "Site" in the model" were included as random effects. Note: percent N values are missing for sample 71 – missing data likely impacted model performance.

```
b
    test burn status effect
Data: lit.soils
Models:
lit.CN.null1: CN_Ratio ~ Depth + (1 | Site/Core) + (1 | Site)
lit.CN.full: CN_Ratio ~ BurnStatus * Depth + (1 | Site/Core) + (1 | Site)
npar AIC BIC logLik deviance Chisq Df Pr(>Chisq) lit.CN.null1 6 334.26 347.83 -161.13 322.26
lit.CN.full
                  8 288.77 306.87 -136.39
                                                272.77 49.483 2 1.798e-11 ***
Signif. codes: 0 '***' 0.001 '**' 0.01 '*' 0.05 '.' 0.1 ' ' 1
Data: lit.soils
Models:
lit.CN.null2: CN_Ratio ~ BurnStatus + (1 | Site/Core) + (1 | Site)
lit.CN.full: CN_Ratio ~ BurnStatus * Depth + (1 | Site/Core) + (1 | Site)
npar AIC BIC logLik deviance Chisq Df Pr(>Chisq) lit.CN.null2 6 330.54 344.12 -159.27 318.54
lit.cn.full
                 8 288.77 306.87 -136.39
                                              272.77 45.767 2 1.153e-10 ***
Signif. codes: 0 '***' 0.001 '**' 0.01 '*' 0.05 '.' 0.1 ' ' 1
d
   # test interaction effect
anova(lit.CN.full, lit.CN.null3)
Data: lit.soils
Models:
 lit.CN.null3: CN_Ratio ~ BurnStatus + Depth + (1 | Site/Core) + (1 | Site)
 lit.CN.full: CN_Ratio ~ BurnStatus * Depth + (1 | Site/Core) + (1 | Site)
               npar AIC BIC logLik deviance Chisq Df Pr(>Chisq) 7 330.56 346.40 -158.28 316.56
 lit.CN.null3
                   8 288.77 306.87 -136.39
                                                 272.77 43.785 1 3.665e-11 ***
 lit.CN.full
Signif. codes: 0 '***' 0.001 '**' 0.01 '*' 0.05 '.' 0.1 ' ' 1
```

Figure B.3. Model results from a a) mixed linear effects model testing the influence of burn status, depth, and the interaction of burn status and depth on carbon to nitrogen ratio in soils. Significance was tested by constructing null models that excluded b) burn status, c) depth, or d) the interaction of burn status and depth and running an ANOVA to compare the null model for each variable in question to the full model. Soil core ID and plot (called "Site" in the model" were included as random effects.

```
# test burn status effect
  anova(lit.d13C.full, lit.d13C.null1)
Data: lit.soils
Models:
lit.d13C.null1: d13C ~ Depth + (1 | Site/Core) + (1 | Site)
lit.d13C.full: d13C ~ BurnStatus + Depth + (1 | Site/Core) + (1 | Site
                   r AIC BIC logLik deviance Chisq Df Pr(>Chisq
6 82.399 96.059 -35.199 70.399
                npar
lit.d13C.null1
lit.d13C.full
                   7 82.939 98.876 -34.470
                                              68.939 1.4592 1
                                                                    0.227
> anova(lit.d13c.full, lit.d13c.null2)
Data: lit.soils
Models:
lit.d13C.null2: d13C ~ BurnStatus + (1 | Site/Core) + (1 | Site)
lit.d13C.full: d13C ~ BurnStatus + Depth + (1 | Site/Core) + (1 | Site)
                        ATC
                                BIC logLik deviance Chisq Df Pr(>Chisq
               npar
                  6 169.108 182.768 -78.554 157.108
lit.d13C.null2
lit.d13C.full
                  7 82.939 98.876 -34.470
                                               68.939 88.168 1 < 2.2e-1
                0 '***' 0.001 '**' 0.01 '*' 0.05 '.' 0.1 ' ' 1
Signif. codes:
```

Figure B.4. Model results from a a) mixed linear effects model testing the influence of burn status and depth on $\delta^{13}C$ stable isotope in soils. Significance was tested by constructing null models that excluded b) burn status or c) depth and running an ANOVA to compare the null model for each variable in question to the full model. Soil core ID and plot (called "Site" in the model" were included as random effects.

```
MODEL INFO:
Observations: 108
Dependent Variable: pH_H20
Type: Mixed effects linear regression
MODEL FIT:
\overline{AIC} = -80.83, BIC = -64.73
Pseudo-R^2 (fixed effects) = 0.12
Pseudo-R^2 (total) = 0.81
FIXED EFFECTS:
                           Est. S.E. t val. d.f.
(Intercept)
                         4.89 0.14 35.95 4.64 0.00
(Intercept)
BurnStatusUnburned
                          0.17 0.19
                                          0.94
                                                   4.00 0.40
                          0.08 0.02 3.50 89.00 0.00
Depth
RANDOM EFFECTS:
              Parameter Std. Dev.
             (Intercept) 0.09
(Intercept) 0.22
 Core:Site
                            0.09
   Site
 Residual
                              0.13
<u>Grouping variables:</u>
             # groups ICC
   Group
 Core:Site 18
Site 6
                        0.12
                        0.66
> # test burn status effect
> anova(lit.pH_H20.full, lit.pH_H20.null1)
Data: lit.pH
Models:
lit.pH_H2O.null1: pH_H2O ~ Depth + (1 | Site/Core) + (1 | Site)
lit.pH_H2O.full: pH_H2O ~ BurnStatus + Depth + (1 | Site/Core) + (1 | S
                 npar AIC BIC logLik deviance Chisq Df Pr(>Chi
lit.pH_H2O.null1 6 -90.138 -74.045 51.069 -102.14
lit.pH_H2O.full 7 -89.328 -70.553 51.664 -103.33 1.1902 1
                                                                     0.2
\mathbf{c}
```

```
> # test depth effect
> anova(lit.pH_H2O.full, lit.pH_H2O.null2)
Data: lit.pH
Models:
lit.pH_H2O.null2: pH_H2O ~ BurnStatus + (1 | Site/Core) + (1 | Site)
lit.pH_H2O.full: pH_H2O ~ BurnStatus + Depth + (1 | Site/Core) + (1
```

Figure B.5. Model results from a a) mixed linear effects model testing the influence of burn status and depth on soil pH measured in water (H₂O). Significance was tested by constructing null models that excluded b) burn status, c) depth, or d) interaction of burn status and depth and running an ANOVA to compare the null model for each variable in question to the full model. Soil core ID and plot (called "Site" in the model" were included as random effects.

```
MODEL INFO:
Observations: 108
Dependent Variable: pH_CaCl2
 Type: Mixed effects linear regression
MODEL FIT:
\overline{AIC} = -84.04, BIC = -67.94
 Pseudo-R^2 (fixed effects) = 0.16
 Pseudo-R^2 (total) = 0.78
FIXED EFFECTS:
                        Est. S.E. t val. d.f. p
 (Intercept) 4.10 0.12 32.88 4.78 0.00
BurnStatusUnburned 0.10 0.17 0.59 4.00 0.59
BurnStatusUnburned
Depth
                             0.19 0.02 7.74 89.00 0.00
RANDOM EFFECTS:
    Group Parameter Std. Dev.
               (Intercept) 0.08
(Intercept) 0.20
0.13
 Core:Site
    Site
 Residual
 <u>Grouping variables:</u>
               # groups ICC
    Group
 Core:Site 18
Site 6
                          0.10
                           0.64
b
Data: lit.pH
Models:
lit.pH_CaCl2.null1: pH_CaCl2 ~ Depth + (1 | Site/Core) + (1 | Site)
lit.pH_CaCl2.full: pH_CaCl2 ~ BurnStatus + Depth + (1 | Site/Core) + (1 |
npar AIC BIC logLik deviance Chisq Df Pr(>Chi
lit.pH_CaCl2.null1 6 -94.414 -78.321 53.207 -106.41
lit.pH_CaCl2.full 7 -92.908 -74.133 53.454 -106.91 0.4946 1 0.4
C
```

Figure B.6. Model results from a a) mixed linear effects model testing the influence of burn status and depth on soil pH measured in 1M calcium chloride (CaCl₂). Significance was tested by constructing null models that excluded b) burn status, c) depth, or d) interaction of burn status and depth and running an ANOVA to compare the null model for each variable in question to the full model. Soil core ID and plot (called "Site" in the model" were included as random effects.

Bulk Density 0-10 cm ANOVA Model Results

Figure B.7. Model results from a one-way ANOVA testing the influence of burn status on bulk density at 0-10 cm.

```
MODEL INFO:
Observations: 417
Dependent Variable: Flux
Type: Mixed effects linear regression
MODEL FIT:
AIC = 292.42, BIC = 316.62
Pseudo-R^2 (fixed effects) = 0.05
Pseudo-R^2 (total) = 0.32
FIXED EFFECTS:
                        Est. S.E. t val. d.f. p
BurnStatusUnburned
Collection
                         0.01 0.01 1.24 405.85 0.22
RANDOM EFFECTS:
           Parameter Std. Dev.
 CollarID (Intercept) 0.20
Site (Intercept) 0.00
Residual 0.31
 Residual
                          0.31
Grouping variables:
          # groups ICC
  Group
 CollarID 29
Site 6
             29
                    0.28
                    0.00
> anova(flux.full, flux.null1)
Data: flux
Models:
flux.null1: Flux ~ Collection + (1 | CollarID) + (1 | Site)
flux.full: Flux ~ BurnStatus + Collection + (1 | CollarID) + (1 | Site)
          npar AIC BIC logLik deviance Chisq Df Pr(>Chisq)
flux.null1 5 279.41 299.58 -134.71 269.41 flux.full 6 277.08 301.28 -132.54 265.08 4.3302 1 0.03744 *
Signif. codes: 0 '*** 0.001 '** 0.01 '* 0.05 '.' 0.1 ' ' 1
c
```

Figure B.6. Model results from a a) mixed linear effects model testing the influence of burn status and collection date on soil carbon dioxide (CO₂) flux. Significance was tested by constructing null models that excluded b) burn status or c) collection and running an ANOVA to compare the null model for each variable in question to the full model. Collar ID and plot (called "Site" in the model" were included as random effects. Soil CO₂ flux values are missing for the 8 May 2022 sample collection date in Plot B2, which may reduce statistical power of our model.

APPENDIX C

FULL STUDY MAP

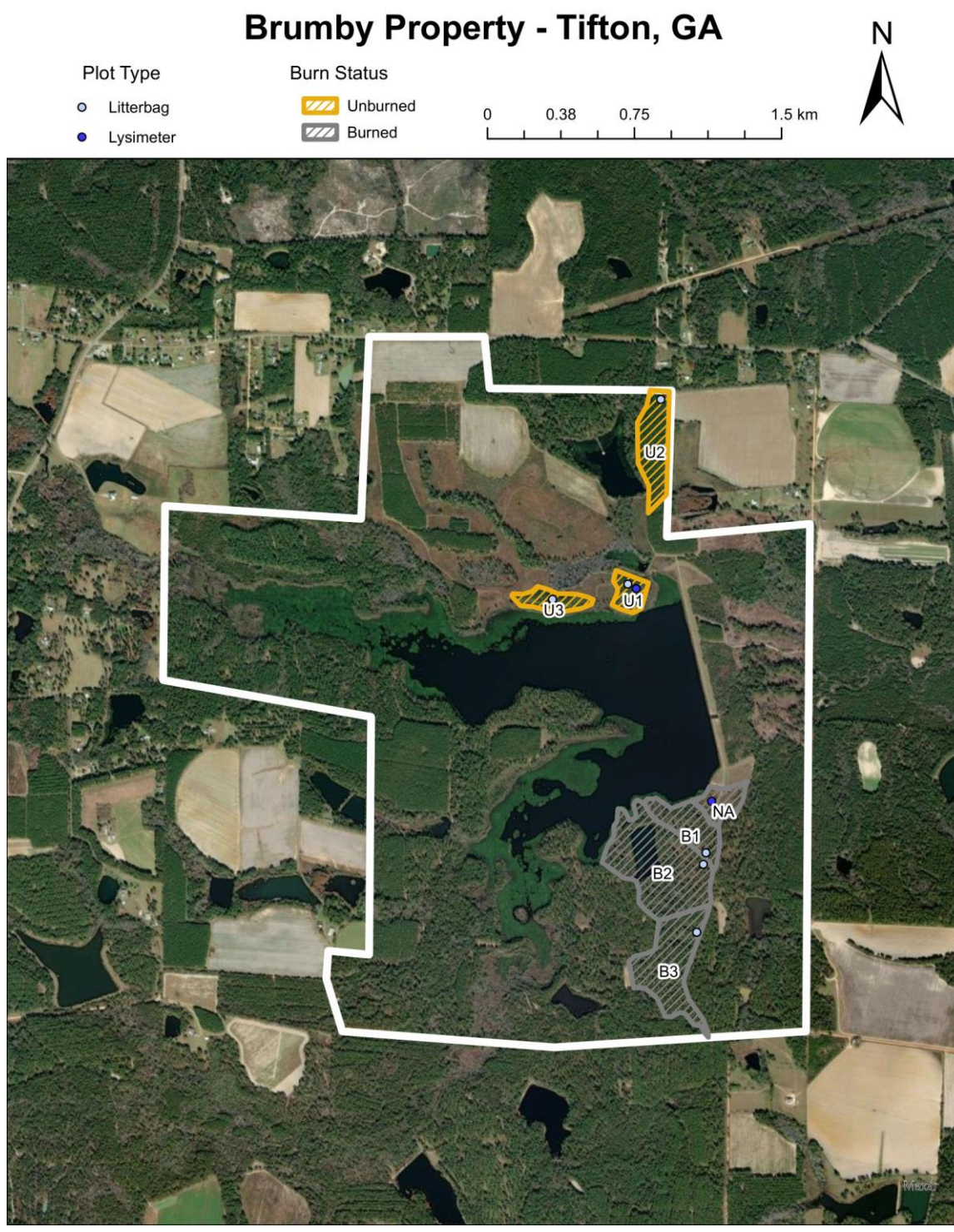


Figure C.1. Map showing all stand and plot locations within the study site. The large water body in the middle of the property is Lake Henry.